

- I AN APPARATUS FOR THE MEASUREMENT OF LIQUID  
DIFFUSION COEFFICIENTS
- II SUPERSATURATION IN HYDROCARBON SYSTEMS
  - 1. n-PENTANE IN THE LIQUID PHASE
  - 2. STATISTICAL PROCEDURES FOR SUPERSATURATION DATA
- III VOLUMETRIC AND PHASE BEHAVIOR OF HYDROCARBON SYSTEMS
  - 1. HYDROGEN-n-HEXANE
  - 2. n-HEPTANE

Thesis by  
William Burt Nichols

In Partial Fulfillment of the Requirements  
For the Degree of  
Doctor of Philosophy

California Institute of Technology  
Pasadena, California

1957

## ACKNOWLEDGMENT

I wish to express my indebtedness to Professor Bruce H. Sage for guidance and encouragement. He has instigated these researches and has continually directed them towards their goals. The assistance of H. Hollis Reamer and Lee T. Carmichael in the operation of the equipment and the work of Willard M. DeWitt, George A. Griffith, Torvald Myklebust, and Seichi Nakawatase in the construction of the apparatus must be gratefully acknowledged. The suggestions of Professors William N. Lacey and William H. Corcoran, both of whom reviewed the manuscript, are appreciated. Virginia Berry and June Gray assisted with the computations and the illustrations. The typing was done by Alethea Miller.

During the course of my graduate work I have been helped greatly by the financial support furnished by a General Petroleum Corporation Fellowship, a Union Carbide and Carbon Corporation Fellowship, and a National Science Foundation Fellowship.

## ABSTRACT

I. An apparatus was constructed for the measurement of Fick diffusion coefficients in the liquid phase under steady state conditions at pressures up to 10,000 psi. and at temperatures from 40 to 460° F. The apparatus consists of a device for the feed of a gas at an accurately known rate, a diffusion cell, and a device identical to the feed equipment for the withdrawal of a gas. The details of construction are given and a tentative method of operation is discussed.

II. 1. A limited number of measurements were made of the effect of the degree of supersaturation on the rate of bubble formation as shown by the time for the first bubble to form in liquid n-pentane. Data were taken at 160° and 280° F. in an isochoric cell and at 160° F. in an isobaric apparatus which is described. The results show that for a given degree of supersaturation the times of bubble formation are widely distributed and must be considered statistically.

II. 2. A procedure for the treatment of supersaturation data is discussed which includes a derivation of a theoretical distribution function for the times of formation of the first bubbles, a regression analysis based on an elementary hypothesis for the dependence of the rate of bubble formation on the degree of supersaturation, and a study of several pertinent confidence intervals.

III. 1. The volumetric behavior of four mixtures of different composition in the binary system hydrogen-n-hexane was investigated at pressures up to 10,000 pounds per square inch for eight temperatures in the interval between 40 and 460° F. The composition of coexisting phases in the heterogeneous region was determined at seven temperatures from 40 to 400° F. and at pressures up to 10,000 pounds per square inch. The results are presented in tabular and graphical form.

III. 2. Prior work on n-heptane by other investigators was extended as a preliminary to the study of the binary system methane-n-heptane. The molal volume of n-heptane is reported in tabular and graphical form as a function of pressure up to 10,000 pounds per square inch at eight temperatures covering the range from 40 to 460° F.

# TABLE OF CONTENTS

PART		PAGE
I	AN APPARATUS FOR THE MEASUREMENT OF LIQUID DIFFUSION COEFFICIENTS . . . . .	1
	Introduction . . . . .	2
	General Arrangement of the Apparatus . . . . .	6
	Operation of Pressure Control and Injector. . . . .	8
	Determination of Composition Gradient . . . . .	11
	Details of Construction . . . . .	14
	Conclusions . . . . .	18
	References . . . . .	20
	Nomenclature . . . . .	21
	Figures . . . . .	22
II	SUPERSATURATION IN HYDROCARBON SYSTEMS . . . . .	30
	1. n-PENTANE IN THE LIQUID PHASE . . . . .	30
	Introduction . . . . .	31
	Statistics . . . . .	33
	Materials . . . . .	37
	Methods and Equipment . . . . .	38
	Experimental Results . . . . .	43
	Literature Cited . . . . .	49
	Nomenclature . . . . .	52
	Figures . . . . .	54
	Tables . . . . .	68
	2. STATISTICAL PROCEDURES FOR SUPERSATURATION DATA . . . . .	72
	Introduction . . . . .	73
	The Basic Distribution Function . . . . .	75
	Regression Analysis . . . . .	80
	Confidence Limits . . . . .	82
	Conclusions . . . . .	88
	References . . . . .	89
	Nomenclature . . . . .	90
III	VOLUMETRIC AND PHASE BEHAVIOR OF HYDROCARBON SYSTEMS . . . . .	92
	1. HYDROGEN-n-HEXANE . . . . .	92
	Introduction . . . . .	93
	Methods and Apparatus . . . . .	94
	Materials . . . . .	98
	Experimental Results . . . . .	99
	Literature Cited . . . . .	103
	Figures . . . . .	104
	Tables . . . . .	111

PART

PAGE

2. n-HEPTANE . . . . . 120

I. AN APPARATUS FOR THE MEASUREMENT  
OF LIQUID DIFFUSION COEFFICIENTS

## INTRODUCTION

In a recent publication (5) Sage and coworkers have described an apparatus for the measurement of Fick diffusion coefficients in the liquid phase. A brief survey of earlier work is also presented in this reference. Their method was to add a gas such as methane to a quiescent liquid (e.g. n-decane) in a constant volume container at such a rate as to maintain a constant pressure within the cell. No material was withdrawn and so the composition and volume of the liquid varied throughout a run. The necessary corrections were substantial and introduced appreciable uncertainty in the reported coefficients. As a result of this earlier work, the present apparatus was designed so as to produce data susceptible to a simple and direct mathematical analysis.

The design of the diffusion cell is based in part upon an apparatus (1) for the measurement of Maxwell diffusion coefficients for gases at pressures up to 60 pounds per square inch under steady state conditions. In this earlier apparatus the less volatile component was introduced as a liquid by an injector similar to that described herein into the diffusion chamber through a porous glass disc at the bottom at a rate such as to maintain a gas-liquid interface at the top of the disc. The liquid evaporated at this interface, and the vapor diffused upward through the stagnant gas. At the top of the diffusion path the vapor was removed by



continuous circulation of the more volatile component. This mixture was then passed through a condenser; the less volatile component was removed and the more volatile component recirculated. The pressure difference between the upper and lower surfaces of the porous disc was determined by a manometer. A constant liquid level in the manometer indicated that a steady state had been attained.

Similarly, the present equipment is to be operated under steady state conditions. A gas is continuously introduced above a liquid surface at a rate equal to the rate of solution in the liquid. This interface is the top of the diffusion path. The bottom of the diffusion path is established by a nest of tubes through which a liquid is circulated. A boiler is used to remove the more volatile component from this circulating stream. The apparatus is designed to withstand pressures up to 20,000psi. at a temperature of 460° F., but the diffusion cell can be operated only in the two phase region of the system under study and so will not generally be used at these extreme conditions.

Only binary systems may be studied and a prior knowledge of their volumetric and phase behavior is required. It is necessary that the fraction of the more volatile component of the bubble point mixture must decrease with increasing temperature at constant pressure. At temperatures below the critical temperature of both components, this requirement is fulfilled. Above the critical temperature of one com-

ponent, this requirement will not be met for all compositions of the system. For example, in the hydrogen-n-hexane system, described in another part of this thesis, at temperatures above 40° F. only at very small fractions of hydrogen does the necessary phase behavior occur.

The Fick diffusion coefficient for component k may be defined by the following equation:\*

$$D_{F,k} = - \frac{\mu_{d,k} \sigma_k}{\frac{\partial \sigma_k}{\partial x}} \quad (1)$$

Equation 1 applies to transport in the x direction only. The total transport of component k in one direction, assuming no convective currents, is

$$\dot{m}_k = \mu \sigma_k + \mu_{d,k} \sigma_k = \mu \sigma_k - D_{F,k} \frac{\partial \sigma_k}{\partial x} \quad (2)$$

The total transport is the sum of the component transports

$$\dot{m} = \sum_{k=1}^{k=n} \dot{m}_k \quad (3)$$

These equations may be found in an excellent summary by Opfell and Sage (3). In the present situation there are only two components; component 1 will be taken to be the lighter component diffusing through the stationary component 2. Under these conditions

$$\dot{m}_2 = 0 \quad (4)$$

$$\dot{m} = \dot{m}_1 \quad (5)$$

---

\*The quantities appearing in the text are defined in the nomenclature which is located after the references.

Since

$$\dot{m} = \mu \sigma \quad (6)$$

$$\mu = \frac{\dot{m}}{\sigma} = \frac{\dot{m}_1}{\sigma} \quad (7)$$

From equations 2 and 7

$$\dot{m}_1 = \dot{m}_1 \frac{\sigma_1}{\sigma} - D_{F,1} \frac{\partial \sigma_1}{\partial x} \quad (8)$$

Rearrangement of equation 8 yields

$$D_{F,1} = \frac{\dot{m}_1}{\frac{\partial \sigma_1}{\partial x}} \left( \frac{\sigma_1}{\sigma} - 1 \right) \quad (9)$$

This exact equation may be approximated by the use of the overall concentration difference and an average value for the ratio  $\frac{\sigma_1}{\sigma}$ . The error in this approximation may be reduced to the desired degree by the use of data taken at smaller concentration differences and diffusion path lengths.

### GENERAL ARRANGEMENT OF THE APPARATUS

The apparatus consists of five major pieces of equipment, two pressure controls  $A_1$  and  $A_2$ , two injectors  $B_1$  and  $B_2$ , and the diffusion cell C, as shown in Figure 1. One pressure control and one injector are operated as a unit, with one pair being used to supply gas at a constant rate or pressure as desired and the other pair to withdraw material similarly. This arrangement permits, by substitution of other equipment for the diffusion cell, the use of the injectors and pressure controls as a steady state flow system. At present each pressure control can be maintained at a constant temperature; the injectors will be thermostated when this refinement becomes justified.

In operation, two main flow paths may be distinguished. The gas is displaced from the first pressure control  $A_1$  by mercury from the first injector  $B_1$  through thermostated lines into the upper chamber D within the diffusion cell above a gas-liquid interface. The gas driven off by the heater in the lower chamber L is withdrawn into the second pressure control  $A_2$  by the operation of the second injector  $B_2$ , which, although it performs the opposite function, will be referred to as an "injector" because it is constructed identically to the first injector.

The flow within the diffusion cell is shown schematically in Figure 1 and may be understood in detail by reference to Figure 2. The gas from the first pressure control

$A_1$  enters the cell in the gas space D and dissolves in the stagnant liquid E, the surface of which may be located by the movable hot wire F. The bottom of the diffusion path is continually swept by the liquid rising through the interstices of the nest of tubes G and descending inside the tubes into the header H. The gas solution enters the heat exchanger J at the bottom, rises around the outside of the tubes, and passes through the heater K, where the dissolved gas is boiled off. The gas in the space L is withdrawn to the pressure control  $A_2$  by the operation of the injector  $B_2$  as shown in Figure 1. The gas liquid interface is maintained between the upper and lower stationary hot wires at M. The liquid passes down through the tubes of the heat exchanger J into the internal pump N and is recirculated through coil P into the nest of tubes G.

OPERATION OF PRESSURE CONTROL AND INJECTOR

Figure 3 is a schematic diagram of the pressure control and associated equipment. In addition to the pressure control A and the injector B, there is shown the air chamber Q, the mercury valve block R, the air pressure valve block S, the safety trap T, and the two pressure gauges U and V. The air chamber Q serves as a reservoir for oil and mercury at approximately the same pressure. Oil is confined within the internal bell by mercury in the bottom of the chamber. The pressure of the air over the mercury outside the bell may be adjusted by the valve block S and is indicated on gauge V. The mercury reservoir is necessary because the volume of the pressure control is many times greater than the volume of the injector. The oil is used in the compensator of the injector and is also used to both lubricate and compensate the lower packing of the injector. Movement of the plunger in the injector is produced by a motor and gearing not shown in Figure 3. The compensator serves to balance the force exerted on the plunger by the mercury in the injector and so to relieve the mechanical drive from the necessity of transmitting this force. Because the oil and mercury are at about the same pressure the packing will keep the mercury substantially free of oil. Because of a slow seepage of the oil through the packing away from the mercury and possible leakage else-

where, over a period of time the oil in the bell of the air chamber becomes displaced by mercury. When the mercury reaches the safety trap T it grounds an electrical contact which furnishes a warning that the oil supply must be replenished.

The mercury valve block R connects the mercury supply in the air chamber Q to the injector B, the pressure control A, and the gauge V, which is thus operated full of mercury. With valves 3 and 4 of the valve block R open, mercury may be displaced from the injector to the lower chamber in the pressure control until the plunger reaches its maximum forward position. By closing valve 4, opening valve 2, and withdrawing the plunger, the injector may be refilled with mercury and the process repeated until the mercury surface in the pressure control rises to the highest point to be allowed. An electrical contact in the side of the pressure control indicates when this level is reached.

Figure 4 is a sectional view of the pressure control. The interior is divided into two chambers by a stainless steel diaphragm W. The upper chamber may be pressured by either a gas or a liquid which will not conduct electricity appreciably. This pressure may be considered a reference pressure and any change in the lower chamber on the other side of the diaphragm will be reflected in a change in position of the center of the diaphragm. A linear transducer X is mechanically linked to the center of the dia-

phragm and converts the displacement into an electrical signal. In turn this signal may be utilized to operate the injector so as to return the pressure in the lower chamber to that in the upper chamber.

A brief description of the electrical components and the electronic circuitry is in order. The linear transducer is a commercial unit manufactured by Crescent Engineering and Research Company. The pertinent characteristics are: linear range 0.12 inches, linearity 0.3%, diameter 0.50 inch, and length 0.50 inch. The probe has a diameter of 0.10 inch. It is used in conjunction with a control system manufactured by the same company. A standard alternating current bridge circuit is utilized, two sides of which are contained within the transducer. A displacement of the core which is directly connected to the diaphragm produces an increase in the reluctance of one coil and a decrease in the other, producing an unbalance in the bridge. The signal from the bridge is rectified and may be recorded or used as an input to a control circuit.

In the present work this signal is applied to a thyatron modulating circuit and a motor control circuit, the construction and operation of which has been described (6). The motor driving the injector is caused to move in such a direction that the pressure in the pressure control is changed and the diaphragm displaced so as to bring the transducer bridge circuit back into balance.



### DETERMINATION OF COMPOSITION GRADIENT

The liquid composition at the gas-liquid interface in the upper chamber of the diffusion cell is determined by the temperature and pressure in that chamber. The composition of the liquid which continually sweeps the top of the nest of tubes is determined by the temperature and pressure prevailing at the gas-liquid interface in the lower chamber. The temperature of the upper interface is the same as that of the bath in which the diffusion cell is immersed. The temperature of the interface in the lower chamber is maintained higher than that of the bath by the heater. The lower of the stationary wires, which are used intermittently to check on the liquid level in the lower chamber, is used otherwise as a platinum resistance thermometer. The pressure within the diffusion cell is not measured directly but is evaluated from a knowledge of the pressure within each pressure control. Owing to the pressure drop through the lines and the diffusion cell the pressure in the second pressure control will be less than that in the first. At the flow rates under consideration, however, this drop will not be great and the average of the two pressures establishes the pressure within the diffusion cell with the necessary accuracy.

The knowledge of the volumetric and phase behavior of the binary system under study permits the calculation of

the concentration difference across the diffusion path from the temperature difference and the pressure. If the diffusion coefficient is a function of the composition, use of the overall composition difference yields an "integral" coefficient. However, by the use of small concentration differences and at several different compositions, the true diffusion coefficient and its dependence on concentration may be established.

A knowledge of the length of the diffusion path is necessary to establish the gradient. The upper interface is located by the movable hot wire which is described in detail later. The lower end of the diffusion path is determined by the location of the nest of tubes and by the rate at which the liquid is circulated. The latter factor causes some uncertainty which must be considered. The diffusion path length may be adjusted over a range of about one inch. The overall concentration difference is fixed by the temperatures in the upper and lower chambers and the pressure of the system. If the injection rate is decreased, the gas-liquid interface in the upper chamber will rise until the diffusion rate has decreased to the value of the injection rate. Conversely the diffusion path may be shortened by increasing the injection rate. By making two runs or sets of runs at two different diffusion path lengths but at the same overall concentration difference the location of the lower end of the path may be calculated, assuming that it does not differ in the two circumstances. This

assumption is not unreasonable and may be checked by a third set of runs. It is to be hoped that, for a given circulation rate, the location remains constant, thus making it unnecessary for the location to be ascertained for each set of measurements.

### DETAILS OF CONSTRUCTION

The cell itself was machined from a forging of columbium-stabilized stainless steel (type 347, 17 to 19 percent chromium, 9 to 12 percent nickel, about 1 percent columbium). This material has the advantage of maintaining its corrosion resistance after heating to temperatures above 800 degrees Fahrenheit. The cell closure, utilizing an unsupported area seal, was constructed from the same material as the cell. The gasket was made of lead and the ratio of closure area to gasket area was 3.45.

The smaller internal parts of the diffusion cell, excepting the nest of tubes, were made from type 416 stainless steel which has 12 to 14 percent chromium and 0.18 to 0.35 percent sulfur for free machining. The nest of tubes was made from stainless-steel hypodermic tubing with an outside diameter of approximately 0.072 inch, and consists of 1471 tubes soldered together at the bottom by a lead-rich solder which melted at 500 degrees Fahrenheit. The nest of tubes was fitted into a cylinder 3.50 inches in diameter, giving an area available for flow of 3.05 square inches inside the tubes and 3.79 square inches between the tubes. The internal pump was used previously in this laboratory (2) and was found to be satisfactory over a wide range of flow rates. The drive for the internal pump is identical with that described in the section of this thesis devoted to the supersaturation apparatus.

The internal heater was wound from 64 feet of 28 gage Nichrome wire to give a rating of 50 watts. First a coil  $3/32$  inch in diameter with 2614 turns was wound; this coil was then wound around a two-inch coil form for ten turns. The coil form was machined from two pieces of transite bolted together; the groove was cut on a  $3/16$ -inch pitch, double thread so that the two ends of the coil were at the top of the coil form.

The use of hot wires for determining the location of a gas-liquid interface has been previously described (7). Figure 5 is a detail of the hot wire which shows the mounting, electrical connection, and pressure seal. Figure 6 presents a schematic diagram of the electrical circuits associated with both the fixed and movable hot wires. The equipment for moving and locating the hot-wire liquid-level indicator is a slight modification of the standard  $3/8$ -inch injector, a drawing of which is shown in Figure 7. The only significant alteration of the injector is the hollow plunger and the electrical head as shown in Figure 5. The plunger was sealed on the outside by Teflon packing and lubricated by oil under full pressure to prevent leakage.

The standard injector with a  $3/8$ -inch plunger is shown in a semi-sectional view in Figure 7. The piston A, driven by the heavy screw B, has a useful travel of 6.75 inches. Vertical movement in the screw is produced by a rotation of the nut C which is in turn driven by the worm

gear D. The upper end of the screw is connected to a plunger E. The packing F and the cylinder G are supplied with oil at a pressure approximately equal to that in the cylinder. The pressure in G relieves the nut C from the necessity of transmitting large forces. Since G contains high pressure oil, it is not necessary to compensate the packing (not shown) for the upper plunger. The injectors are similar to those previously described (4, 5, 6).

The pressure control cells were made from two different stainless steels; the first one was machined from a forging of type 416 and the second from type 430. The 430 was undesirable from the standpoint of difficulty of machining. Figure 4 shows three fluid connections to the cell: a sample line at the top of the lower chamber; a mercury line at the bottom; and interconnection between the upper and lower chambers. Not shown is another sample connection identical with the one shown, a connection through a valve into the bottom of the lower chamber, and a mercury trap which is shown schematically in Figure 3. The unsupported area principle is utilized again for the closure of the pressure control cell. The stainless steel diaphragm is similar to, but larger than, one reported earlier (8). The center of the diaphragm is mechanically fastened to the probe of the linear transducer. Two of the three seals for the electrical leads from the transducer are shown in Figure 4. Two other electrical connections are not shown: the mercury level contact in the trap

and the side contact which indicates when the mercury has risen to the limit of safety. The three agitated liquid baths for the diffusion cell and the pressure controls are similar to those used on many projects in the laboratory, and a brief description may be found in the section of this thesis devoted to the supersaturation project. The interconnections between the two pressure controls and the diffusion cell are constructed from small (0.072-inch diameter) stainless steel tubing which is inside 0.250-inch diameter copper tubing. Oil, maintained at a constant temperature, is circulated in the annular space between the tubes; the outside of the copper tubing is insulated with asbestos strips. The temperature of the lines is not important in itself but must be maintained constant.

### CONCLUSIONS

One of the pressure controls herein described has been used for a short time to maintain a constant pressure in the supersaturation apparatus. The supersaturation cell is kept at a constant temperature but the volume of several connecting lines varies with room temperature; this variation would cause a fluctuation in pressure if the pressure control were not functioning. The formation of a bubble within the supersaturation cell also tends to change the pressure. The brief experience has shown that the pressure control is capable of maintaining a constant pressure within better than 0.1 percent at a pressure of approximately 1000 pounds per square inch providing the volume does not change at a rate greater than the maximum injection rate.

The largest part of the error in the diffusion coefficient will probably be contributed by the unsteadiness of the diffusion path. Previous experience with an analogous apparatus (1) indicates that if the position of the interface in the upper chamber does not fluctuate appreciably, the error in the diffusion coefficient to be expected is of the order of 0.5 percent. The error due to fluctuations of the liquid level is not susceptible to calculation without a detailed knowledge of the magnitude and frequency of the fluctuations. The apparatus must be run so as to minimize these effects.



Another possible source of error is convection currents in the liquid in the upper chamber. At present, no steps are being taken to eliminate them; instead, reliance is being placed upon the density gradient to maintain the liquid completely stagnant. It is very probable that the convection currents will appear only at the higher liquid circulation rates and in this case a low rate of circulation can be used. The convection currents are potentially dangerous since the only way of determining their presence is to find the measured diffusion coefficients unreasonable. If they are proven to exist by future measurements it should be possible by the use of tubes or dividers in the liquid to eliminate the convection currents.

## REFERENCES

1. Carmichael, L. T., Reamer, H. H., and Sage, B. H. Washington, D.C. Amer. Doc. Inst., Doc. No. 4611 (1955).
2. Carmichael, L. T., and Sage, B. H. Ind. Eng. Chem. 44 2728 (1952).
3. Opfell, J. B., and Sage, B. H. Ind. Eng. Chem. 47 918 (1955).
4. Reamer, H. H., Corcoran, W. H., and Sage, B. H. Ind. Eng. Chem. 45 2699 (1953).
5. Reamer, H. H., Opfell, J. B., and Sage, B. H. Ind. Eng. Chem. 48 275 (1956).
6. Reamer, H. H., and Sage, B. H. Rev. Sci. Inst. 24 362 (1953).
7. Sage, B. H., and Lacey, W. N. Am. Inst. of Mining Met. Engrs. Technical Publication 2269.
8. Schlinger, W. G., and Sage, B. H. Ind. Eng. Chem. 42 2158 (1950).

NOMENCLATURE

$D_{F,k}$  Fick diffusion coefficient of component k  
sq. ft./sec.

$k$  Component k

$\dot{m}_k$  Transport rate of component k lb./sq.ft.-sec.

$u$  hydrodynamic velocity ft./sec.

$u_d$  diffusional velocity ft./sec.

$u_k$  transport velocity of component k  
lb./sq.ft.-sec.

$\mathcal{L}$  length in transport direction ft.

$\sigma$  specific weight lb./cu.ft.

$\sigma_k$  concentration of component k lb./cu.ft.

LIST OF FIGURES

1. Flow Diagram
2. Section of Diffusion Cell
3. Pressure Control and Associated Equipment
4. Section of Pressure Control
5. Detail of Hot Wire Assembly
6. Hot Wire Circuits
7. Details of Injector

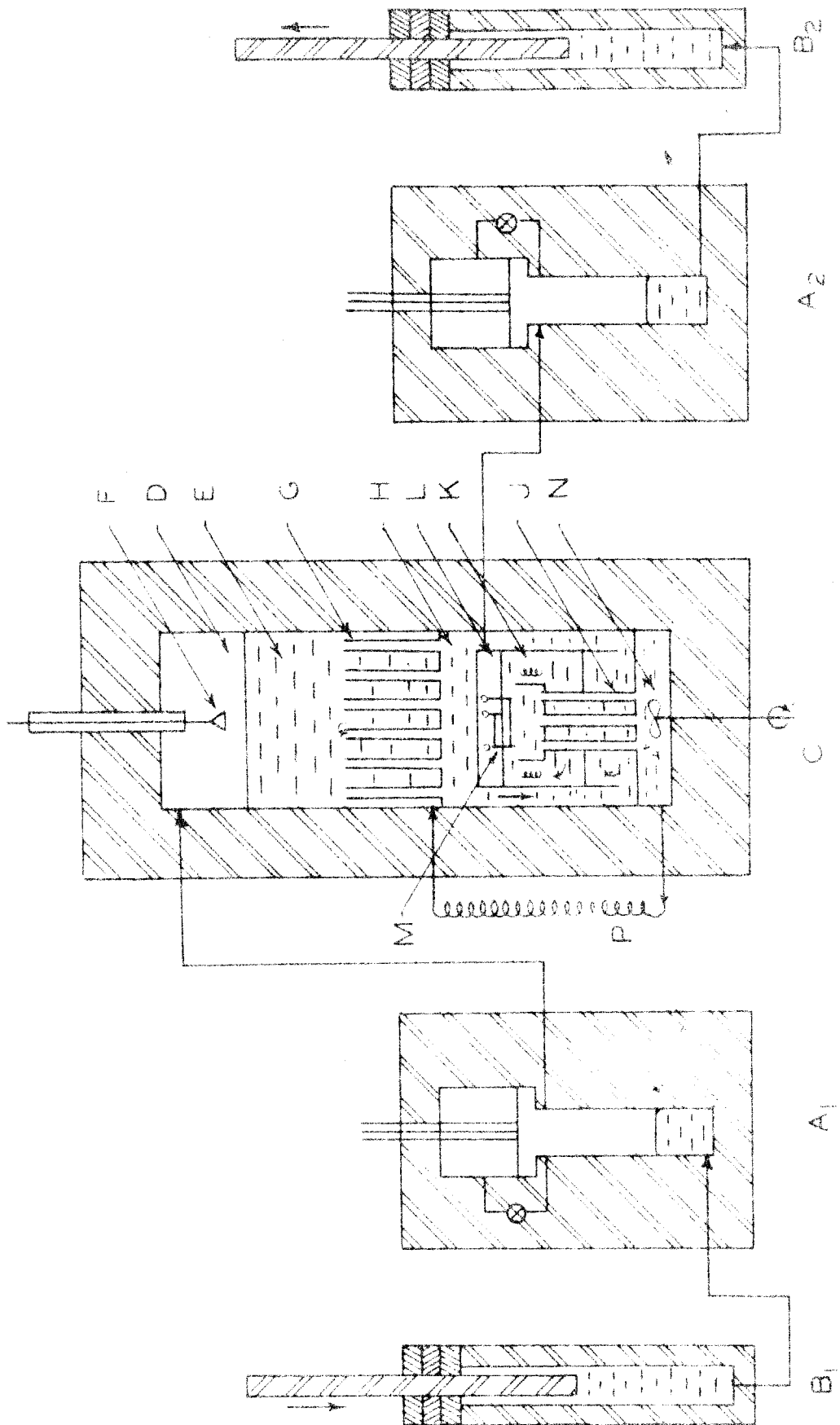


Figure 1. Flow Diagram

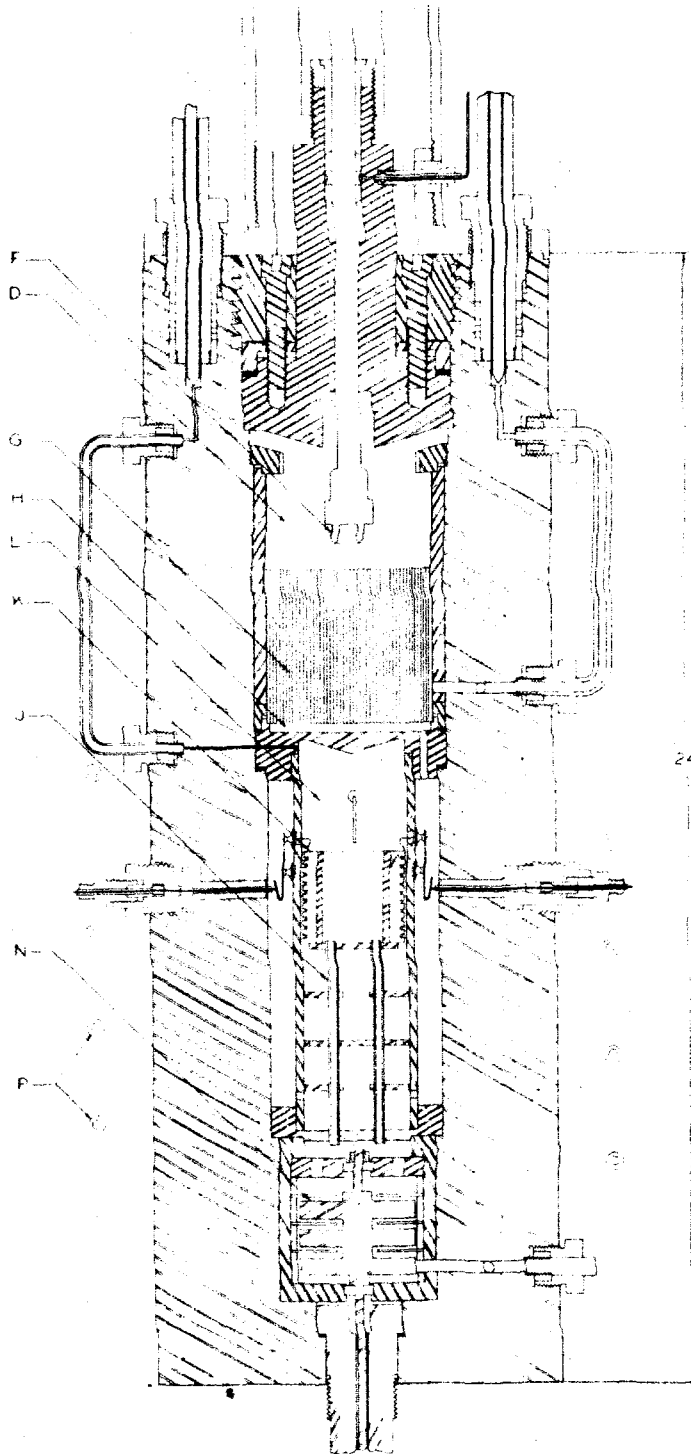


Figure 2. Section of Diffusion Cell

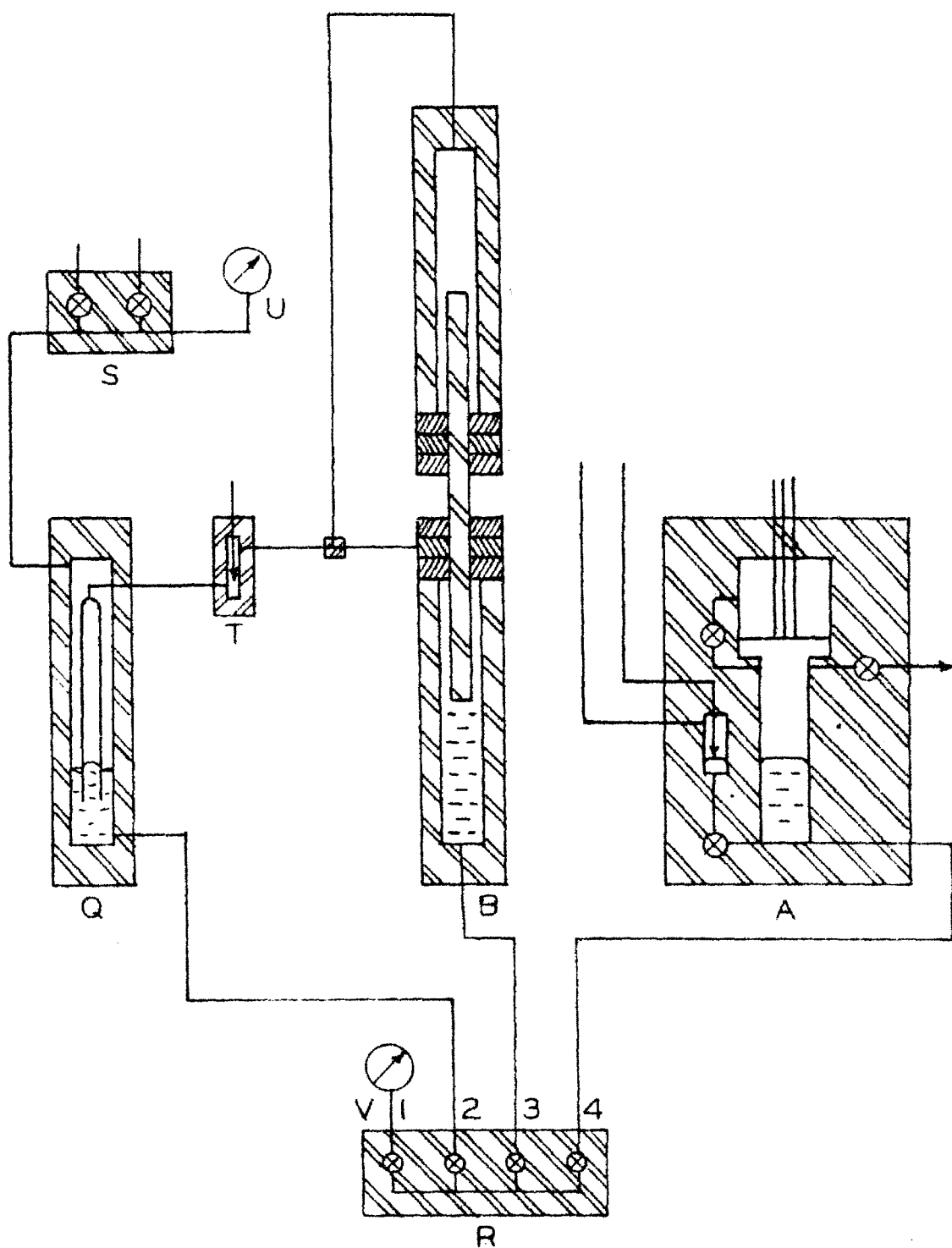


Figure 3. Pressure Control and Associated Equipment

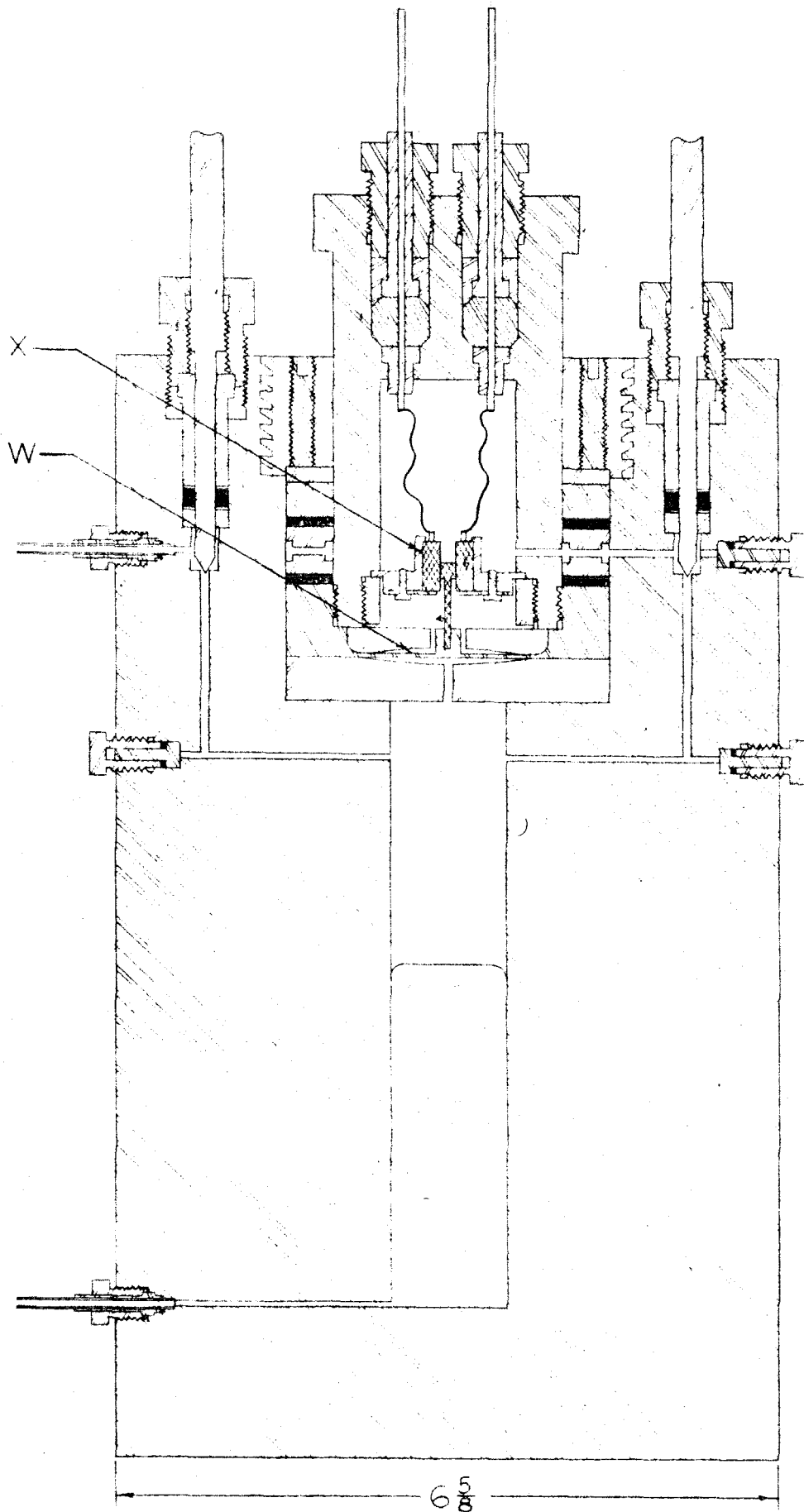
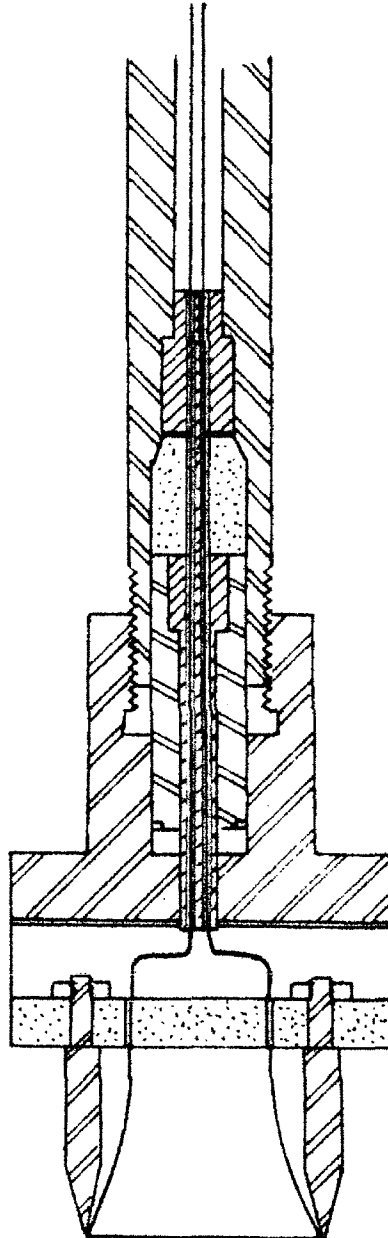


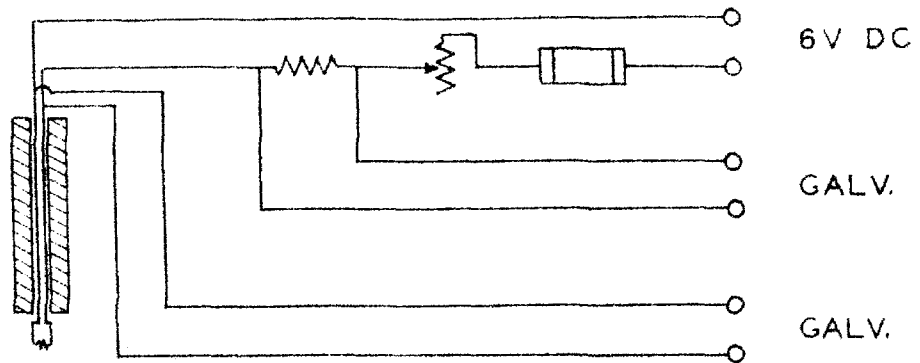
Figure 4. Section of Pressure Control



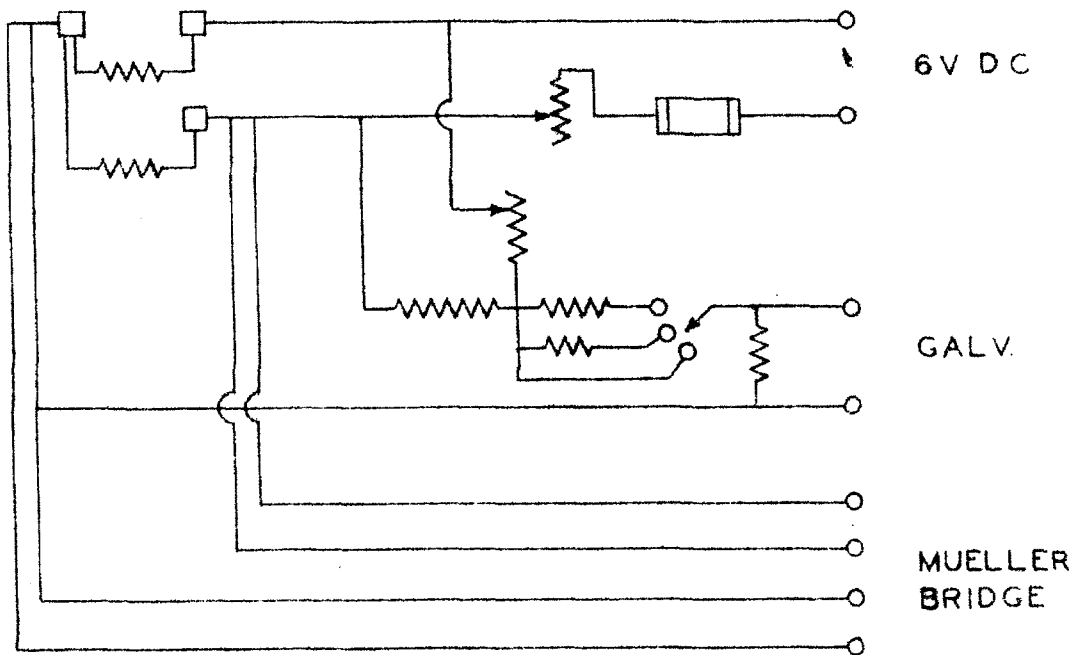


SCALE : TWICE FULL SIZE

Figure 5. Detail of Hot Wire Assembly



MOVABLE HOT WIRES



FIXED HOT WIRES

Figure 6. Hot Wire Circuits

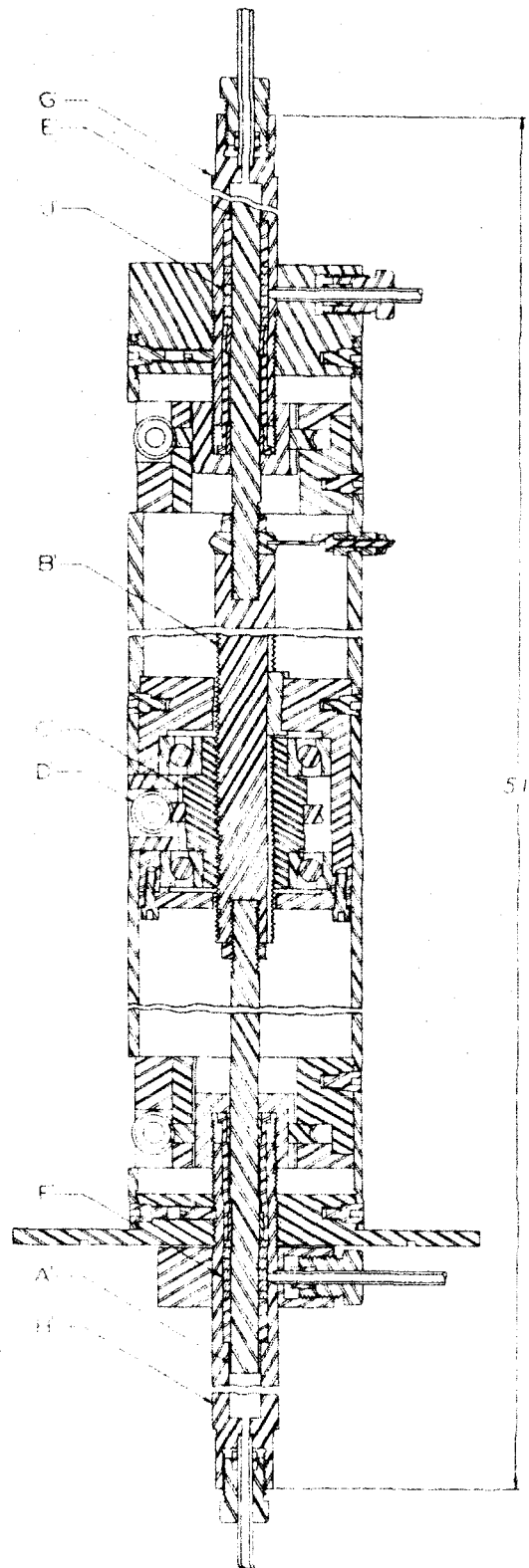


Figure 7. Details of Injector

II. SUPERSATURATION IN HYDROCARBON SYSTEMS

1. n-PENTANE IN THE LIQUID PHASE

SUPERSATURATION IN HYDROCARBON SYSTEMS. n-PENTANE  
IN THE LIQUID PHASE

W. B. Nichols, L. T. Carmichael, and B. H. Sage

California Institute of Technology  
Pasadena, California

INTRODUCTION

A knowledge of the probability of the formation of bubbles in a supersaturated hydrocarbon liquid is of technical interest in problems associated with the production and refining of petroleum. Some experimental investigations of attainable tensions in liquids have been made. Vincent (46, 47) studied the maximum tension in a mineral oil while Gardescu (14) found it was possible to maintain hydrocarbon mixtures at pressures significantly below bubble point for short periods of time. Kennedy and Olson (21) investigated the formation of bubbles in liquid mixtures of kerosene and methane and found it was possible to maintain a supersaturation of as much as 770 pounds per square inch for short intervals. The influence of solid surfaces upon the duration of a given degree of supersaturation in liquids was investigated by Marboe and Weyl (26) whereas the effect of viscous flow upon such phenomena was reported by Jha (20). The behavior of supersaturated solutions of electrolytes was studied by Akhumov and Rozen (1) while the stability of salt solutions was investigated by Tovbin and Krasnova (45). The

attainable tension in water was measured by a number of investigators (3,4,9,31,42,43) who obtained measurements varying from 750 to over 3,000 pounds per square inch. More recently cavitation in aqueous solution has been studied in some detail (32,33,49). The thermodynamics of such systems was considered by Gibbs (15) and extended by Goranson (16).

Related phenomena are found in gases when they are maintained at pressures in excess of vapor pressures. The spontaneous formation of nuclei in gases was studied by Sander and Damköhler (40). However, it has been found in wind tunnels that the extent of such supersaturation of air or nitrogen is small (10,27). Some study of the process of the evolution of gas from liquids was made by Burrows and Preece (5) while the factors influencing nucleation in boiling heat transfer was studied by Sabersky and Gates (37). The foregoing investigators have established the fact that the time that a particular solution will remain in a strained state must be evaluated statistically.

The theory of liquids (7,8,23,24) indicates that there exist significant fluctuations in the state variables at a point as a function of time. For this reason it is to be expected that there will be wide variations in the time during which a system will remain in the strained condition even though the macroscopic state is held invariant. It is beyond the objective of this discussion to consider the theory of supersaturation in liquids. Measurements of

the time that n-pentane was maintained in a strained condition were established at three temperatures. The results confirm earlier (19) findings that supersaturation in hydrocarbon liquids must be investigated statistically.

### STATISTICS

The statistical theory of liquids is usually based upon the Lennard-Jones and Devonshire equations of state (24) which were improved by Kirkwood (23) and have been considered rather intensively by Dahler and Hirschfelder (7,8). The results of Hirschfelder follow the work of Fürth (12,13). All of these theories of the molecular properties of liquids emphasize the fluctuations in the properties of liquids at a point with time. For this reason it is to be expected that the formation of bubbles in a strained liquid will be randomly distributed in time. Hunt (19) made a simple evaluation of the probability of a bubble being formed in a given time interval.

It is postulated for present purposes that the times of formation of bubbles are distributed at random. Such a situation is referred to as a "discontinuous stationary stochastic process" (2,25,35). Under these conditions the Poisson distribution has been shown to apply by a well established proof (11, 22).

With such a distribution the probability of n bubbles forming in the time interval from 0 to  $\theta$  is given by:

$$P_n(0, \theta) = \frac{(k\theta)^n}{n!} e^{-k\theta} \quad (1)$$

In Equation 1  $k\theta$  is the expected number of bubbles formed within the time interval. The probability of no bubbles forming in the interval from 0 to  $\theta$  may be established from

$$Q(0, \theta) = e^{-k\theta} \quad (2)$$

The mean value of times for the first bubble to form may be evaluated from the following equation (11):

$$\bar{\theta} = \frac{1}{\dot{m}_b} = \int_0^{\infty} k\theta e^{-k\theta} d\theta = \frac{e^{-k\theta}}{k} (k\theta - 1) \Big|_0^{\infty} = \frac{1}{k} \quad (3)$$

The reciprocal of the rate of bubble formation may be equated to the mean time for the first bubble to form

$$k = \dot{m}_b \quad (4)$$

Probability of the first bubble forming between  $\theta$  and  $\theta + d\theta$  is given by

$$P(\theta, \theta + d\theta) = \dot{m}_b e^{-\dot{m}_b \theta} d\theta \quad (5)$$



The associated variance may be described by (11)

$$(\sigma')^2 = \int_0^{\infty} (\theta - \bar{\theta})^2 \dot{m}_b e^{-\dot{m}_b \theta} d\theta = \frac{1}{\dot{m}_b^2} \quad (6)$$

From the foregoing it follows that the standard deviation is the reciprocal of the rate of bubble formation as indicated in Equation 7,  $\dot{m}_b$  always being positive,

$$\sigma' = \frac{1}{\dot{m}_b} \quad (7)$$

Integration of Equation 5 followed by rearrangement results in the following relation between the cumulative distribution and the time:

$$\ln[1 - P(0, \theta)] = -\dot{m}_b \theta \quad (8)$$

In accordance with Equation 8, a plot of  $\ln[1 - P(0, \theta)]$  as a function of time should yield a straight line if the formation of a bubble is randomly distributed in time.

The work associated with the formation of a stable spherical bubble may be approximated by the expression (15),

$$\underline{w} = \frac{16 \pi \gamma^3}{3(p_b - p)^2} \quad (9)$$

In the derivation of Equation 9 the variation of interfacial

tension with radius (44) was neglected.

It might be expected that the rate of bubble formation might follow the general theory of Arrhenius. Under this hypothesis the number of bubbles formed per unit time in the volume would be approximated by

$$\dot{m}_b = Ae^{-\left(\frac{16\pi\gamma^3}{3(P_b - P)^2}\right) \frac{1}{bT}} \quad (10)$$

From Equation 10 it would be expected that the natural logarithm of the mean time for the formation of the first bubble would be a linear function of the reciprocal of the square of the supersaturation pressure, as indicated in the equation,

$$\ln A\bar{\theta}_b = \ln \bar{\theta}_b + \ln A = \frac{\alpha}{(P_b - P)^2} \quad (11)$$

Equation 11 has been used to correct some of the experimental data to a fixed supersaturation pressure,  $(P_b - P^\circ)$ , by assuming that

$$\ln \theta_b^\circ - \ln \theta_b = \frac{\alpha}{(P_b - P^\circ)^2} - \frac{\alpha}{(P_b - P)^2} \quad (12)$$

The following approximate equation was used to correct the small deviations of the experimental data from conditions

of constant strain:

$$\beta = \frac{(\theta_b)_c}{\theta_b} = \frac{\bar{\theta}_m^*}{\theta_b(P_b - P)^*} \int_0^{\theta_b} \frac{P_b - P}{\bar{\theta}_m} d\theta \quad (13)$$

The integral in equation 13 was evaluated graphically. The relation of the mean time  $\bar{\theta}_m$  for the first bubble to form with pressure is given by Equation 11.

In accordance with the central limit theorem (29) for a population with a finite variance  $\sigma^2$  and mean  $\mu$ , the distribution of the sample mean approaches the normal distribution with variance  $\frac{\sigma^2}{n}$  and mean  $\mu$  as the sample size  $n$  increases. As a consequence of this theorem, the 95% confidence interval for the mean rate of bubble formation of  $n$  points is asymptotically  $\pm \frac{1.960}{\sqrt{n}}$  times the measured rate. Thus for a sample of 100 points, the 95% confidence interval is  $\pm 19.6\%$  of the measured rate.

It should be emphasized that the above discussion leaves much to be desired from the standpoint of classical statistics but appears to yield a simple means of analysis of the experimental data obtained.

## MATERIALS

The n-pentane used in this investigation was obtained as pure grade from the Philips Petroleum Co. and was reported to contain not more than 0.01 mole fraction of material other than n-pentane. It was used for these pre-

liminary measurements without purification except for deaeration by prolonged refluxing at reduced pressure. The deaerated sample showed a specific weight at atmospheric pressure of 38.775 pounds per cubic foot at 77° F. as compared to a value of 38.791 pounds per cubic foot at a temperature of 77° F. reported by Rossini (36). An index of refraction at 77° F. of 1.35475 was obtained for the D-lines of sodium as compared to a value of 1.35472 reported by Rossini for an air saturated sample. The vapor pressure at 160° F. was found to be 42.4 pounds per square inch and at 278.94° F. it was 183.6 pounds per square inch, which agreed satisfactorily with accepted values (39).

#### METHODS AND EQUIPMENT

In principle, the method employed in this investigation involved maintaining one relatively small portion of the system at a somewhat higher temperature than the remainder thus localizing the region in which supersaturation occurred. Such an arrangement permitted the configuration of the system subjected to strain to be relatively simple, without interfaces, packing glands, and acute angles which might have a significant influence upon the time-strain relationships of the system.

Figure 1 portrays schematically the nature of the equipment employed. It consists of the pressure vessel A provided with a stainless steel thimble B. The three-stage centrifugal pump C is utilized to circulate the fluid

from the entrance of the pump upward through the tube D located at the center of the thimble B. Mercury is introduced or withdrawn from the vessel at E. A multi-lead copper constantan thermocouple is used to determine the temperature of thimble B relative to the bath K shown in Figure 3, and the leads are shown schematically at F and F' in Figure 1. An electric heater G, is used to maintain the temperature of the thimble at desired values up to  $40^{\circ}$  F. above that of the pressure vessel A.

The system is brought to equilibrium at some predetermined temperature and is maintained at a pressure well above the bubble-point pressure for a specified time, usually several hours. During this period the pump C is operated only intermittently. The temperature of the thimble B is then raised a predetermined amount in order to bring the bubble-point pressure of the fluid within the thimble B above that of the main body of liquid. The pressure is then carefully reduced to a value just above the bubble-point pressure of the main body of liquid by the withdrawal of mercury. The situation existing under these circumstances is shown in Figure 2, in which the equilibrium vapor pressure of n-pentane is shown as a function of temperature. The pressure within the vessel is indicated at P corresponding to the equilibrium temperature  $T_e$ . The vessel A is maintained at  $T_A$  and thus the state H corresponds to the conditions within the pressure vessel A. The temperature at B of Figure 1 is shown at state J. The

equilibrium bubble-point pressure at  $T_B$  is above the pressure in the vessel thus yielding a supersaturated or strained state at J. The magnitude of the supersaturation pressure is given by

$$P_s = P_b - P \quad (14)$$

It is apparent from consideration of Figure 2 that the equipment described herein is only suitable for use with systems in which the equilibrium bubble-point pressure increases with an increase in temperature.

Figure 3 shows the general arrangement of the associated equipment. The pressure vessel A of Figure 1 is shown within the agitated silicone bath K of Figure 3. The thimble B is located above the three-stage centrifugal pump C and the tube D serves to introduce the fluid from the pump into the thimble. The bath K is provided with an impeller L which is driven by means of gears through the packing gland M. Rotation of the impeller circulates the silicone fluid within the bath upward around the outside shell and downward around the vessel A. A mercury-oil interface is provided in N so that the pressure can be measured by the balance P (38).

The quantity of mercury within the pressure vessel A is controlled by the chamber R which is connected to it by means of stainless steel tubing approximately 0.09 inch in inside diameter, as is shown in Figure 3. A bell

S is provided within the chamber R to supply oil to the compensated shaft-cylinder combination T (6) which seals the shaft driving the impeller of the pump C. Gauges and valves at U permit the introduction and withdrawal of mercury and the determination of the approximate pressure in the vessels A and R.

The temperature of the agitated silicone bath K is controlled through a modulated circuit which has been described (34). Temperatures are related to the international platinum scale by means of a strain-free platinum resistance thermometer (28). For the ready determination of pressure as a function of time, a strain gauge type of transducer V is provided to aid in control of operations, whereas the mechanical injector W is used to maintain isobaric conditions.

The system is brought to physical equilibrium at a pressure markedly higher than P shown in Figure 2 and the thimble heated to an appropriate value  $T_B$ . The pressure is then gradually decreased to a chosen value P which yields a known degree of supersaturation. The supersaturation of the state is determined from the temperature of the thimble B and the pressure as determined by the balance P of Figure 3. These data, together with a knowledge of the vapor pressure of the compound as a function of temperature, permit the supersaturation pressure to be calculated. The transducer V is employed to follow the small random variations in pressure as a function of time. The dependent

variable is the time at which the strained state returns to equilibrium by the formation of a bubble.

Details of the pressure vessel A and thimble B are shown in Figure 4. The vessel was constructed of a chrome-nickel steel. It was found advantageous to employ a different type of stainless steel for the closure in order to avoid galling between closely mating parts which were immersed in silicone. A three-stage centrifugal pump C constructed of chrome-nickel steel was used to attain equilibrium. The location of the thermocouple leads of Figure 1 is shown at F and F'. An electric heater G was used to maintain the thimble B at the desired temperature.

The details of the shaft-cylinder combination are shown in Figure 5. A clearance of approximately  $2 \times 10^{-5}$  inches was provided between the shaft X and the cylinder Y. The cylinder was so arranged as to yield some pressure compensation by elastic deformation which reduced the clearance at the higher pressures. The introduction of oil at Z in a lantern near the middle of the cylinder permitted the virtual elimination of leakage and resulted in negligible contamination of a particular sample over a period of several months residence in the equipment.

For a number of preliminary measurements a spherical, isochoric vessel was employed. The primary equipment consisted of a spherical stainless steel shell provided with a flexible diaphragm of the aneroid type through which the



pressure within the vessel was measured as a function of time. Details of construction of this vessel and the associated temperature control equipment were described earlier in some detail (41). The vessel was filled with n-pentane liquid at a temperature of approximately 40° F. When heated, the pressure rose to about 1000 pounds per square inch above vapor pressure where it was held under nearly isobaric, isothermal conditions for several hours. The temperature was then gradually lowered until the pressure within the vessel was an appropriate amount below the vapor pressure of n-pentane and the system was then maintained under isothermal conditions until a bubble was formed. The associated rapid rise in pressure to substantially the vapor pressure at the temperature in question was used as an indication of bubble formation. It was found that even careful control of temperature with respect to time during adjustment to the prescribed value was not sufficiently precise to avoid marked variations in the pressure with respect to time during the period of strain. For this reason the equipment was not found suitable for extensive investigation of the phenomena of supersaturation in hydrocarbon liquids.

#### EXPERIMENTAL RESULTS

A typical set of experimental results obtained with the isochoric equipment for n-pentane is shown in Figure 6. The points shown correspond to the pressures measured with the

balance P of Figure 3 as a function of time. In addition nearly a continuous record of pressure was obtained by means of the strain gauge transducer V. From the data of Figure 6 the supersaturation pressure or strain was computed and depicted in Figure 7. In this instance an average supersaturation pressure of 4.54 pounds per square inch was maintained for a period of 8630 seconds or approximately 2.4 hours before a bubble was formed. A consideration of Figures 6 and 7 indicates that the technique involving an isochoric vessel leaves much to be desired in the way of maintaining a constant value of supersaturation pressure for an extended period. Also some difficulty was experienced in bringing the supersaturation to a predetermined value as the temperature was gradually reduced. As a result the supersaturation was changing with respect to time for a significant part of the total period. Such behavior still further complicated the statistical analysis of the results.

The results of some twenty measurements of n-pentane with the isochoric equipment are recorded in Table I for temperatures near 160° and 280° F. In this instance the average values of supersaturation pressure and time of strain have been indicated. The standard deviation of the variation in pressure with time was included as well as the uncorrected time of strain. The details of the calculation of the average pressure and the corrected time of strain for isobaric conditions of strain were discussed

in an earlier section. A total volume of 0.00876 cubic foot and a surface area of 0.22245 square foot were involved.

Figure 8 shows typical results for n-pentane obtained with the heated thimble equipment described above. In this instance the sample is maintained under isothermal conditions throughout the period of strain. Only a total of 0.000411 cubic foot of sample with a surface area of 0.0567 square foot within the thimble is subjected to the strain and the conditions are nearly isobaric. For this reason it is possible to obtain the results for a particular set of conditions directly from a series of experimental measurements such as the one submitted in Figure 8. A summary of the experimental results obtained with the heated thimble equipment is recorded in Table II.

Utilizing the information of Table II, adjusted by Equation 11 for small deviations from isobaric conditions, there is obtained and shown in Figure 9 the natural logarithm of the time of strain as a function of the supersaturation pressure. In order to show the applicability of equation 11, the natural logarithm of the time of strain is shown as a function of the reciprocal of the square of the supersaturation pressure in Figure 10. As predicted by Equation 7, there is a marked deviation from the straight line fitted to the data by standard statistical methods (30). The data of Figures 9 and 10 are based upon a temperature of 160° F. and were obtained from the thimble

equipment. The data from the isochoric equipment were obtained over a significant range of strains while those for the heated thimble apparatus were restricted to two to three rather narrow ranges of supersaturation pressures. The results of the corrections for non-isobaric conditions are recorded in Table I. It should be emphasized that these corrections, which were made by iterative application of the methods of analysis described earlier, are only approximations that permit the experimental results to be compared under the conditions of constant strain.

Utilizing the corrected data, there is shown in Figure 11 the probability of a bubble not being formed under one typical condition of strain as a function of time. To calculate the ordinate of this figure, the probability of a bubble forming up to a given time was approximated by the ratio of the number of trials with supersaturation times less than that of, but including, the trial in question to the total number of trials. This approach to the evaluation of probability leaves much to be desired (17,18) but affords a simple means of presenting the nature of supersaturation phenomena. As was indicated earlier the confidence limits for such an analysis are poor with the small number of investigations reported here for each set of conditions. A straight line was fitted to the data shown by the points of Figure 11 by the method of least squares. In accordance with Equation 8, the line should pass through the origin with a slope equal to the negative reciprocal of

the mean time. The intercepts and slopes were compared with "Student's t test" (50) and no significant difference was found. The standard deviation of the times from the mean time was computed and is shown in Table III. The agreement is good for the number of points involved. A "chi squared test" (50) of the frequency of occurrence of points within various intervals does not indicate any significant discrepancy between the data and the theoretical distribution, but it does point up the need for a large amount of data under constant conditions. These results indicate that the proposed distribution is followed by these data and indicate that the formation of bubbles is random with respect to time as was predicted from the theory of liquids (19).

Utilizing the data of Table III, the probability of a bubble forming as a function of time for a given degree of strain is shown in Figures 12 and 13. The rather poor confidence limits described earlier apply to the information of these figures. For this reason rather wide disagreements from such prediction are to be encountered for a particular case.

The data obtained with the isochoric equipment involved nearly 21 times the volume of n-pentane and nearly 4 times the surface area that was employed in the investigation with the heated thimble equipment. Each set of measurements was corrected to a unit volume basis for inclusion in the summary of experimental data presented in

Tables I and II. It is of interest to note that after making this correction there is little to choose in a statistical sense between the experimental data from the two pieces of equipment. The data from the two types of equipment are in rough agreement when compared on a unit volume basis. The data are insufficient in number to establish the effect of surface on bubble formation.

These preliminary results serve to indicate that a large number of experimental trials are required for the determination of the statistical behavior of supersaturated hydrocarbon liquids. Furthermore, the data of Figure 13 indicate a marked shift in the probability function as the temperature increases. The probability of a bubble being formed at a given degree of supersaturation was much greater for a particular time of strain at 280° F. than was the case at 160° F. It remains for further experimental work to establish whether or not these trends which have been indicated by this limited study are reflected in the general behavior of supersaturated hydrocarbon liquids.

#### ACKNOWLEDGMENT

This work was a contribution from Research Project 37 of the American Petroleum Institute at the California Institute of Technology. H. H. Reamer and W. M. DeWitt contributed to the experimental program while Virginia Berry and Betty Kendall aided in the preparation of the results in a form suitable for publication. W. N. Lacey reviewed the manuscript.

LITERATURE CITED

1. Akhumov, E. I., and Rozen, B. Ya., Zhur. Fiz. Khim. (USSR) 27, 1760 (1953).
2. Arley, N., and Buch, K. R., "Introduction to the Theory of Probability and Statistics," John Wiley and Sons, Inc., New York, 1950.
3. Briggs, L. J., J. Appl. Phys., 21, 721 (1950).
4. Budgett, H. M., Proc. Roy. Soc., (London) A86, 25 (1912).
5. Burrows, G., and Preece, F. H., Trans. Inst. Chem. Engrs., (London) 32, 99 (1954).
6. Carmichael, L. T., and Sage, B. H., Ind. Eng. Chem., 44, 2728 (1952).
7. Dahler, J. S., and Hirschfelder, J. O., Technical Report WIS-ONR-12, University of Wisconsin, 15 October 1954.
8. Dahler, J. S., and Hirschfelder, J. O., Technical Report WIS-ONR-15, University of Wisconsin, 3 January 1955.
9. Dixon, H. H., Sci. Proc. Roy. Dublin Soc., 14, N. S. No. 16, 229 (1914).
10. Faro, I., Small, T. R., and Hill, F. K., J. Appl. Phys., 23, 40 (1952).
11. Fry, T. C., "Probability and Its Engineering Uses," D. Van Nostrand Co., Inc., New York, 1928.
12. Furth, R., Proc. Cambridge Phil. Soc., 37, 252 (1941).
13. Ibid., 276.
14. Gardescu, I. I., Oil Gas J., 30, No. 41, 22 (1931).
15. Gibbs, J. W., "Collected Works" Vol. I, Longmans Green and Co., New York, 1931.
16. Goranson, R. W., "Thermodynamic Relations in Multi-Component Systems," Carnegie Institution of Washington, Washington, D. C., 1930.
17. Gumbel, E. J. "Probability tables for the Analysis of Extreme Value Data," U.S. Department of Commerce, National Bureau of Standards AMS-22 Washington (1953).

18. Gumbel, E. J. "Statistical Theory of Extreme Values and Some Practical Applications," U.S. Department of Commerce, National Bureau of Standards, AMS-33 Washington (1954).
19. Hunt, E. B., Jr., private communication, January 8, 1954.
20. Jha, S. D., Kolloid-Z., 137, 162 (1954).
21. Kennedy, H. T., and Olson, C. R., Trans. Am. Inst. Mining Met. Engrs., 195, 271 (1952).
22. Khinchin, A. I., "Asymptotische Gesetze der Wahrscheinlichkeitsrechnung," Chelsea Publishing Co., New York, 1948.
23. Kirkwood, J. G., J. Chem. Phys., 18, 380 (1950).
24. Lennard-Jones, J. E., and Devonshire, A. F., Proc. Roy. Soc., (London) A163, 53 (1937).
25. Liepmann, H. W., Z. angew. Math. u. Phys., 3, 321, 407 (1952).
26. Marboe, E. C., and Weyl, W. A., J. Soc. Glass Technol., 32, 281 (T) (1948).
27. McLelland, C. H., and Williams, T. W., Natl. Advisory Comm. Aeronaut. Tech. Note 3302, October, 1954.
28. Meyers, C. H., Bur. Standards J. Research, 9, 807 (1932).
29. Mood, A. M., "Introduction to the Theory of Statistics," McGraw-Hill Book Co., Inc., New York, 1950.
30. Ibid., Chap. 13.
31. Myer, J., Z. Elektrochem., 17, 743 (1911).
32. Parkin, B. R., and Kermeen, R. W., Hydrodynamics Laboratory, California Institute of Technology, Report No. E-35.2, December, 1953.
33. Plesset, M. S., J. Appl. Mechanics, 16, 277 (1949).
34. Reamer, H. H., and Sage, B. H., Rev. Sci. Instr., 24, 362 (1953).
35. Rice, S. O., Bell System Tech. J., 23, 282 (1944); 24, 46 (1945).



36. Rossini, F. D., et al., "Selected Values of the Physical and Thermodynamic Properties of Hydrocarbons and Related Compounds," Carnegie Press, Pittsburgh, 1953.
37. Sabersky, R. H., and Gates, C. W., Jr., Jet Propulsion, 25, 67 (1955).
38. Sage, B. H., and Lacey, W. N., Trans. Am. Inst. Mining Met. Engrs., 136, 136 (1940).
39. Sage, B. H., and Lacey, W. N., "Thermodynamic Properties of the Lighter Paraffin Hydrocarbons and Nitrogen," 1950.
40. Sander, A., and Damköhler, G., Naturwissenschaften, 31, 460 (1943). Translation Natl. Advisory Comm. Aeronaut. Tech. Mem. 1368, November, 1953.
41. Schlinger, W. G., and Sage, B. H., Ind. Eng. Chem., 42, 2158 (1950).
42. Temperley, H. N. V., Proc. Phys. Soc., (London) 58, 436 (1946).
43. Temperley, H. N. V., and Chambers, L. G., Proc. Phys. Soc., (London) 58, 420 (1946).
44. Tolman, R. C., J. Chem. Phys., 17, 333 (1949).
45. Tovbin, M. V., and Krasnova, S. I., Zhur. Fiz. Khim. (USSR) 25, 161 (1951).
46. Vincent, R. S., Proc. Phys. Soc., (London) 53, 126 (1941).
47. Ibid., 55, 41 (1943).
48. Wilks, S. S., "Mathematical Statistics," Princeton University Press, Princeton, 1943.
49. Williams, J. A., and Little D. J., Trans. Inst. Chem. Engrs., (London) 32, 174 (1954).
50. Youden, W. J., "Statistical Methods for Chemists," Chap. 5, John Wiley and Sons, Inc., New York, 1951.

# NOMENCLATURE

A	frequency factor in Arrhenius rate expression
b	specific gas constant
d	differential operator
e	base of natural logarithm
k	parameter in Poisson distribution
$\ln$	natural logarithm
n	statistical sample size
$\dot{n}_b$	rate of bubble formation, bubbles/sec. cu.ft.
P	pressure lb./sq.in.
$P_b$	bubble point pressure lb./sq.in.
$P_b - P^0$	fixed supersaturation pressure lb./sq.in.
$P_s$	supersaturation pressure lb./sq.in.
$\mathcal{P}$	probability of bubble being formed
Q	probability of bubble not being formed
T	temperature degrees Rankins
$\underline{w}$	work necessary to form stable spherical bubble, ft. lb. or Btu
$\alpha$	$\frac{16\pi\gamma^3}{3bT} \quad (\text{lb./sq.in.})^2$
$\beta$	correction factor
$\gamma$	interfacial tension lb./ft.
$\Delta$	difference
$\theta$	time, sec.
$\bar{\theta}$	mean time for first bubble to form, sec.
$\theta_b$	time of strain to first bubble, sec.

- $\theta_b^\circ$  time of strain to first bubble adjusted to fixed supersaturation pressure ( $P_b - P^0$ ), sec.
- $\bar{\theta}_b$  mean time to first bubble for specific conditions, sec.
- $(\theta_b)_c$  corrected time to first bubble for non-isobaric conditions of strain, sec.
- $\bar{\theta}_m$  mean time corresponding to a given value of supersaturation pressure, sec.
- $\mu$  statistical mean
- $\sigma'$  standard deviation

Superscript

time average of quantity during run

## LIST OF FIGURES

1. Schematic Arrangement of Equipment
2. Pressure-Temperature Diagram for n-Pentane
3. Arrangement of Associated Equipment
4. Sectional View of Pressure Vessel
5. Details of Shaft-Cylinder Combination
6. Sample of Experimental Results with Isochoric Equipment
7. Supersaturation Pressure for n-Pentane as a Function of Time
8. Experimental Results with Heated Thimble Equipment
9. Effect of Strain upon Duration of Supersaturation
10. Applicability of Arrhenius Equation to Supersaturation
11. Probability of a Bubble Not Being Formed
12. Probability of a Bubble Being Formed in Heated Thimble Equipment
13. Probability of a Bubble Being Formed in Isochoric Equipment

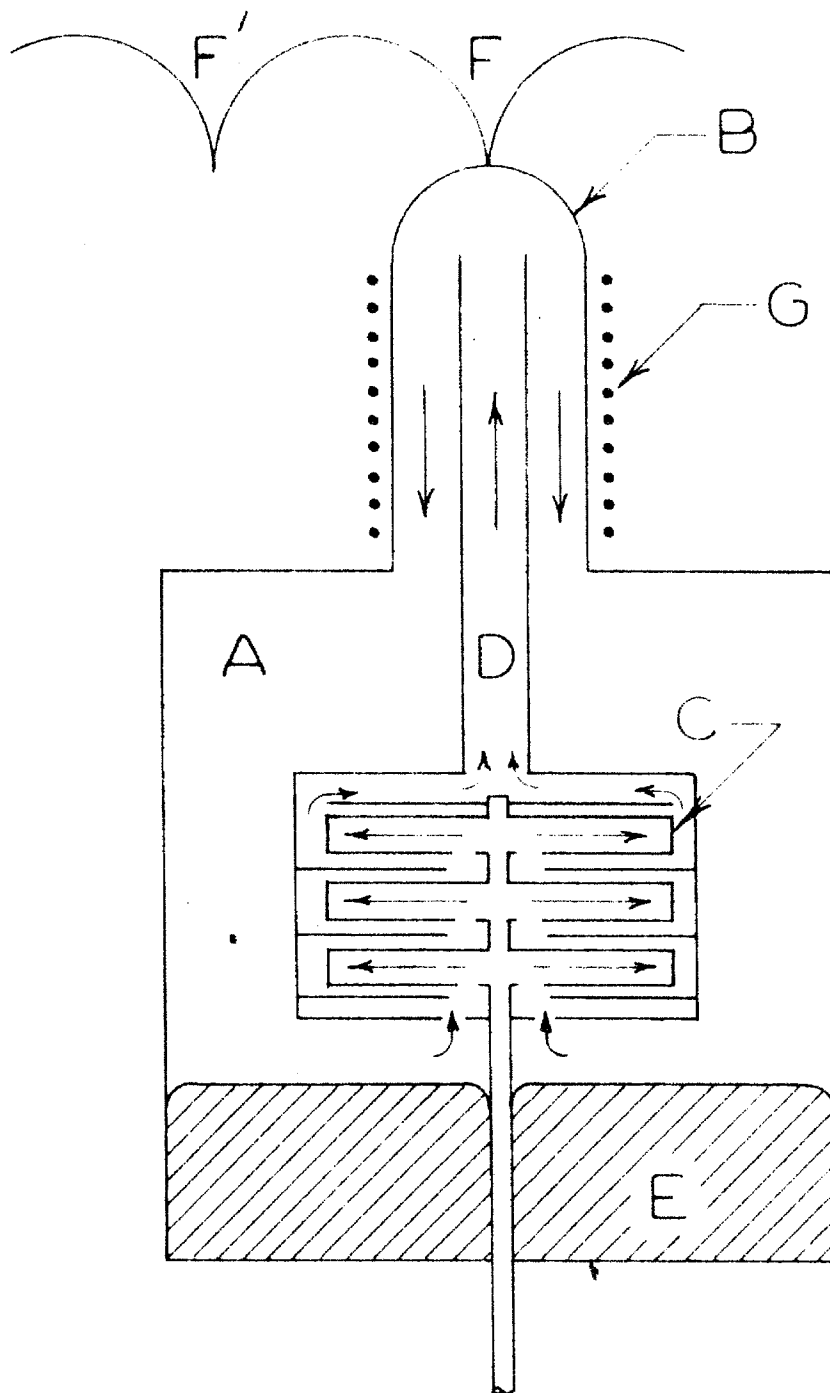


Figure 1. Schematic Arrangement of Equipment

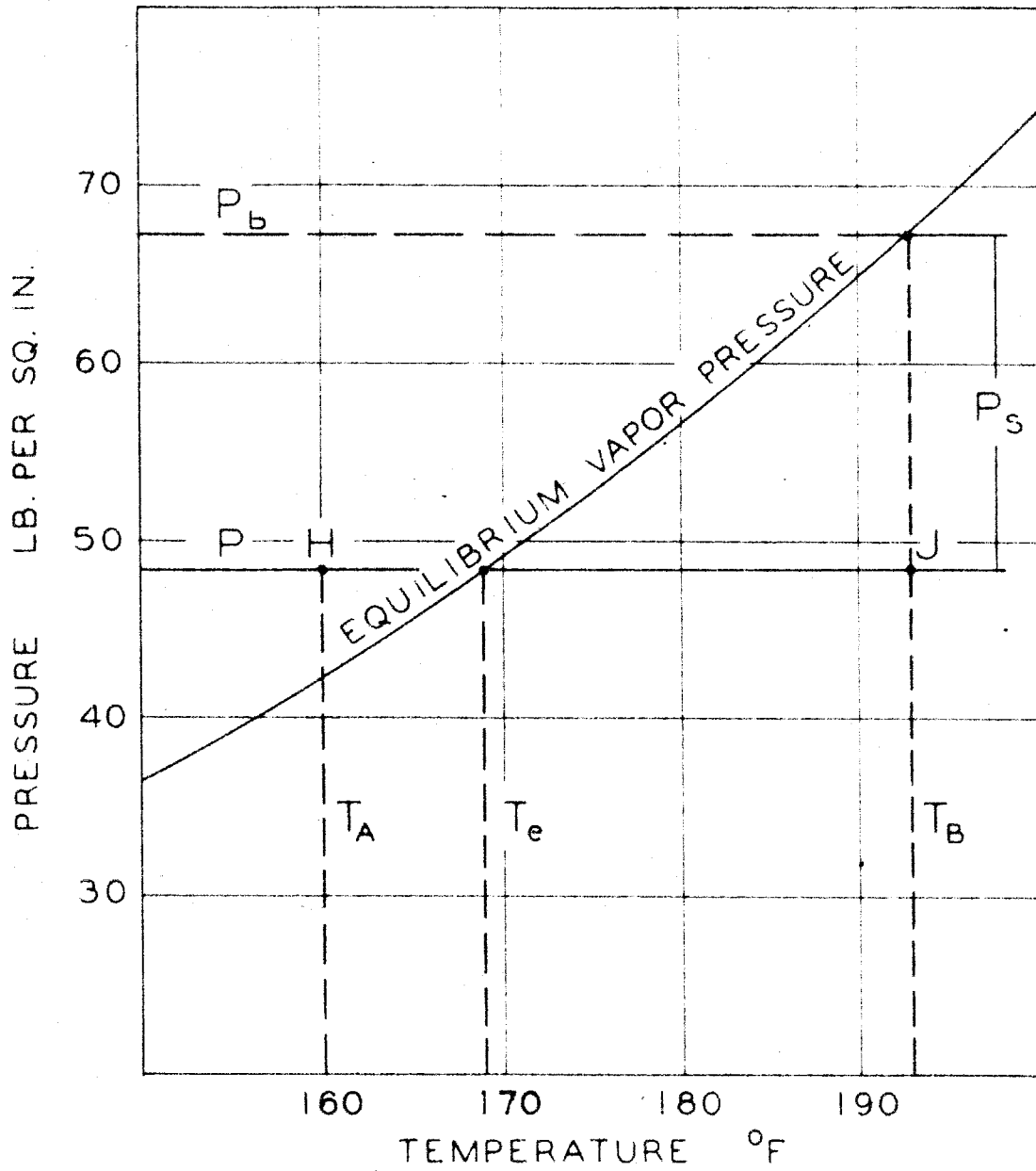


Figure 2. Pressure-Temperature Diagram for n-Pentane



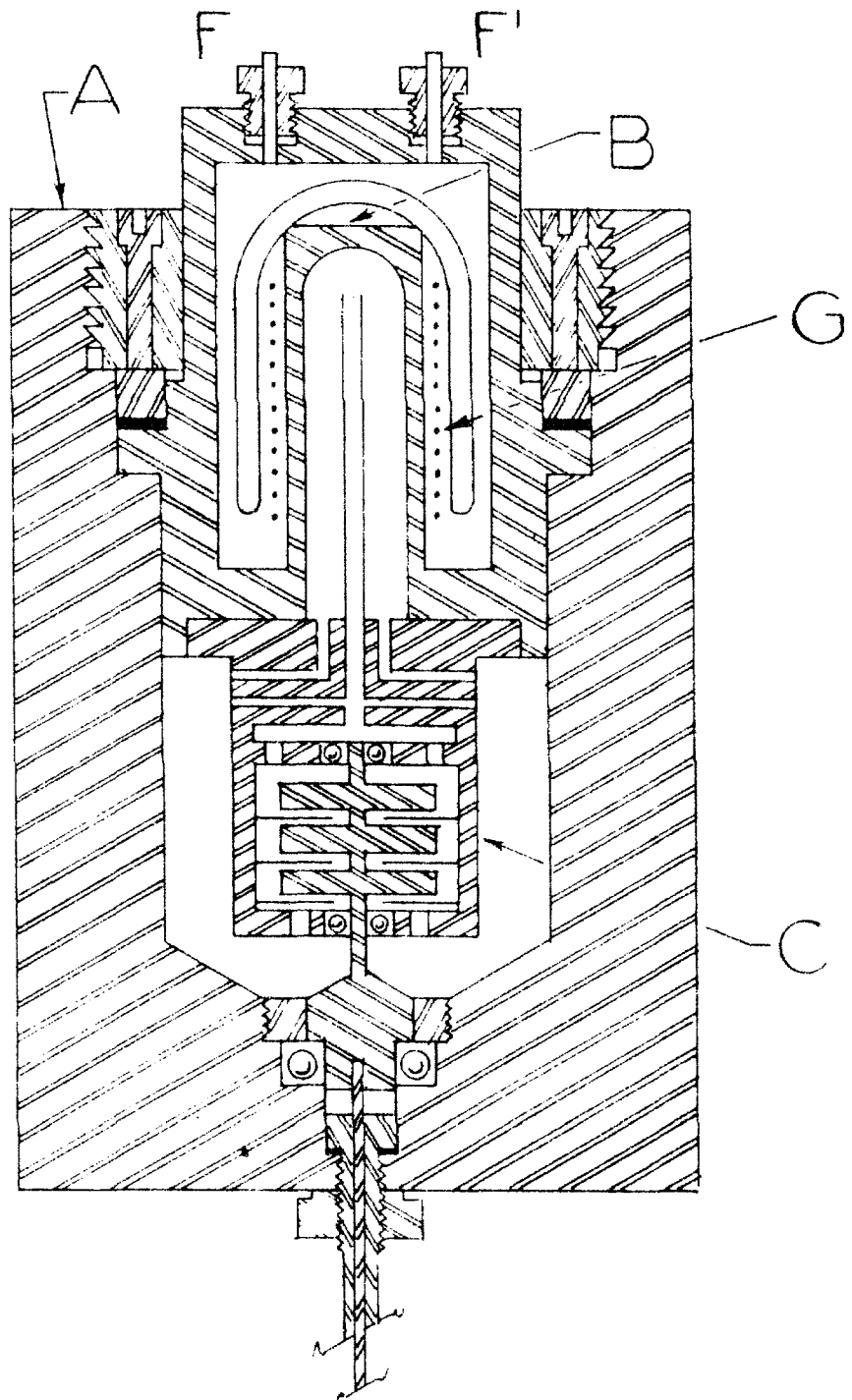


Figure 4. Sectional View of Pressure Vessel



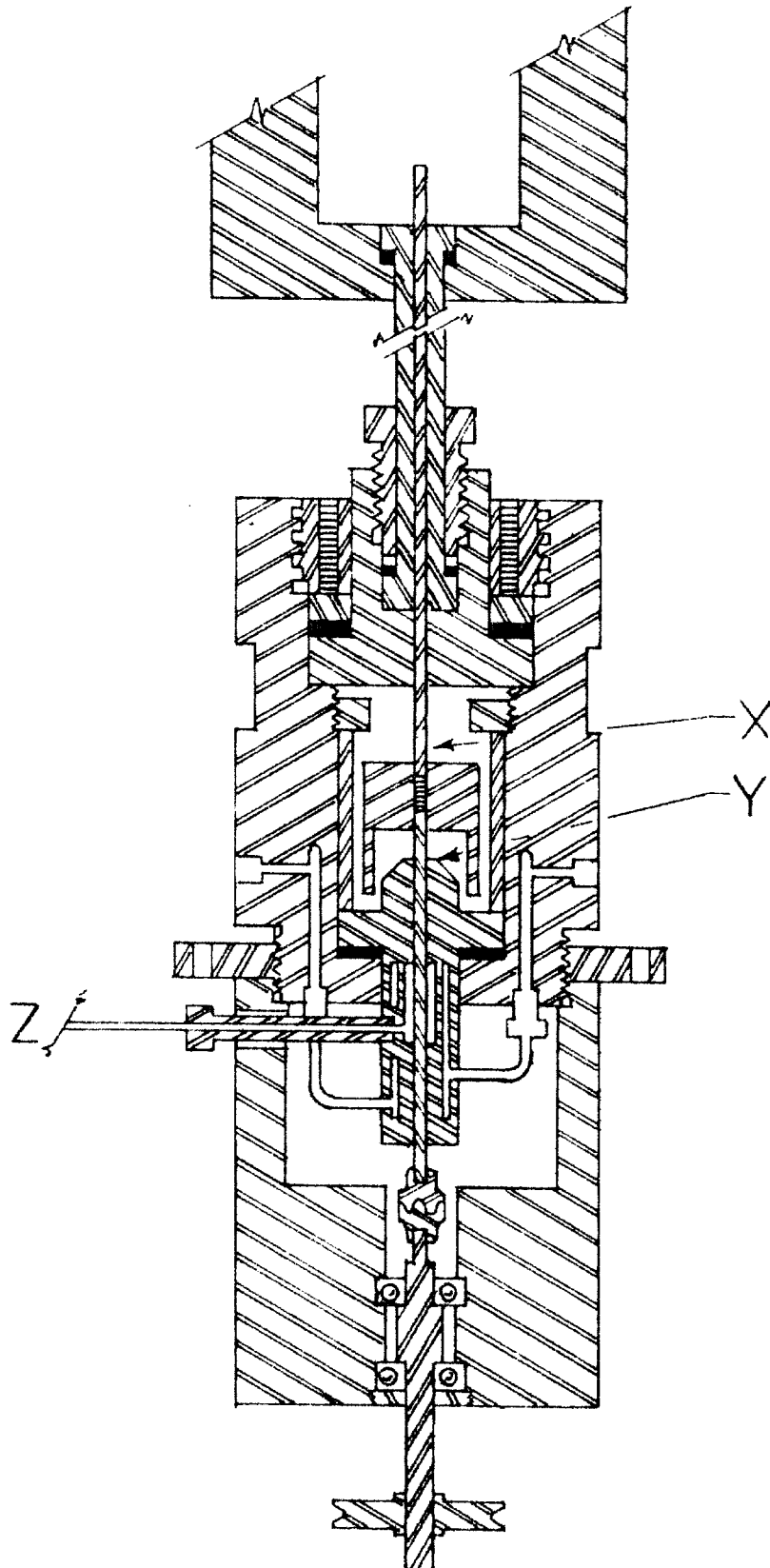


Figure 5. Details of Shaft-Cylinder Combination

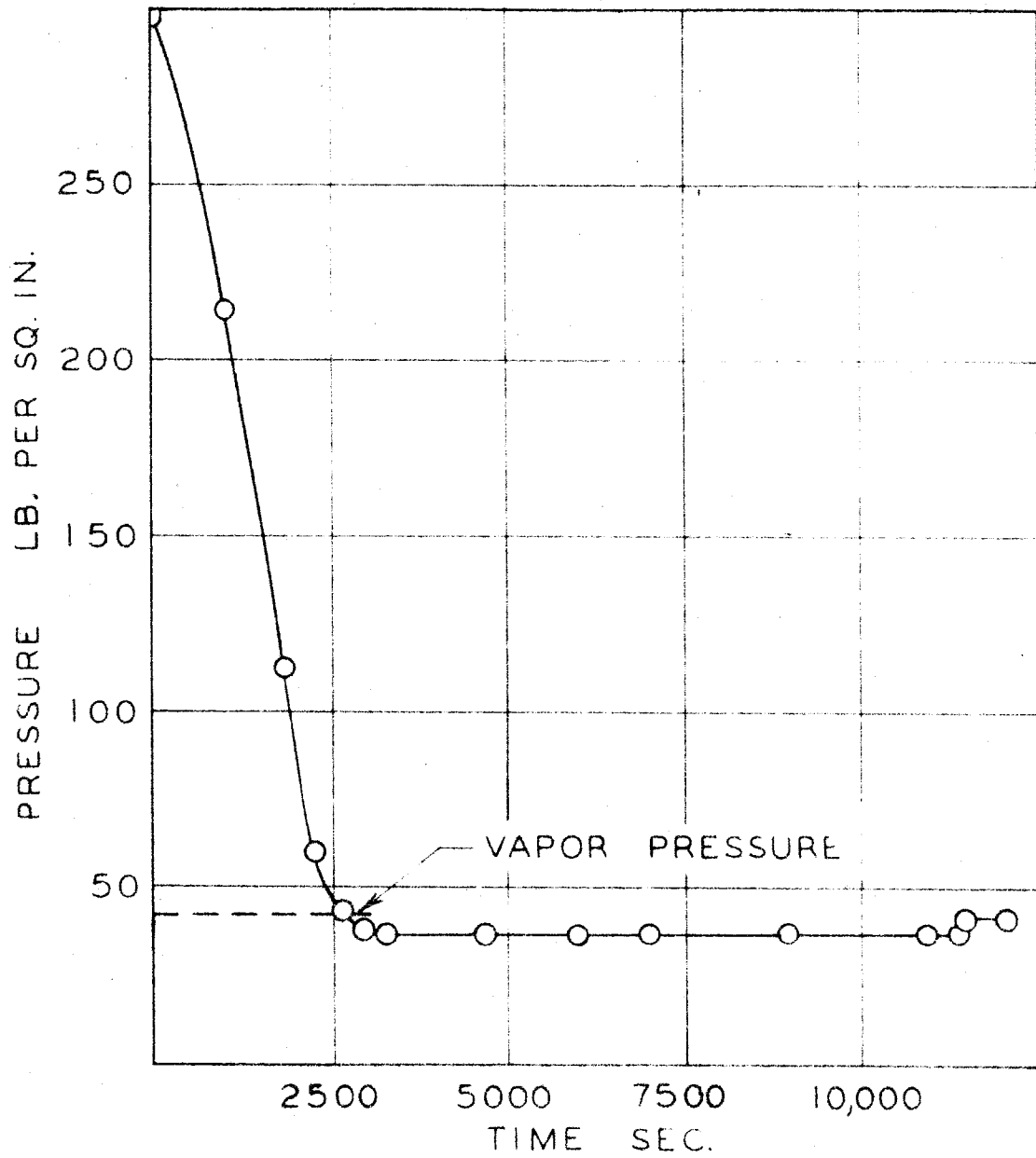


Figure 6. Sample of Experimental Results with Isochoric Equipment

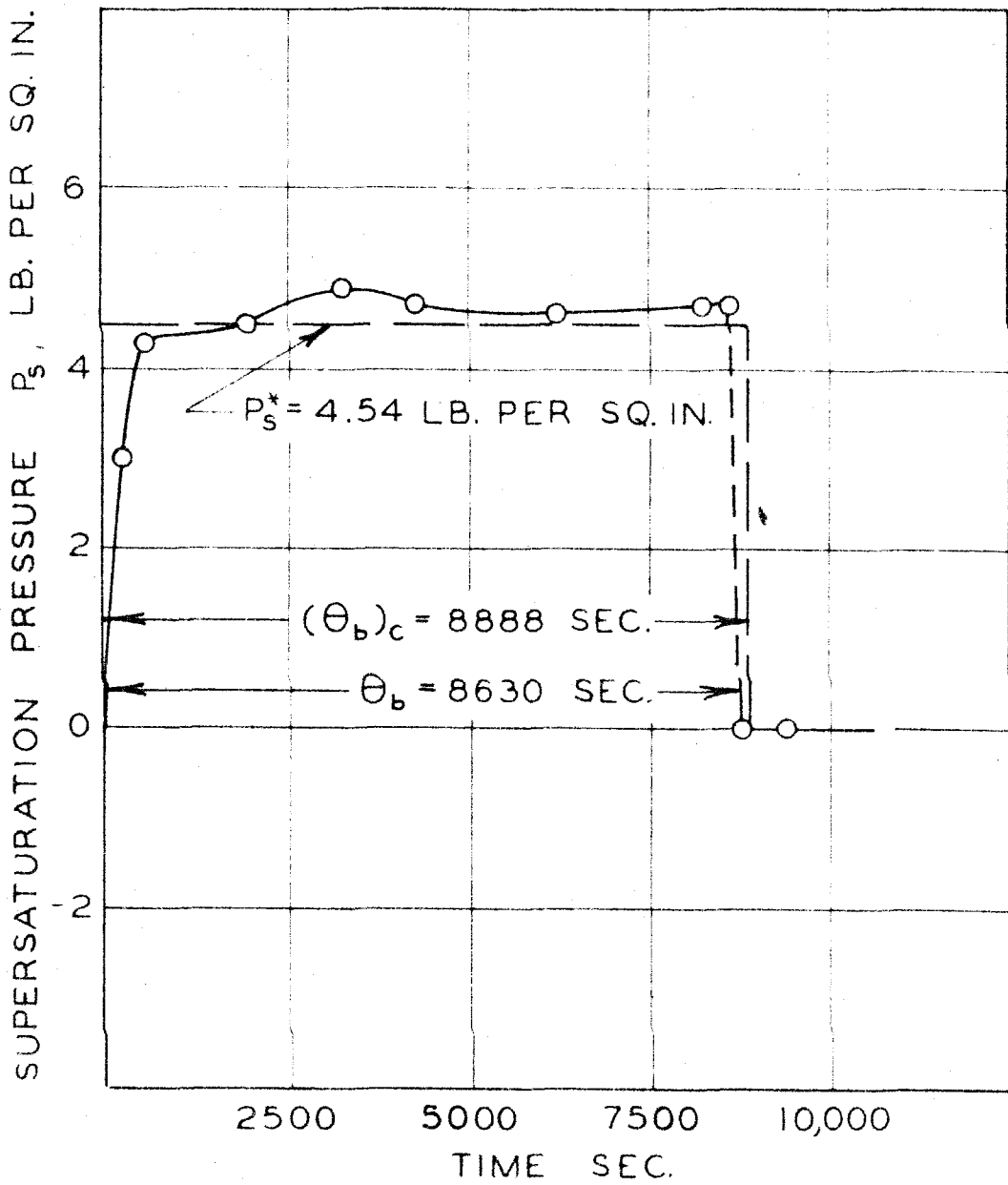


Figure 7. Supersaturation Pressure for n-Pentane as a Function of Time

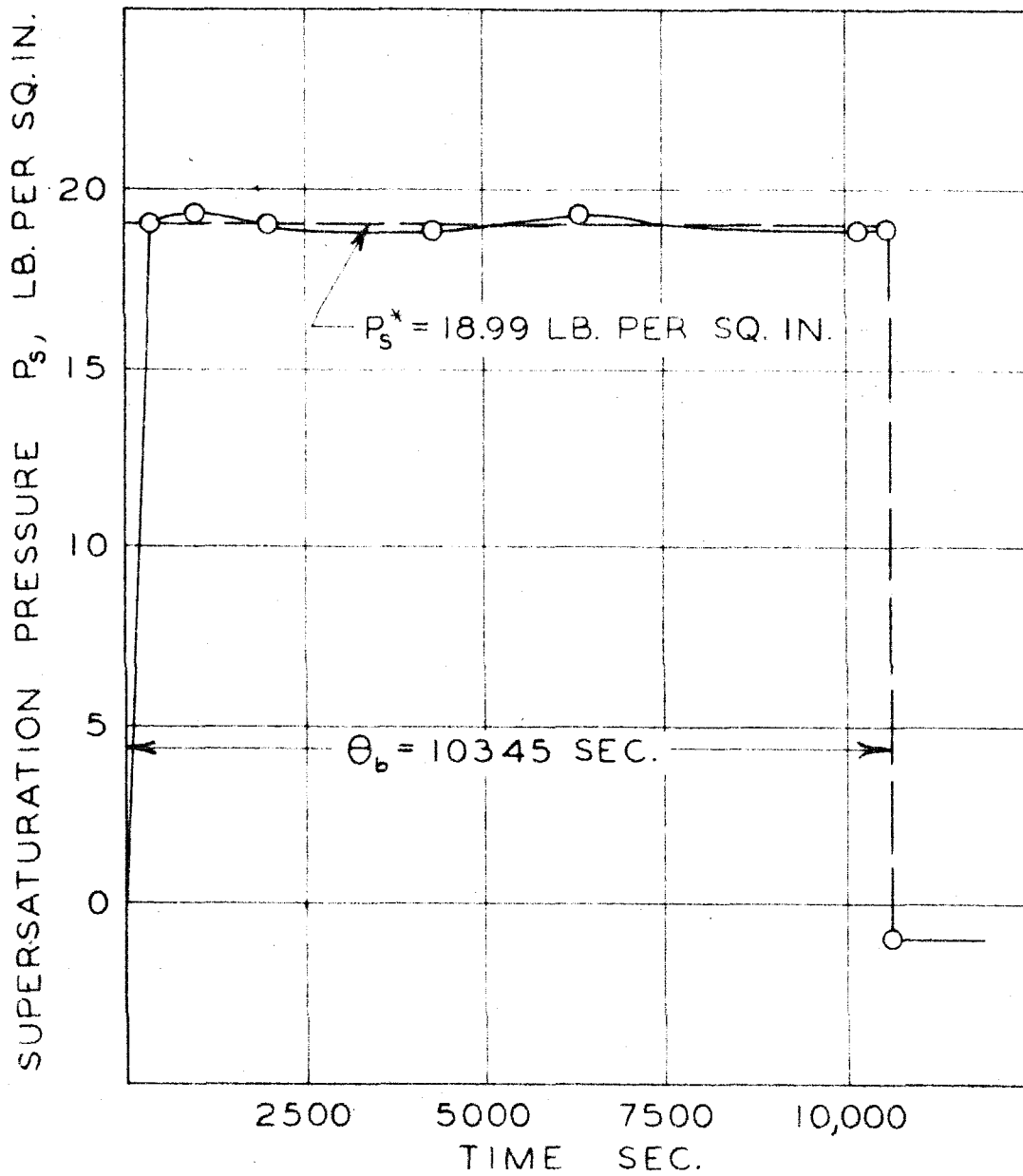


Figure 8. Experimental Results with Heated Thimble Equipment

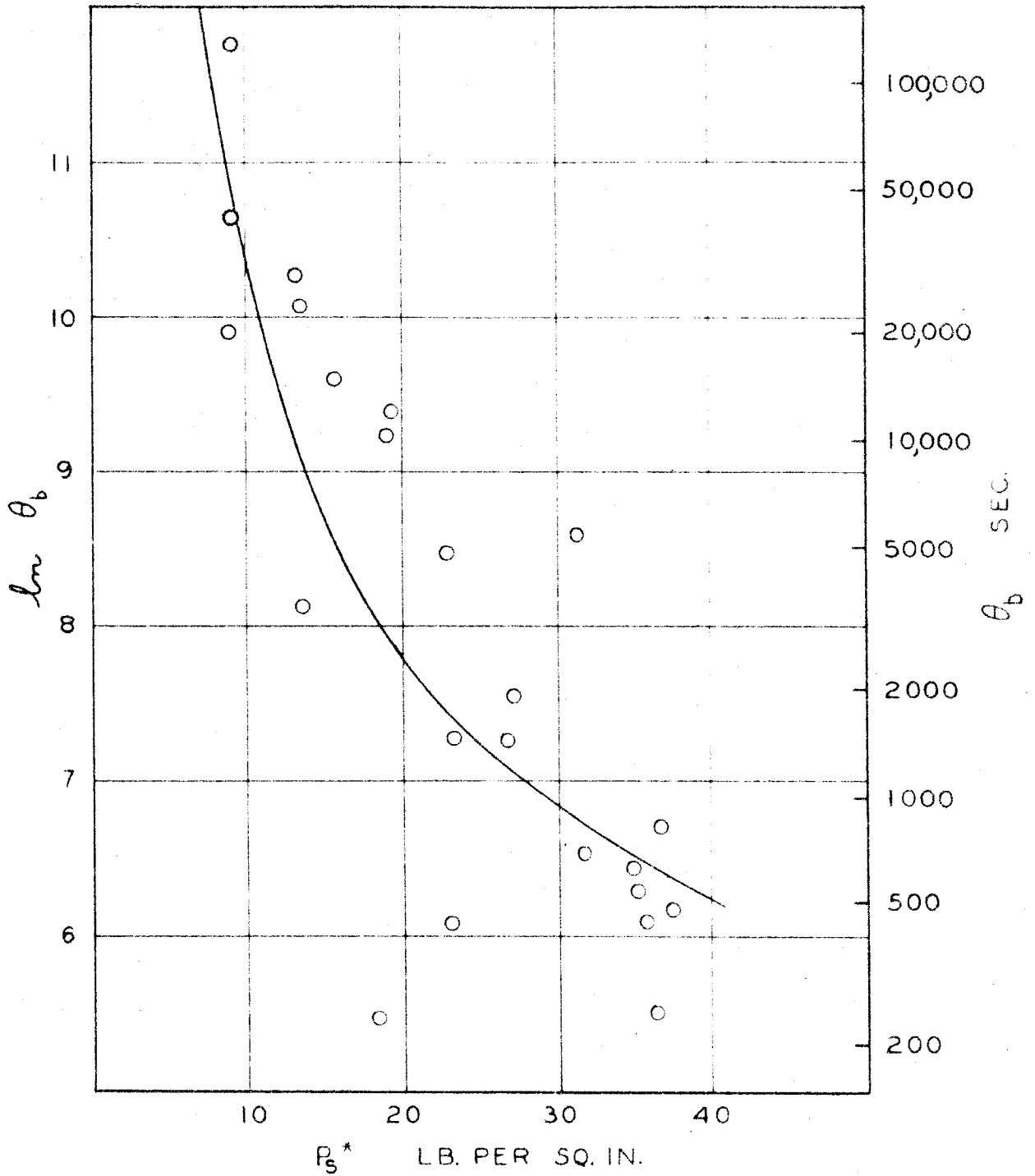


Figure 9. Effect of Strain upon Duration  
of Supersaturation

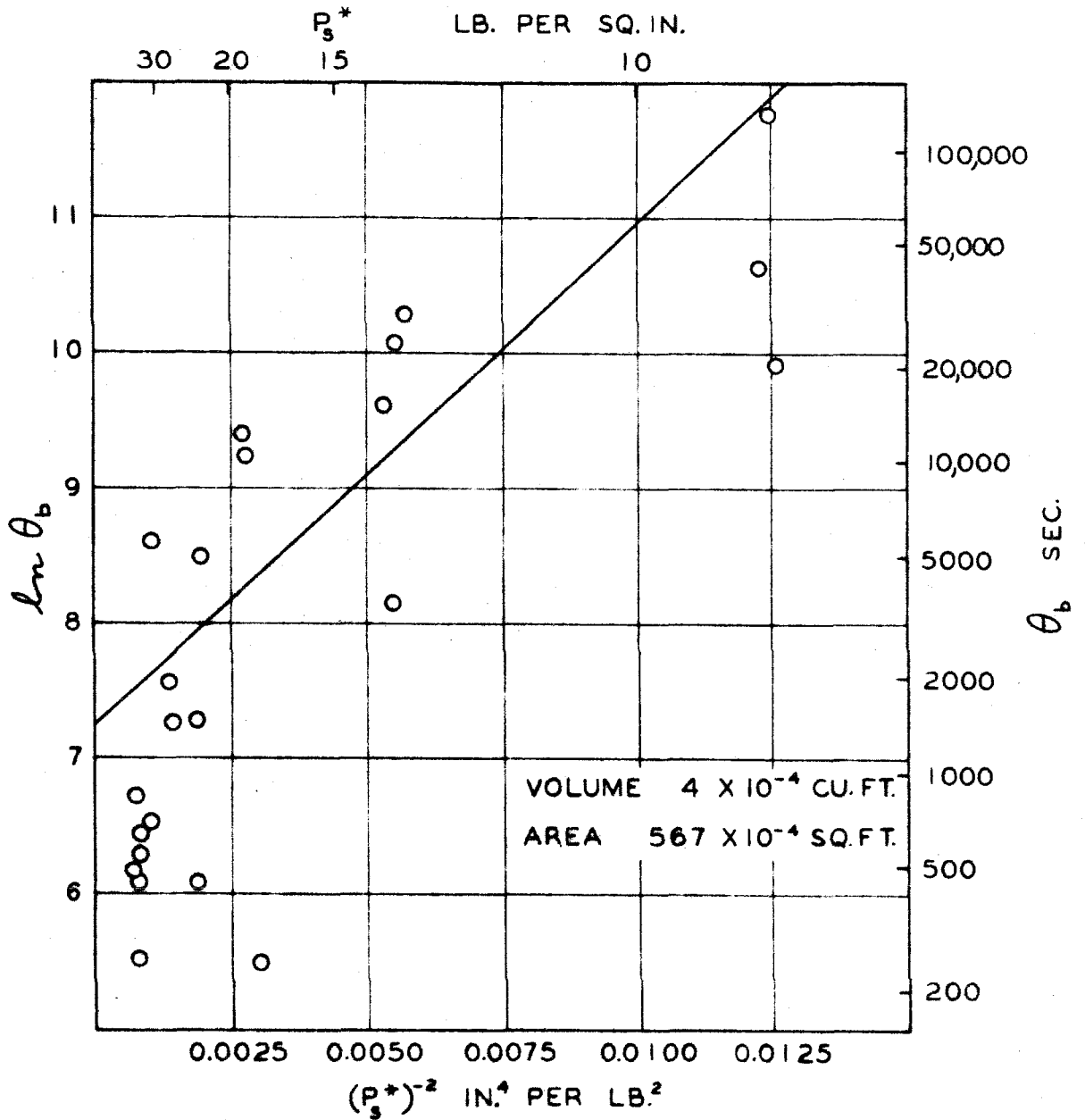


Figure 10. Applicability of Arrhenius Equation to Supersaturation

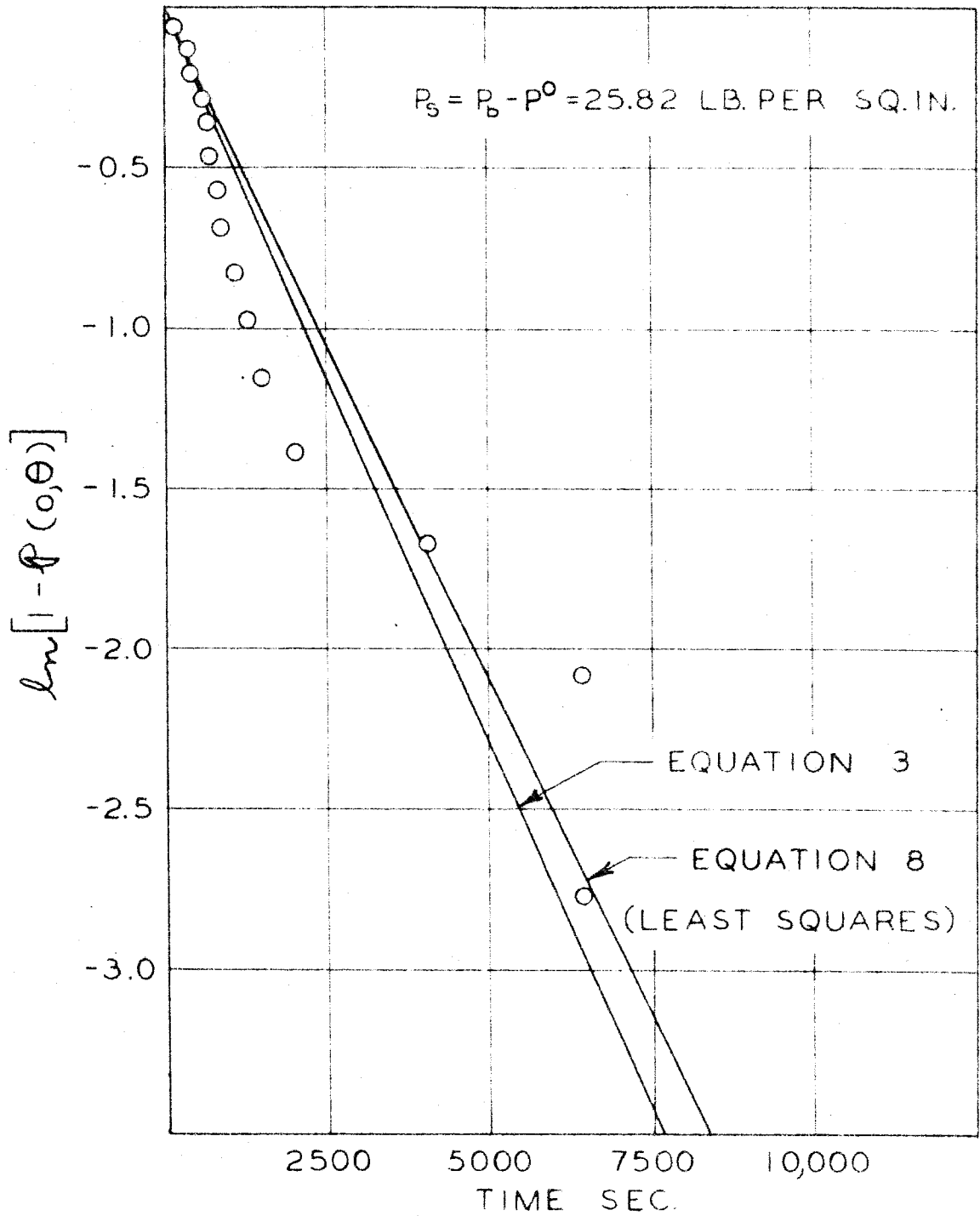


Figure 11. Probability of a Bubble Not Being Formed

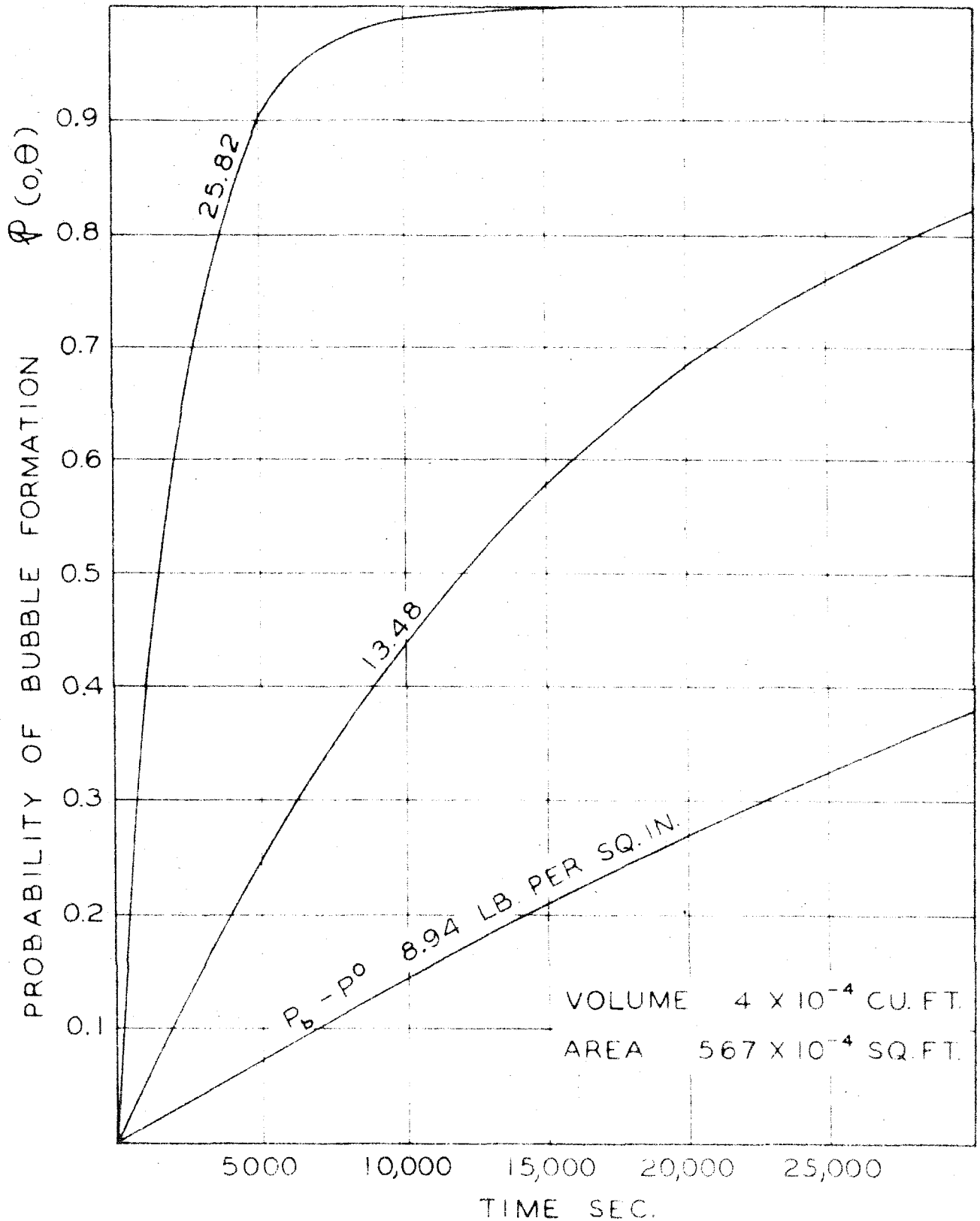


Figure 12. Probability of a Bubble Being Formed in  
Heated Thimble Equipment



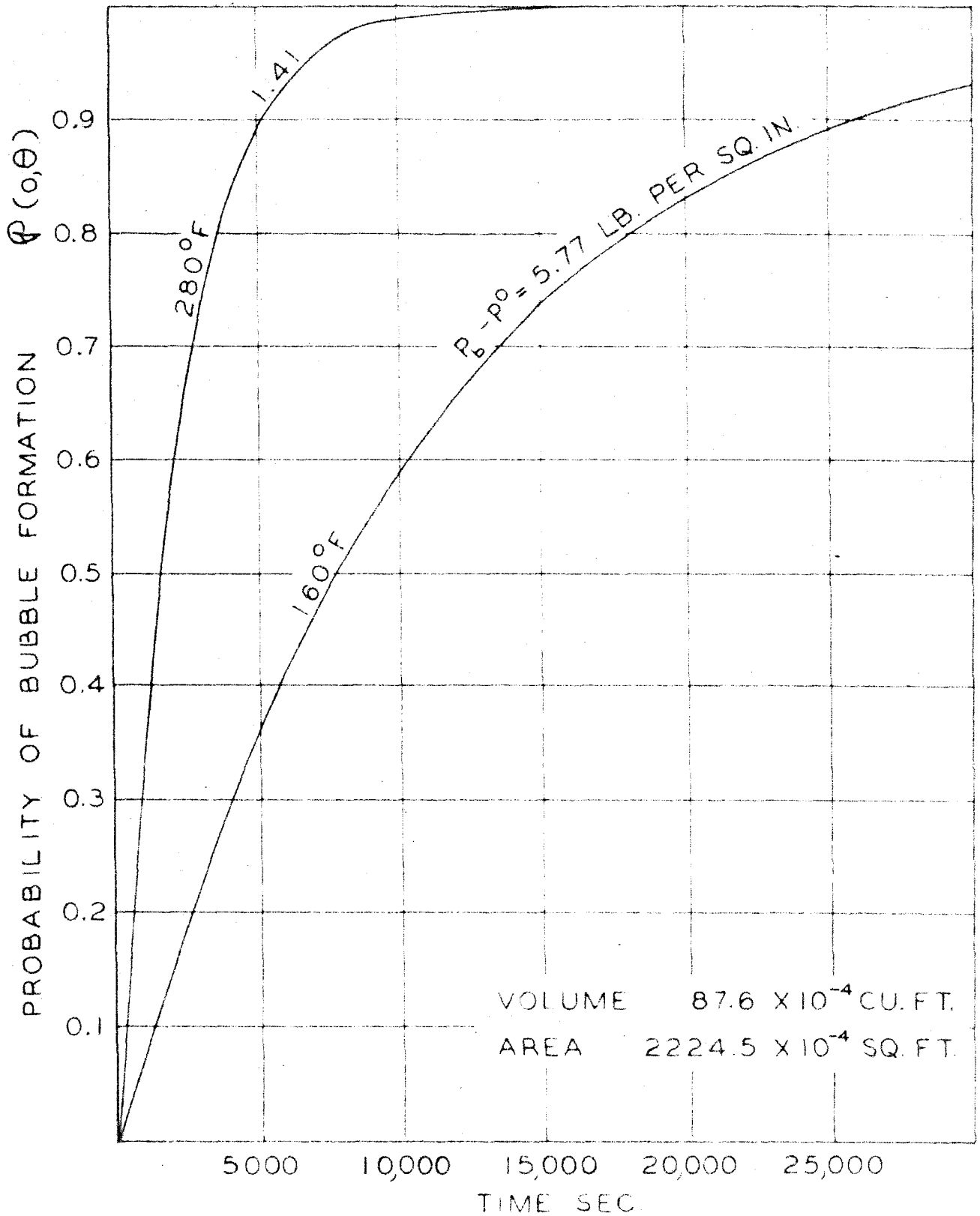


Figure 13. Probability of a Bubble Being Formed in Isochoric Equipment

## LIST OF TABLES

- I. Summary of Experimental Results for n-Pentane in Isochoric Equipment
- II. Summary of Experimental Results for n-Pentane in Heated Thimble Equipment
- III. Comparison of Predicted and Experimental Standard Deviations

TABLE I. SUMMARY OF EXPERIMENTAL RESULTS FOR n-PENTANE IN ISOCHORIC EQUIPMENT

Identification	Number of Experimental Points	Supersaturation Pressure	Standard Deviation	Bubble Formation Time	Correction Factor	Rate of Bubble Formation
		Lb./Sq. Inch	Lb./Sq. Inch	Sec.		Bubbles/Sec. Cu.Ft.
160° F.						
9218	5	2.767 <sup>a</sup>	0.4274	4425	1.0106	0.026
9220	14	4.040	0.5255	16319	1.0125	0.007
9226	8	4.542	0.6189	8630	1.0299	0.013
9228	4	6.034	1.8726	4730	1.2469	0.019
9230	7	5.709	0.5436	9315	1.0191	0.012
9232	6	6.034	2.5914	4155	1.1336	0.024
9234	6	7.354	0.8679	6420	1.0276	0.017
9236	13	6.766	0.2498	17040	1.0018	0.007
9238	13	7.553	0.6739	23300	0.9994	0.005
9242	16	4.520	1.0337	29820	0.9998	0.004
9246	4	16.322	5.6901	1710	0.9865	0.068
9252	14	14.506	0.7235	7185	1.0011	0.014
280° F.						
9268	6	1.548 <sup>a</sup>	0.6243	855	0.9930	0.133
9270	3	1.230	0.3554	1098	1.0980	0.104
9274	7	1.262	0.6628	4288	1.0066	0.027
9276	4	2.002	0.7292	3563	1.1802	0.032
9278	6	1.261	0.6068	2750	1.1364	0.042
9280	6	1.555	0.4716	3157	1.0000	0.036
9282	3	1.314	0.2924	1481	1.1052	0.077
9284	4	1.611	0.6884	994	0.9803	0.115

<sup>a</sup> Average supersaturation pressure

TABLE II. SUMMARY OF EXPERIMENTAL RESULTS FOR n-PENTANE IN  
HEATED THIMBLE EQUIPMENT

Identi- fication	Number of Experimental Points	Supersaturation Pressure	Standard Deviation	Bubble Formation Time	Rate of Bubble Formation
		Lb./Sq. Inch	Lb./Sq. Inch	Sec.	Bubbles/Sec. Cu.Ft.
160° F.					
19078	2	18.29 <sup>a</sup>	0.0000	242	10.054
19078	28	13.21	0.5653	29265	0.083
19082	7	18.99	0.2286	10345	0.235
19082	14	13.74	0.4930	14854	0.164
19086	7	19.23	0.2673	12023	0.202
19086	23	13.47	0.3376	23735	0.103
19090	2	23.05	0.0000	437	5.568
19090	17	8.91	0.4050	20062	0.121
19096	3	23.14	0.0000	1457	1.670
19102	21	9.02	0.1844	41250	0.059
19104	3	22.78	0.8520	4805	0.506
19104	64	8.96	0.4405	126900	0.019
19107	3	26.56	0.1155	1418	1.716
19107	2	27.04	0.7778	1899	1.281
19107	3	13.51	0.2754	3414	0.713
19114	5	31.34	1.0663	5454	0.446
19118	1	31.65	0.0000	682	3.568
19120	2	36.27	0.2121	246	9.891
19120	2	37.42	0.7071	480	5.069
19130	2	35.10	0.2828	540	4.506
19130	2	36.75	0.0707	823	2.956
19135	2	35.57	0.1442	442	5.505
19135	2	34.92	0.7071	624	3.899

<sup>a</sup> Average supersaturation pressure.

TABLE III. COMPARISON OF PREDICTED AND EXPERIMENTAL STANDARD DEVIATIONS

Number of Points	Temperature ° F.	Supersaturation Pressure Lb./Sq.In.	Mean Time To First Bubble Sec.	Standard <sup>a</sup> Deviation Sec.	Rate of Bubble Formation	
					Bubbles/Sec. Cu.Ft.	Eq.(8)
Isochoric	12	5.77 <sup>b</sup> 1.41	11278	8521	0.010	0.011
	8		2262	1317	0.050	0.049
Heated Thimble	16	25.82 13.48 8.94	2177	2499	1.117	1.019
	4		17457	10354	0.139	0.132
	3		164485	57692	0.038	0.057

<sup>a</sup> Deviation from mean time<sup>b</sup> Fixed supersaturation pressure  $P_b - P^0$

II. SUPERSATURATION IN HYDROCARBON SYSTEMS

2. STATISTICAL PROCEDURES FOR SUPERSATURATION DATA

## INTRODUCTION

An apparatus for the measurement of rates of bubble formation in hydrocarbon systems is described elsewhere in this thesis together with the first data taken with the equipment. The description there of the numerical procedures for the handling of the data is necessarily brief. It is the purpose of this section of the thesis to elaborate upon these procedures and to consider possible additional methods. For the sake of clarity, the derivation of the distribution function of times for the first bubble to form which was presented in the preceding part of this thesis is reproduced here in slightly extended form.

The present treatment is based upon a simple picture of the mechanism of bubble formation (5) and follows the suggestions of Hunt (4). In a supersaturated solution, that is, a liquid which is at a pressure which is less than the bubble point pressure, there is a critical size of bubble, generally microscopic. If a bubble is formed in the liquid which is less than this critical size, the bubble will collapse. If the bubble is larger than the critical size it will grow until equilibrium is attained. These bubbles are created by local fluctuations in the state properties of the system. Thus a supersaturated solution will remain in a non-equilibrium state until a fluctuation occurs which is of sufficient magnitude to

form a bubble of critical size. Since these fluctuations are random, the formation of bubbles should be randomly distributed in time.



# THE BASIC DISTRIBUTION FUNCTION

Without any assumption with regard to the effect of surface or volume on the rate of bubble formation, it is postulated that the probability of a bubble forming in any given time interval in a fixed system is the same for all time intervals of the same size. Data points distributed in such a manner are referred to as "individually at random" (2). In an idealized situation where the formation of a bubble does not affect the probability of another bubble forming (not attained experimentally in this work), the probability of bubbles forming in a given time interval is independent of the number of bubbles forming in any other time interval which does not intersect the given interval. Such a set of data points is said to be distributed "collectively at random" (2). For points distributed individually and collectively at random, the probability of  $n$  points lying within a subinterval of length is given by the Poisson distribution (2)

$$P_n(0, \theta) = \frac{(k\theta)^n}{n!} e^{-k\theta} \quad (1)$$

where  $k\theta$  is the expected number of bubbles formed within the time interval. The probability of no bubbles forming in the interval from 0 to  $\theta$  may be established from

$$P_0(0, \theta) = e^{-k\theta} \quad (2)$$

Equation 2 has a simple interpretation. The quantity represents the probability of no bubble forming in a time interval of unit length. Since this probability is the same for all unit intervals, the probability of no bubble forming up to time  $\theta$  is  $(e^{-k})^\theta$  or  $e^{-k\theta}$ . This result follows directly from the postulate that the bubbles are distributed "individually at random." Under the experimental conditions herein reported only the first bubble is of interest and so the collective randomness postulate is not pertinent.

The probability of no bubbles forming up to  $\theta$ , as given by equation 2 is equal to the probability of the first bubble forming at some time later than  $\theta$ , and so

$$e^{-k\theta} = \int_{\theta}^{\infty} f(\theta) d\theta = 1 - \int_0^{\theta} f(\theta) d\theta \quad (3)$$

where  $f(\theta)$  is the distribution function of times for the first bubble to form. The second equality follows directly from the definition of a distribution function. Upon differentiation, equation 3 yields

$$-ke^{-k\theta} = -f(\theta) \quad (4)$$

$$f(\theta) = ke^{-k\theta} \quad (5)$$

The mean time for the first bubble to form is given by

$$\bar{\theta} = \int_0^{\infty} \theta f(\theta) d\theta = \int_0^{\infty} k\theta e^{-k\theta} d\theta = \frac{1}{k} \quad (6)$$

The variance is

$$\begin{aligned} \sigma^2 &= \int_0^{\infty} (\theta - \bar{\theta})^2 f(\theta) d\theta = \int_0^{\infty} (\theta^2 - 2\theta\bar{\theta} + \bar{\theta}^2) f(\theta) d\theta \\ &= k\left(\frac{2}{k^3}\right) + \frac{1}{k^2} - \frac{2}{k^2} = \frac{1}{k^2} \end{aligned} \quad (7)$$

The standard deviation is therefore

$$\sigma = \frac{1}{k} \quad (8)$$

Under conditions in which the formation of the first bubble does not affect the probability of the formation of another bubble (this situation may be approximated in an oil field), the reciprocal of the mean time for the first bubble to form is the rate of bubble formation for the given volume

$$\dot{n}_b = \frac{1}{\bar{\theta}} = k \quad (9)$$

If the bubble forms at random throughout the volume of the sample, a rate of bubble formation per unit volume may be calculated by dividing  $\dot{n}_b$  by the volume of the sample.

The probability of no bubble forming in the interval from 0 to  $\theta$  is given by equation 2 as  $e^{-k\theta}$ . The probability

of the first bubble forming in this interval must then be

$$P(0, \theta) = 1 - e^{-k\theta} = 1 - e^{-\dot{m}_b \theta} \quad (10)$$

Rearrangement of equation 10 yields

$$\ln[1 - P(0, \theta)] = -\dot{m}_b \theta \quad (11)$$

In accordance with equation 11, a plot of  $\ln[1 - P(0, \theta)]$  versus  $\theta$  should yield a straight line with a slope equal to the negative reciprocal of the mean time.

As a first approximation, the Arrhenius equation may be applied to the rate of bubble formation.

$$\dot{m}_b = Ae^{-\frac{W}{RT}} \quad (12)$$

The exponential form arises from the equilibrium distribution of embryos derived from a consideration of the mechanism for embryo formation (7). The work necessary to form a bubble of critical size (the size past which the bubble will continue to grow) corresponds closely to an activation energy. An expression has been derived by Gibbs (3) for this work.

$$\frac{W}{RT} = \frac{16\pi\gamma^3}{3(P_b - P)^2} \quad (13)$$

The variation of surface tension with radius has been discussed (8) and the effect on the work expression was shown (1). From equations 12 and 13,

$$\ln \dot{m}_b - \ln A = -\frac{16\pi\delta^3}{3AT(P_b-P)^2} \quad (14)$$

or

$$\ln \bar{\theta}_b + \ln A = \frac{\alpha}{(P_b-P)^2} \quad (15)$$

It is desirable during the course of the experimental program to make groups of runs at various chosen degrees of supersaturation. As the supersaturation pressure could not be set exactly, equation 15 was used to adjust the data to a chosen degree of supersaturation by taking the factor to be constant from one point to another. For adjustments of the order of two pounds per square inch, equation 15 should be quite adequate; its validity over a much wider range has not been proved.

# REGRESSION ANALYSIS

In accordance with equation 15, the following hypothesis will be made:

$$\ln \frac{\mu_i}{a} = \frac{\alpha}{S_i^2} \quad ; \quad \mu_i = a e^{\alpha/S_i^2} \quad (16)$$

where  $S_i$  has been written for  $P_b - P$  and  $\mu_i$  for the  $\bar{\theta}$  corresponding to  $P_b - P$ . The density may be put in the form

$$f(t_i) = \frac{1}{\mu_i} e^{-t_i/\mu_i} \quad (17)$$

by denoting the time for the first bubble to form by  $t_i$ . Substitution of equation 16 into equation 17 yields

$$f(t_i) = \frac{1}{a} e^{-\alpha/S_i^2} e^{-(\frac{1}{a} t_i e^{-\alpha/S_i^2})} \quad (18)$$

The likelihood (6) is

$$L = \prod_{i=1}^n \frac{1}{a} e^{-\alpha/S_i^2} e^{-(\frac{1}{a} t_i e^{-\alpha/S_i^2})} \quad (19)$$

The logarithm of the likelihood has its maximum at the same point as does the likelihood and is simpler to maximize.

$$\begin{aligned} \ln L &= \sum_{i=1}^n \left[ (-\alpha/S_i^2) - \ln a - \frac{1}{a} t_i e^{-\alpha/S_i^2} \right] \\ &= -\sum_{i=1}^n \alpha/S_i^2 - n \ln a - \frac{1}{a} \sum_{i=1}^n t_i e^{-\alpha/S_i^2} \end{aligned} \quad (20)$$

By differentiating separately with respect to  $a$  and  $\alpha$  and setting both derivatives equal to zero the maximum may be located.

$$\frac{\partial \ln L}{\partial a} = -\frac{n}{a} + \frac{1}{a^2} \sum_{i=1}^n t_i e^{-\alpha s_i^{-2}} = 0 \quad (21)$$

Solving for  $a$

$$a = \frac{1}{n} \sum_{i=1}^n t_i e^{-\alpha s_i^{-2}} \quad (22)$$

$$\frac{\partial \ln L}{\partial \alpha} = -\sum_{i=1}^n s_i^{-2} + \frac{1}{a} \sum_{i=1}^n t_i s_i^{-2} e^{-\alpha s_i^{-2}} = 0 \quad (23)$$

$$a \sum_{i=1}^n s_i^{-2} = \sum_{i=1}^n t_i s_i^{-2} e^{-\alpha s_i^{-2}} \quad (24)$$

A combination of equations 22 and 24 results in

$$\sum_{i=1}^n t_i s_i^{-2} e^{-\alpha s_i^{-2}} = \frac{1}{n} \left( \sum_{i=1}^n t_i e^{-\alpha s_i^{-2}} \right) \left( \sum_{i=1}^n s_i^{-2} \right) \quad (25)$$

Equation 25 must be solved by a lengthy trial and error procedure; a value for  $\alpha$  is chosen and the sums are calculated. Different values for  $\alpha$  are tried until one is found for which equation 25 is satisfied. Equation 22 is then used to calculate the corresponding value for  $a$ .

### CONFIDENCE LIMITS

Two somewhat different methods for making a run have been considered. The most straightforward procedure is to continue a run until a bubble has formed and to record the time of the run. This is the method which was used to obtain the data reported herein. An alternative procedure is to select the total time for each run in a series and, at the end of this time, record only whether a bubble has formed or not; these results may be analyzed statistically by the use of the binomial distribution. The latter procedure has the advantage of simplifying the experimental program. Providing some estimate of the mean time is available, a cut-off time may be chosen which is convenient for the operation of the equipment. The former method has the important advantage of obtaining more information per run. Thus, if the same number of runs are made by each plan, a more accurate estimate of the mean will be obtained by allowing each run to go to completion, but the time involved for the runs will be much greater. For confidence intervals of the same length, the complete run program requires many fewer runs, and somewhat less total time for the runs. The preparation time for each run is at the disposal of the experimenter, but, since it might well be a significant variable and must be studied even-



tually as part of the experimental program,\* the preparation time may be of the order of the time for a run. For this reason it is an important advantage to keep the number of runs as low as possible, and so the complete run procedure was adopted.

The pertinent confidence intervals will be calculated in justification of the foregoing conclusions. The exact confidence intervals for the parameter of a binomial distribution has been given by Mood (6). The 95 percent confidence upper limit  $p_1$  is given by the value of  $p$  for which

$$\sum_{y=0}^l \binom{n}{y} p^y (1-p)^{n-y} = 0.025 \quad (26)$$

and the lower limit  $p_2$  is the value of  $p$  for which

$$\sum_{y=l}^n \binom{n}{y} p^y (1-p)^{n-y} = 0.025 \quad (27)$$

The value 0.025 was chosen so as to equalize the error at each end of the distribution. These partial binomial sums may be found by the use of Pearson's tables of the incomplete beta function since

$$\sum_{y=0}^l \binom{n}{y} p^y (1-p)^{n-y} = 1 - F(p; l, n-l-1) \quad (28)$$

---

\* Recently an investigation of both preparation time and procedure was inaugurated in connection with studies on the methane-n-decane system.

and

$$\sum_{y=l}^m \binom{m}{y} p^y (1-p)^{m-y} = F(p; l-1, m-l) \quad (29)$$

For large values of  $m$  beyond the range of Pearson's tables the normal approximation to the binomial distribution may be used. Again for the 95 percent confidence interval,

$$P\left[\hat{p} - 1.960 \sqrt{\frac{\hat{p}(1-\hat{p})}{m}} < p < \hat{p} + 1.960 \sqrt{\frac{\hat{p}(1-\hat{p})}{m}}\right] \cong 0.95 \quad (30)$$

where  $\hat{p}$  is the maximum likelihood estimator for  $p$  and is simply the fraction of successes (runs with bubble formation) found experimentally. The confidence interval for the parameter may be converted to a confidence interval for the rate of bubble formation by the use of equation 11; the result for equation 30 is

$$P\left[\frac{\ln\left\{1 - \hat{p} + 1.960 \sqrt{\frac{\hat{p}(1-\hat{p})}{m}}\right\}}{\ln\{1-\hat{p}\}} < \frac{\dot{m}_b}{\hat{m}_b} < \frac{\ln\left\{1 - \hat{p} - 1.960 \sqrt{\frac{\hat{p}(1-\hat{p})}{m}}\right\}}{\ln\{1-\hat{p}\}}\right] \cong 0.95 \quad (31)$$

In accordance with the central limit theorem (4) for a population with a finite variance  $\sigma^2$  and mean  $\mu$ , the distribution of the sample mean approaches the normal distribution with variance  $\frac{\sigma^2}{n}$  and mean  $\mu$  as the sample size

$m$  increases. Thus, for the rate of bubble formation as estimated by the method of complete runs,

$$P\left[\left(1 - \frac{1.960}{\sqrt{n}}\right) < \frac{\dot{m}_b}{\hat{m}_b} < \left(1 + \frac{1.960}{\sqrt{n}}\right)\right] \cong 0.95 \quad (32)$$

As a numerical example, take 50 trials in which a bubble forms 25 times. The 95 per cent confidence interval for  $p$  is

$$P[0.355 < p < 0.645] = 0.95 \quad (33)$$

Converting by equation 11,

$$P[0.632 < \frac{\dot{m}_b}{\hat{m}_b} < 1.492] = 0.95 \quad (34)$$

For a probability of a bubble forming of 0.5, the cut-off time should be taken as  $0.632\bar{\theta}$  or  $0.693\bar{\theta}$ . Thus for fifty runs the total time of the runs is  $(50)(0.693\bar{\theta}) = 34.7\bar{\theta}$ . The length of the confidence interval is  $1.492 - 0.632 = 0.860$ . From equation 32 twenty-one runs must be carried to completion to establish the rate within this confidence interval; the time for these runs is directly  $21\bar{\theta}$ . For somewhat shorter cut-off times, the discrepancy in times is slightly less, but the difference in number of runs becomes much greater. Since the preparation time for a run is large, the method of complete runs is highly advantageous from the standpoint of time.

The outstanding disadvantage of adopting the policy of complete runs is the absolute necessity of completing a run once it is commenced. For example, the equipment in the laboratory is shut down each week by 8 AM Saturday. If a run is stopped before completion it cannot fail to bias the data, since the interrupted run is more likely to be a long run than a short one. Some information is furnished by the uncompleted run, but not as much as by a normal run. By taking less information from the complete runs, that is, by considering only whether a bubble has formed by the time at which the incomplete run was cut off, the data may be treated in a statistically sound manner; this procedure is, however, just the same as the binomial method but without the advantage of a suitably chosen cut-off time. If the run is completely disregarded, the remaining data are obviously biased; similarly, but to a smaller degree, if all the information furnished by each run is used, the data are biased because in the aggregate the longer runs have been given less weight than they have deserved. Probably the best solution to this problem is to refuse to start a run when it is desirable to stop the apparatus sooner than 2.3 times the mean time of the previous runs; only one out of ten runs would be expected to exceed this value. By a suitable choice of this time, the fraction of runs which would exceed the time may be held to any level desired. It would seem that the savings in time indicated above are sufficient justification for the

loss of time caused by shutting the apparatus down sooner than otherwise necessary.

### CONCLUSIONS

1. A simplified treatment of the theory of liquids indicates that the times for the first bubble to form are distributed according to

$$f(\theta) = ke^{-k\theta} \quad (5)$$

2. The effect of the degree of supersaturation on the mean time for the first bubble to form may possibly be given by an equation of the form of

$$\ln \bar{\theta}_b + \ln A = \frac{\alpha}{(p_b - p)} \quad (15)$$

3. The line which best fits the data when plotted according to equation 15 can be found by a trial and error procedure.

4. The procedure whereby the runs are allowed to continue until a bubble forms is more efficient than the method of stopping each run at the end of a given time; that is, the time necessary to establish a mean rate of bubble formation within a certain percentage by the former method is much less than by the latter.

REFERENCES

1. Buff, F. P., J. Chem. Phys., 19, 1951 (1951).
2. Fry, T. C., "Probability and Its Engineering Uses,"  
D. Van Nostrand Co., Inc., New York, 1928.
3. Gibbs, J. W., "Collected Works" Vol. I, Longmans  
Green and Co., New York, 1931.
4. Hunt, E. B., Jr., private communication to B. H. Sage,  
January 8, 1954.
5. La Mer, V. K., Ind. Eng. Chem., 44, 1270 (1952).
6. Mood, A. M., "Introduction to the Theory of Statistics"  
McGraw-Hill Book Co., Inc., New York, 1950.
7. Reiss, H., Ind. Eng. Chem., 44, 1284 (1952).
8. Tolman, R. C., J. Chem. Phys., 17, 333 (1949).

NOMENCLATURE

A	frequency factor in Arrhenium rate equation
a	reciprocal of A
k	specific gas constant
$F(p, l, n)$	$\int_0^p \frac{(l+n+1)!}{l!n!} x^l (1-x)^n dx$ , the incomplete beta function
$f(\theta)$	distribution function of time for the first bubble to form
i	running index
k	parameter in Poisson distribution
L	likelihood function
l	number of runs in which bubble forms before cut off time
n	number of sample points; the nth sample point
$\dot{n}_b$	rate of bubble formation
P	pressure
$P_b$	bubble point pressure
P	probability; probability of bubble being formed
$P_n$	probability of n bubbles being formed
p	probability of bubble being formed before cut-off time
$p_1$	upper confidence limit for p
$p_2$	lower confidence limit for p
$S_i$	degree of supersaturation ( $P_b - P$ ) for ith sample point
T	absolute temperature
$t_i$	time for the first bubble to form for ith sample point



$w$	work necessary to form bubble of critical size
$y$	number of runs in which a bubble forms
$\alpha$	$\frac{16\pi\gamma^3}{3kT}$
$\gamma$	interfacial tension lb./ft.
$\theta$	time for the first bubble to form
$\bar{\theta}$	population mean of times for the first bubble to form
$\bar{\theta}_b$	sample mean of times for the first bubble to form
$\mu_i$	mean time corresponding to $s_i$
$\sigma$	standard deviation
$\wedge$	maximum likelihood estimator
$\binom{n}{y}$	$\frac{n!}{y!(n-y)!}$

### III. VOLUMETRIC AND PHASE BEHAVIOR OF HYDROCARBON SYSTEMS

#### 1. HYDROGEN-n-HEXANE

## VOLUMETRIC AND PHASE BEHAVIOR IN THE HYDROGEN-n-HEXANE SYSTEM

W. B. Nichols, H. H. Reamer and B. H. Sage

California Institute of Technology

Pasadena, California

### INTRODUCTION

Only limited investigations of the volumetric and phase behavior of binary systems involving hydrogen and hydrocarbons at high pressures are available. The phase behavior of the hydrogen-n-propane system has been investigated (2) and the solubility of hydrogen has been determined in a number of hydrocarbons (4,5). These limited data do not permit a general correlation of the effect of the characteristics of the hydrocarbon components upon the phase behavior of such systems of the partial volume (7) of hydrogen in hydrocarbon liquids.

In order to extend the knowledge of the volumetric and phase behavior of hydrogen-hydrocarbon systems, an experimental study of the hydrogen-n-hexane system was carried out at temperatures between 40° and 460° F. and for pressures up to 10,000 pounds per square inch. The investigation included a direct evaluation of the composition of the gas phase in heterogeneous mixtures of these components as well as measurements of the specific volume of four mixtures as a function of pressure and temperature.

The volumetric behavior of hydrogen has been investigated in detail and it is beyond the scope of the present discussion to present a review of these data. However, for present purposes the measurements of Wiebe and Gaddy (15) and Deming and Shupe (3) were employed. The latter data appeared to describe the volumetric behavior of hydrogen within the above-described range and temperatures with an uncertainty less than 0.2%. Recently the volumetric behavior of n-hexane has been studied (14). This work is in good agreement with the earlier measurements of Kelso and Felsing (6). The measurements of the volumetric behavior of n-hexane in the liquid phase are known throughout the range of pressure and temperatures of interest with an uncertainty of approximately 0.25%. There is no experimental information available except at pressures above atmospheric to describe the volumetric behavior of n-hexane in the gas phase except for states at temperatures above the critical, where some measurements are reported by Kelso and Felsing (6).

The above-described experimental information concerning the volumetric behavior of hydrogen and of n-hexane suffices for present needs and permits the experimental data for their mixtures to be smoothed with respect to composition. The behavior of hydrogen and n-hexane are not reported here.

#### METHODS AND APPARATUS

It is the purpose of this investigation to determine

the specific volume as a function of pressure and temperature for a series of mixtures of hydrogen and n-hexane of chosen compositions. In principle, the experimental methods involved the confinement of a sample mixture of known composition and weight in a stainless steel pressure vessel over mercury.

Effective volume of this chamber was varied by the introduction or withdrawal of mercury. Mechanical agitation was provided to hasten the attainment of physical equilibrium within and between the phases. The details of the experimental apparatus used for this purpose have been described (13). Pressures were measured by means of a balance utilizing a piston cylinder combination (13). This instrument was calibrated against a vapor pressure of carbon dioxide (1). Recent experience with such an instrument (11) indicates that the pressures within the apparatus relative to the vapor pressure of carbon dioxide at the ice point were known within 0.2 pound per square inch or 0.10%, whichever was the larger measure of uncertainty.

The stainless steel vessel containing the hydrocarbons under investigation was immersed in an agitated liquid bath the temperature of which was controlled with a resistance thermometer through a modulating electronic circuit (10). The temperature of the agitated liquid bath was related to the international platinum scale by means of a strain-free platinum resistance thermometer of the coiled filament type (8). This unit was compared with the indi-

cations of a similar instrument which had been calibrated recently by the National Bureau of Standards. The temperature of the contents of the pressure vessel was known within  $0.02^{\circ}$  F. of the international platinum scale throughout temperature interval between  $40^{\circ}$  and  $460^{\circ}$  F.

The n-hexane was introduced by weighing bomb techniques (13) and the hydrogen by volumetric methods involving the measured change in volume of constant pressure under isothermal conditions.

The weight of the mixtures was known within 0.05% for all four compositions investigated. Experience with the equipment indicates that the relative probable error in specific volume at pressures below 5000 pounds per square inch was approximately 0.25%. This probable error increased gradually at the higher pressure to a relative value of 0.5% at 10,000 pounds per square inch. The larger uncertainties, at the higher pressures resulted from difficulties in obtaining reproducible calibrations of the instrument under these conditions.

Some difficulty was experienced from thermal rearrangement of the n-hexane at temperatures of  $400^{\circ}$  and  $460^{\circ}$  F. The existence of this thermal rearrangement was indicated by comparison of the equilibrium volumetric behavior near the bubble point for samples at  $100^{\circ}$  F. which had been subject to investigation at  $400^{\circ}$  and  $460^{\circ}$  F. An increase in bubble point pressure of as much as 10 pounds per square inch was experienced in the case of the mixtures rich in

n-hexane. For this reason it should be emphasized that in the vicinity of bubble point, measurements at 400° and 460° F. are subject to an additional uncertainty beyond that just described. However, this thermal rearrangement did not significantly modify the volumetric behavior in the condensed liquid or in the heterogeneous region at specific volumes several times that of bubble point.

In order to establish the composition of the gas phase of heterogeneous mixtures of hydrogen and n-hexane it was found desirable to determine the mole fraction of each of the components by direct measurement. It was not found desirable to utilize volumetric measurements at constant composition to obtain these data. The small change in composition which was experienced at dew point with large changes in pressure throughout the greater part of the temperature interval covered by this investigation render measurements at constant composition ineffective.

As a result of the marked difference in volatility between the components partial condensation at liquid nitrogen temperatures was employed. The sample of the gas phase was removed from the heterogeneous mixture under isobaric-isothermal conditions and passed through a special weighing bomb (13) which was maintained at liquid nitrogen temperatures. To insure that all the n-hexane was removed the hydrogen was passed through a second weighing bomb also maintained at liquid nitrogen temperatures. The total quantity of hydrogen involved was determined by volumetric meas-

urement in a large glass vessel maintained at 100° F. The change in pressure within this vessel was determined by means of a mercury-in-glass manometer used in conjunction with a cathetometer. The n-hexane and a small quantity of dissolved hydrogen were permitted to warm to room temperature in the weighing bombs and then were re-cooled to liquid nitrogen temperatures and the hydrogen removed by prolonged evacuation. No difficulty was experienced in obtaining measurements reproducible within 0.001 mole fraction n-hexane. Measurements upon samples of known compositions yielded results within this error. The techniques developed for partial condensation should have permitted the composition of the gas phase in heterogeneous mixtures of hydrogen and n-hexane to be determined within 0.002 mole fraction.

#### MATERIALS

The hydrogen was obtained from a commercial manufacturer and was prepared electrolytically. It was reported to contain less than 0.002 mole fraction of material other than hydrogen and water. The gas was passed through liquid nitrogen, a chamber containing platinum wire heated to approximately 800° F., and again through a coil immersed in liquid nitrogen. This treatment was followed by contact with activated charcoal and anhydrous calcium sulphate. The foregoing processes were carried out at the pressures in excess of 500 pounds per square inch. Mass spectrographic



analysis of hydrogen so purified indicated it to contain less than 0.001 mole fraction of material other than hydrogen.

The n-hexane was obtained as research grade from the Phillips Petroleum Company which reported it to contain not more than 0.003 mole fraction of material other than n-hexane. This hydrocarbon was dried over metallic sodium, and solidified at liquid nitrogen temperatures. It was maintained at a relatively high vacuum in the solid state for an extended period to complete the removal of noncondensable gases. A value of 40.871 for the specific weight at 77° F. was obtained for the air-free sample as compared to 40.878 reported by Rossini (12) for an air saturated sample at the same temperature. The index of refraction relative to the D-lines of sodium at 77° F. was 1.37225 as compared to 1.37226 reported by Rossini (12) for air-saturated n-hexane.

#### EXPERIMENTAL RESULTS

Measurements of the volumetric behavior of four mixtures of hydrogen and n-hexane were investigated. A large sample of each mixture was first introduced and measurements made for pressures from approximately 1000 to 10,000 pounds per square inch. The sample was then brought to a single phase state and approximately 80% of it removed. The remaining smaller sample was then investigated over the same temperature interval to obtain data for pressures below 1000 pounds per square inch. Figure 1 shows the

experimental information obtained for a mixture relatively rich in n-hexane. Similar experimental information was obtained for each of the three other samples investigated. The detailed record of experimental data obtained in the course of this volumetric study is available (9). Only three of the mixtures are reported. Because a different method for loading the sample was used for the mixture containing 2.98 mole percent hydrogen, the error in the molal volumes for this mixture was much greater than the uncertainty connected with the others.

The composition of the coexisting phase as determined from condensation analysis of samples withdrawn under isobaric-isothermal conditions from the gas phase of heterogeneous mixtures of hydrogen and n-hexane is shown in Figure 2. The scale of the figure in the vicinity of pure n-hexane was enlarged markedly in order to illustrate the behavior of the gas phase in somewhat greater detail. The points shown for the liquid phase were obtained from discontinuities in the isothermal first derivative of specific volume as a function of pressure. The data obtained in the course of the measurement of the composition of the gas phase in heterogeneous mixtures of hydrogen and n-hexane are also available (9).

Figure 3 presents the product of the molal equilibrium ratios for hydrogen and for n-hexane as a function of pressure for each of the several temperatures investigated. The use of the product of pressure and the equilibrium ratio was

employed in order to present the behavior in greater detail than is possible by the use of the equilibrium ratio alone. The equilibrium ratio for n-hexane in the hydrogen-n-hexane system is shown plotted on a logarithmic scale versus pressure in Figure 4. The equilibrium ratios shown in Figures 3 and 4 were computed from the information presented in Figures 1 and 5. Figure 5 is a pressure-temperature diagram for this binary system. The rapid increase in the initial pressure with a decrease in temperature from the critical state of the pure hydrocarbon was previously noted in the hydrogen-propane system (2). The maxcondentherm locus shown in Figure 5 is the locus of points representing the maximum condensation temperature for a system of constant composition.

Figure 6 shows the molal volume as a function of composition at 400° F. This temperature was chosen to illustrate the behavior of a composition rich in hydrogen. For lower temperatures the dew point line lies much closer to the right hand axis. The requirement that the isobars in the heterogeneous region be straight lines on a plot such as shown in Figure 6 was used to smooth the volumetric data taken in this region.

Table I records the molal volume for even values of pressure and temperature for the three experimentally studied compositions. In the liquid phase a standard estimate of error of 0.000036 cubic feet per pound mole was found for the experimental data from the smooth curves from

which the information of Table I was obtained. The standard estimate of error in the heterogeneous region was 0.00044 cubic feet per pound mole. The much larger deviation in the heterogeneous region probably results from a lack of strict attainment of equilibrium, particularly at states remote from the bubble point. The standard estimate of error assumed that all the uncertainty existed in specific volume and none was associated with the evaluation of pressure, temperature, and composition. The data of Table I are smooth with respect to composition within the small uncertainty associated with graphical operations involving volumetric data for n-hexane, hydrogen, and the three experimental mixtures reported.

Table II presents the compositions and molal volumes of the liquid and gas phases of heterogeneous mixtures of hydrogen-n-hexane for seven temperatures between 40° and 400° F. In addition the molal equilibrium ratios for hydrogen and n-hexane for each temperature were included. Table III records a number of the properties at the unique states in the heterogeneous region.

#### ACKNOWLEDGMENT

This work was in part supported by the General Petroleum Corporation through scholarship grants to D. E. Stewart, W. C. Windham, and C. H. Viens. Virginia Berry and June Gray assisted with the calculations and the preparation of the figures, while W. N. Lacey reviewed the manuscript.

LITERATURE CITED

1. Bridgeman, O. C., J. Am. Chem. Soc., 49, 1174 (1927).
2. Burriss, W. L., Hsu, N. T., Reamer, H. H., and Sage, B. H., Ind. Eng. Chem., 45, 210 (1953)
3. Deming, W. E., and Shupe, L. E., Phys. Rev., 40, 848 (1932).
4. Ipatieff et al., Oil and Gas J., 32, 14 (1933).
5. Kay, W. B., Chem. Rev., 29, 501 (1941).
6. Kelso, E. A., and Felsing, W. A., J. Am. Chem. Soc., 62, 3132 (1940).
7. Lewis, G. N., Proc. Am. Acad., 43, 259 (1907).
8. Meyers, C. H., Bur. Standards J. Research, 9, 807 (1932).
9. Nichols, W. B., Reamer, H. H., and Sage, B. H., Am. Doc. Inst., Washington, D.C., Doc. No. (1957).
10. Reamer, H. H., and Sage, B. H., Rev. Sci. Inst., 24, 362 (1953).
11. Reamer, H. H., and Sage, B. H., Rev. Sci. Inst., 26, 592 (1955).
12. Rossini et al., "Selected Values of Physical and Thermodynamic Properties of Hydrocarbons and Related Compounds," Carnegie Press, Pittsburgh, 1953.
13. Sage, B. H., and Lacey, W. N., Trans. AIME, 136, 136 (1940).
14. Stewart, D. E., Sage, B. H., and Lacey, W. N., Ind. Eng. Chem., 46, 2529 (1954).
15. Wiebe, R., and Gaddy, V. L., J. Am. Chem. Soc., 60, 2300 (1938).

LIST OF FIGURES

1. Sample Experimental Volumetric Measurements for Mixture Containing 0.1895 Mole Fraction Hydrogen
2. Composition of Coexisting Phases in Hydrogen-n-Hexane System
3. Equilibrium Ratios for Hydrogen and n-Hexane
4. Equilibrium Ratio for n-Hexane
5. Pressure-Temperature Diagram for Hydrogen-n-Hexane System
6. Molal Volume as a Function of Composition at 400° F.

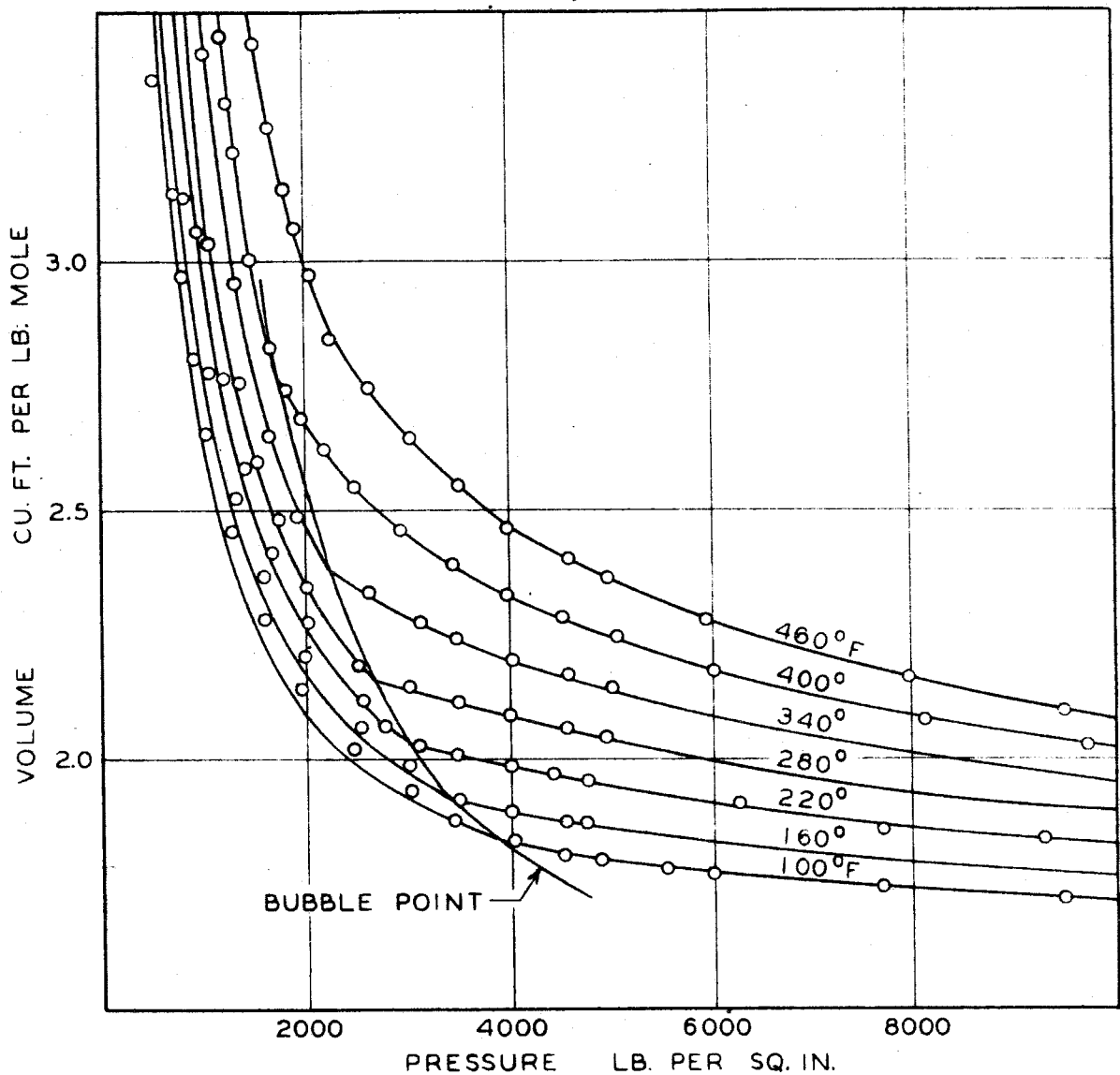


Figure 1. Sample Experimental Volumetric Measurements for Mixture Containing 0.1895 Mole Fraction Hydrogen

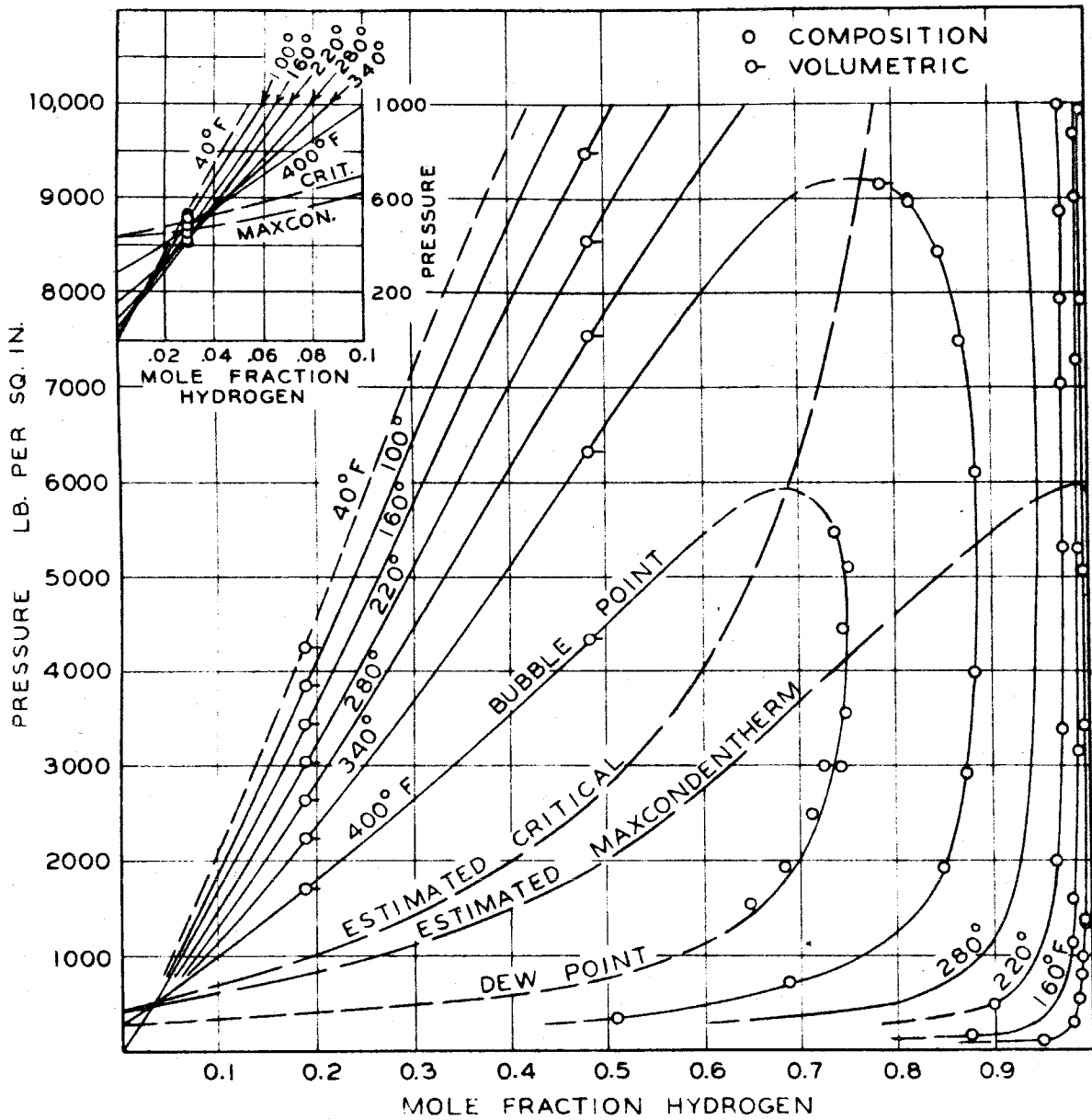


Figure 2. Composition of Coexisting Phases in Hydrogen-n-Hexane System



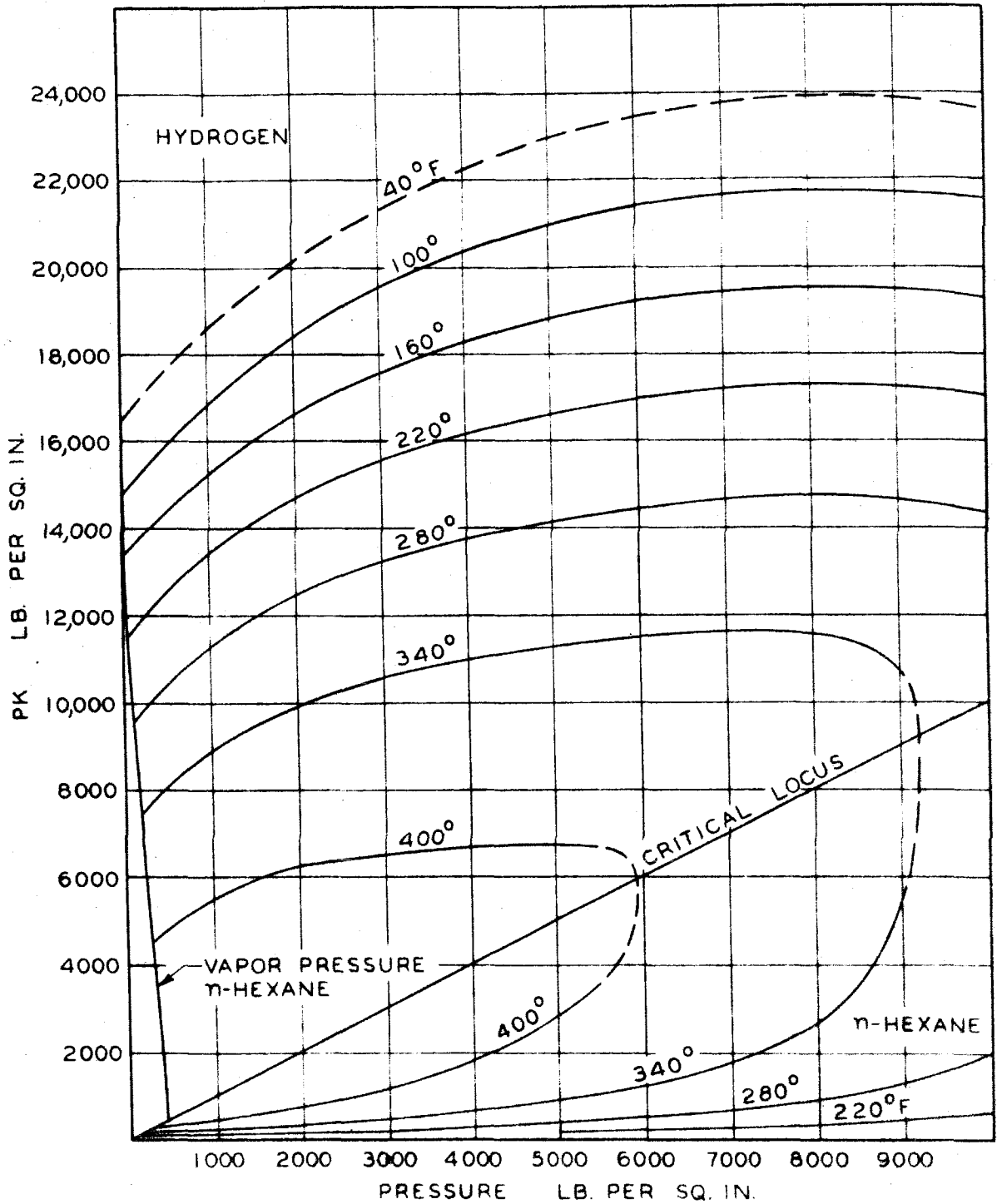


Figure 3. Equilibrium Ratios for Hydrogen and n-Hexane

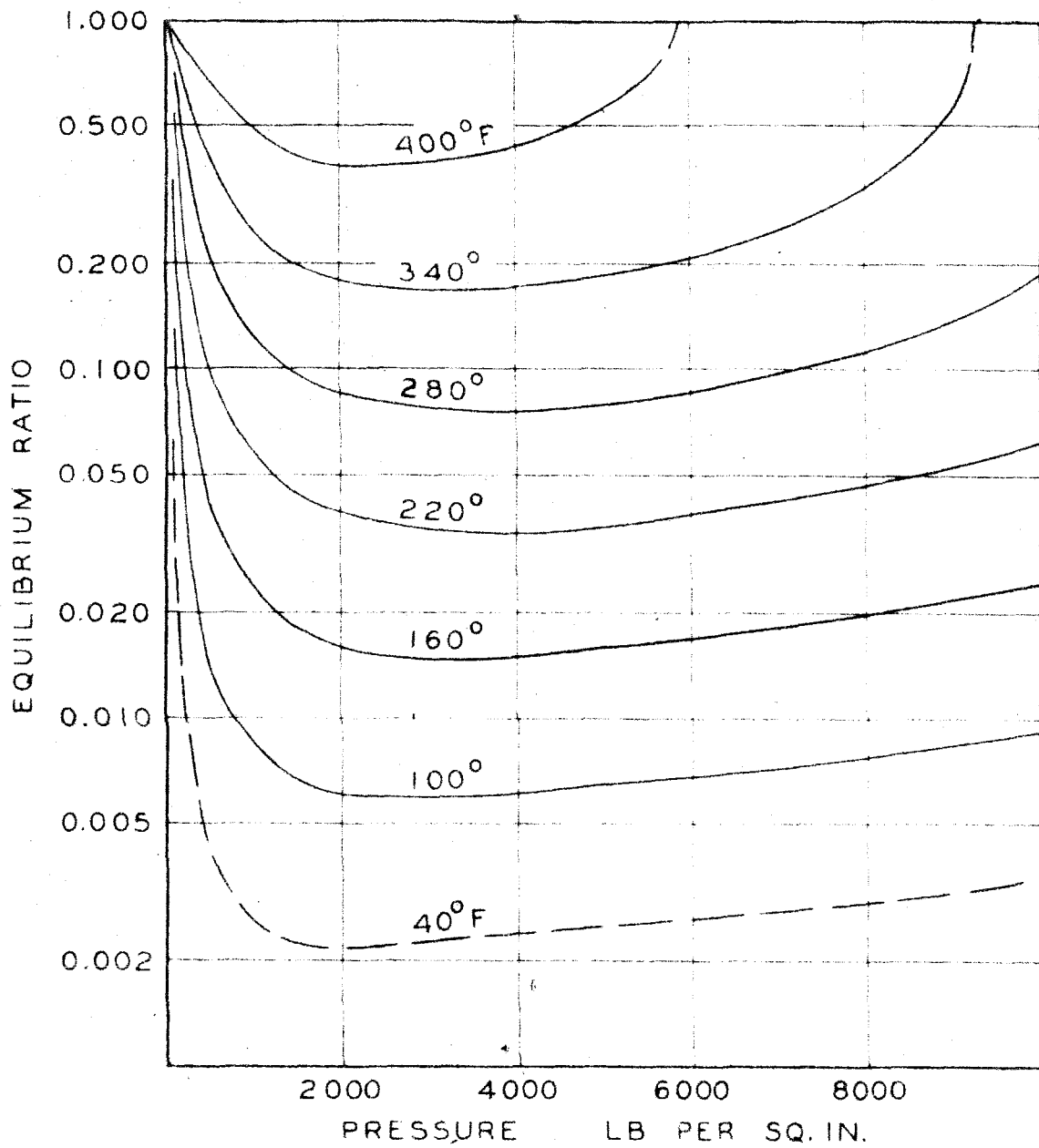


Figure 4. Equilibrium Ratio for n-Hexane

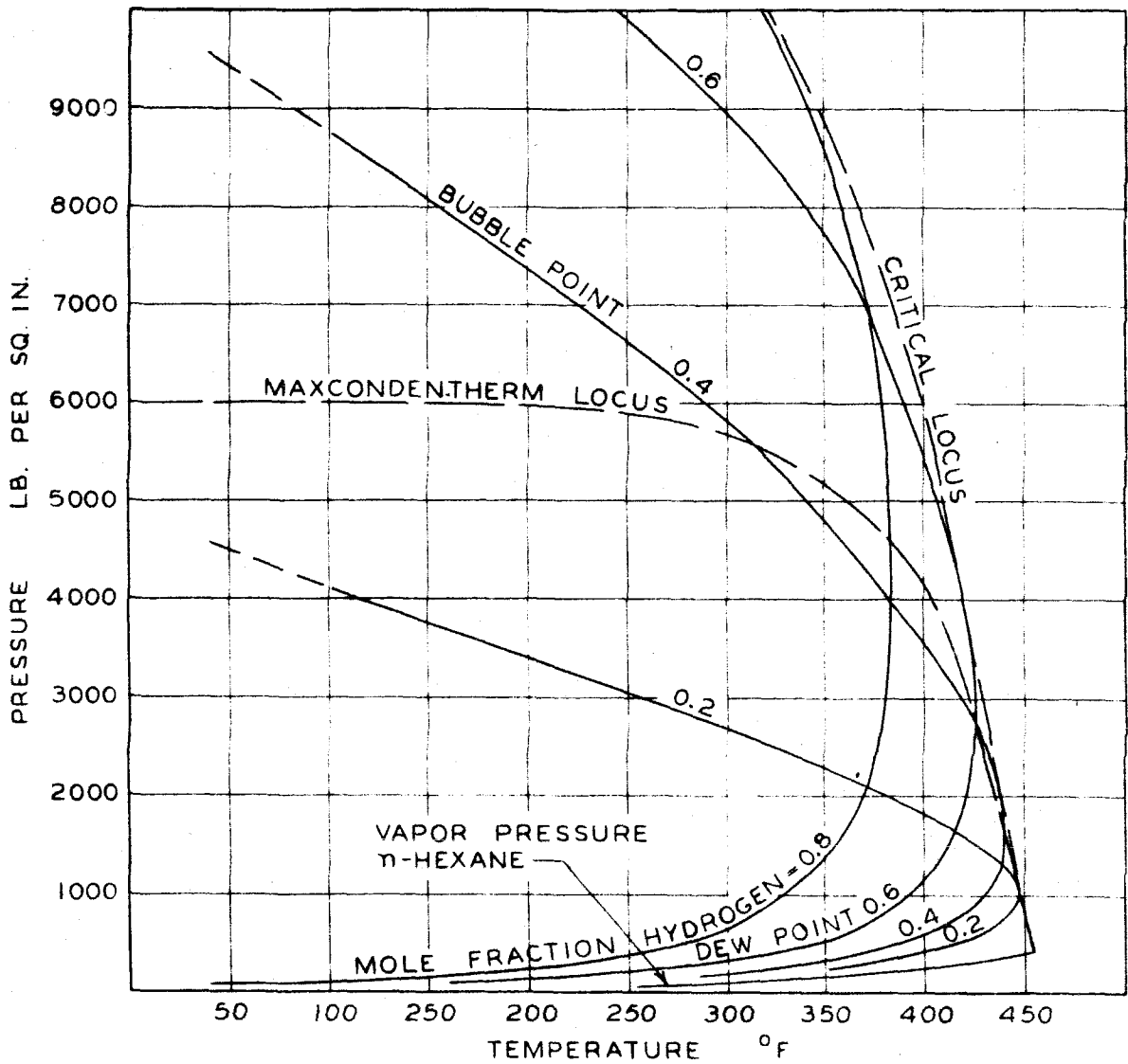


Figure 5. Pressure-Temperature Diagram for  
Hydrogen-n-Hexane System

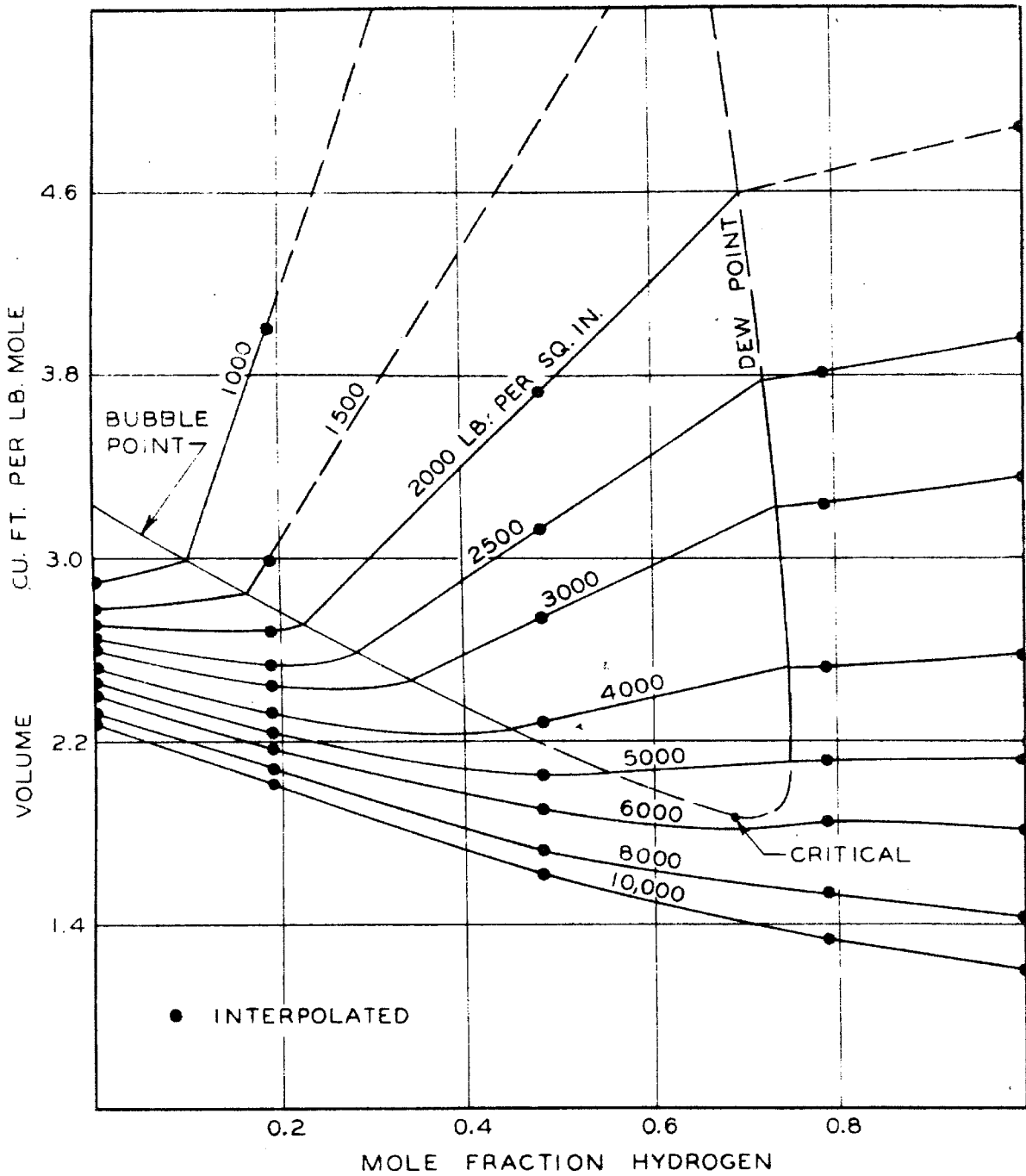


Figure 6. Molal Volume as a Function of Composition at 400° F.

LIST OF TABLES

- I. Molal Volumes for Mixtures of Hydrogen and n-Hexane
- II. Properties of the Coexisting Gas and Liquid Phases  
in the Hydrogen-n-Hexane System
- III. Estimated Properties at the Unique States in the  
Hydrogen-n-Hexane System

TABLE I. MOLAL VOLUMES FOR MIXTURES OF HYDROGEN AND n-HEXANE

Pressure Lb./Sq.Inch	Temperature °F.						
	40	100	160	220	280	340	400
Dew Point	(9) <sup>a</sup>	(17)	(40)	(77)	(127)	(220)	(425)
Bubble Point	(4240) <sup>a</sup>	(3840)	(3430)	(3030)	(2640)	(2225)	(1705)
	1.770	1.844	1.924	2.030	2.166	2.381	2.792
	6.78 <sup>b</sup>	-	-	-	-	-	-
200	4.09	4.47	4.87	5.51	6.34	-	-
400	3.25	3.40	3.65	4.05	4.59	5.30	-
600	2.758	2.920	3.10	3.40	3.72	4.20	-
800	2.500	2.641	2.782	3.02	3.19	3.53	-
1000	2.304	2.406	2.537	2.681	2.840	3.07	4.96
1250	2.170	2.275	2.367	2.487	2.617	2.784	4.00
1500	2.080	2.170	2.260	2.363	2.458	2.607	3.36
1750	2.010	2.092	2.168	2.256	2.352	2.473	2.985
2000	1.960	2.034	2.109	2.185	2.267	2.382	2.778
2250	1.919	1.985	2.052	2.128	2.200	2.347	2.679
2500	1.885	1.946	2.007	2.076	2.163	2.319	2.605
2750	1.861	1.918	1.973	2.037	2.148	2.289	2.542
3000	1.820	1.870	1.917	2.008	2.114	2.240	2.493
3500	1.788	1.833	1.893	1.984	2.084	2.200	2.451
4000	1.762	1.808	1.877	1.966	2.063	2.166	2.384
4500	1.756	1.791	1.859	1.946	2.039	2.135	2.330
5000	1.737	1.770	1.833	1.909	1.992	2.082	2.283
6000	1.722	1.756	1.812	1.886	1.954	2.039	2.244
7000	1.706	1.742	1.796	1.861	1.931	2.006	2.174
8000	1.693	1.726	1.778	1.844	1.910	1.980	2.124
9000	1.678	1.711	1.764	1.828	1.892	1.954	2.084
10,000							2.049
							2.021
							2.077

<sup>a</sup> Values in parentheses represent pressures expressed in pounds per square inch absolute<sup>b</sup> Volume expressed in cubic feet per pound mole

TABLE I. (Cont.)

Pressure Lb./Sq.Inch	Temperature °F.							
	40	100	160	220	280	340	400	460
Dew Point	(34) <sup>a</sup>	(40)	(85)	(140)	(221)	(336)	(738)	
	-	-	-	-	-	-	-	
Bubble Point			(9500) <sup>b</sup>	(8575)	(7560)	(6320)	(4330)	
	-	-	1.424	1.497	1.597	1.756	2.193	
200	-	-	-	-	-	-	-	-
400	-	-	-	-	-	-	-	-
600	-	-	-	-	-	-	-	-
800	4.29 <sup>c</sup>	4.70	-	-	-	-	-	-
1000	3.63	3.97	4.23	4.86	-	-	-	-
1250	3.11	3.36	3.65	3.98	4.34	4.93	4.80	4.75
1500	2.768	2.997	3.22	3.48	3.78	4.21	4.15	4.20
1750	2.522	2.724	2.913	3.13	3.37	3.73	3.74	3.72
2000	2.341	2.517	2.678	2.863	3.08	3.36	3.39	3.41
2250	2.202	2.361	2.506	2.670	2.857	3.09	3.12	3.18
2500	2.091	2.226	2.361	2.513	2.678	2.879	2.912	2.997
2750	1.996	2.127	2.250	2.384	2.531	2.707	2.740	2.698
3000	1.923	2.041	2.150	2.278	2.411	2.562	2.471	2.483
3500	1.800	1.901	2.004	2.108	2.222	2.343	2.286	2.324
4000	1.716	1.800	1.898	1.981	2.077	2.181	2.152	2.202
4500	1.641	1.733	1.804	1.889	1.963	2.052	2.050	2.026
5000	1.585	1.662	1.738	1.806	1.874	1.948	1.903	1.903
6000	1.506	1.565	1.627	1.683	1.738	1.796	1.801	1.814
7000	1.443	1.497	1.549	1.595	1.642	1.702	1.724	1.744
8000	1.397	1.442	1.486	1.528	1.567	1.638	1.665	1.683
9000	1.348	1.399	1.437	1.475	1.519	1.590	1.619	
10,000	1.338	1.367	1.396	1.433	1.485	1.558		

TABLE I. (Cont.)

Pressure lb./Sq. Inch	Temperature °F.					Mole Fraction Hydrogen = 0.7878				
	40	100	160	220	280	340	400	460		
Dew Point	(61) <sup>a</sup>	(79)	(127)	(292)	(494)					
Bubble Point	-	-	-	-	-	-	-	-		
200	-	-	-	-	-	-	-	-		
400	-	-	-	-	-	-	-	-		
600	-	-	-	-	-	-	-	-		
800	-	-	-	-	-	-	-	-		
1000	-	-	-	-	-	-	-	-		
1250	3.95 <sup>c</sup>	4.35	4.09	4.49	4.30	4.27	4.19	4.51		
1500	3.38	3.74	3.60	3.92	3.83	3.83	3.81	4.09		
1750	2.977	3.78	3.21	3.50	3.46	3.48	3.51	3.76		
2000	2.681	2.949	2.920	3.18	3.17	3.20	3.23	3.48		
2250	2.448	2.683	2.686	2.917	2.926	2.966	3.22	3.04		
2500	2.266	2.478	2.504	2.702	2.727	2.613	2.82	3.04		
2750	2.109	2.309	2.335	2.526	2.413	2.343	2.522	2.715		
3000	1.986	2.165	2.087	2.248	2.182	2.137	2.294	2.464		
3500	1.787	1.926	1.898	2.037	1.999	1.974	2.113	2.262		
4000	1.636	1.763	1.757	1.890	1.860	1.840	1.974	2.113		
4500	1.520	1.638	1.640	1.749	1.642	1.740	1.846	1.960		
5000	1.427	1.528	1.470	1.552	1.489	1.572	1.664	1.763		
6000	1.288	1.369	1.336	1.409	1.375	1.442	1.526	1.612		
7000	1.184	1.258	1.240	1.308	1.280	1.337	1.419	1.494		
8000	1.109	1.177	1.167	1.224	1.212	1.270	1.332	1.403		
9000	1.051	1.121	1.118	1.158						
10,000	1.018	1.065								



TABLE II. PROPERTIES OF THE COEXISTING GAS AND LIQUID PHASES IN THE

HYDROGEN-n-HEXANE SYSTEM

Pressure Lb./Sq.Inch	Mole Fraction Hydrogen Dew Point	Volume Cu.Ft./Lb. Mole	Mole Fraction Hydrogen Bubble Point	Volume Cu.Ft./Lb. Mole	Equilibrium Ratio	
					Hydrogen	n-Hexane
40° F.						
1.107 <sup>a</sup>	0	-	0	2.064	-	1.0000
500	0.996	-	0.028	2.022	35.19	0.0041
1000	0.998	- <sup>b</sup>	0.054	1.980	18.53	0.0026
1500	0.998	3.80 <sup>b</sup>	0.078	1.945	12.88	0.0023
2000	0.998	2.914	0.099	1.912	10.04	0.0022
2500	0.998	2.381	0.120	1.880	8.288	0.0023
3000	0.998	2.023	0.140	1.850	7.103	0.0023
3500	0.998	1.768	0.160	1.818	6.238	0.0024
4000	0.998	1.577	0.179	1.790	5.562	0.0024
4500	0.998	1.429	0.199	1.754	5.024	0.0025
5000	0.998	1.311	0.218	1.721	4.588	0.0026
6000	0.998	1.132	0.256	1.659	3.904	0.0027
7000	0.998	1.007	0.294	1.598	3.391	0.0028
8000	0.998	0.9150	0.334	1.531	2.988	0.0030
9000	0.998	0.8449	0.376	1.472	2.654	0.0032
10,000	0.998	0.7920	0.422	1.414	2.365	0.0035
100° F.						
4.954 <sup>a</sup>	0	-	0	2.148	-	1.0000
500	0.986	-	0.031	2.095	31.81	0.0144
1000	0.992	- <sup>b</sup>	0.059	2.050	16.81	0.0085
1500	0.994	4.24 <sup>b</sup>	0.084	2.015	11.83	0.0066
2000	0.995	3.24	0.108	1.975	9.209	0.0061
2500	0.995	2.643	0.131	1.940	7.595	0.0058
3000	0.995	2.242	0.153	1.900	6.503	0.0061
3500	0.995	1.958	0.175	1.870	5.686	0.0061
4000	0.995	1.744	0.196	1.830	5.077	0.0062
4500	0.995	1.578	0.217	1.800	4.585	0.0064
5000	0.995	1.445	0.238	1.772	4.181	0.0066
6000	0.995	1.245	0.279	1.698	3.566	0.0069
7000	0.995	1.104	0.322	1.620	3.090	0.0074
8000	0.995	1.000	0.366	1.545	2.719	0.0079
9000	0.995	0.9221	0.412	1.461	2.415	0.0085
10,000	0.995	0.8607	0.461	1.390	2.158	0.0093

<sup>a</sup>Vapor pressure of n-Hexane

<sup>b</sup>Volumes at dew point calculated

<sup>c</sup>Critical state

TABLE II. (Cont.)

Pressure Lb./Sq.Inch	Mole Fraction Hydrogen Dew Point	Volume Cu.Ft./Lb. Mole	Mole Fraction Hydrogen Bubble Point	Volume Cu.Ft./Lb. Mole	Equilibrium Ratio	
					Hydrogen	n-Hexane
160° F.						
15.82 <sup>a</sup>	0	-	0	2.256	-	1.0000
500	0.961	-	0.034	2.195	28.69	0.0403
1000	0.978	-	0.064	2.140	15.28	0.0235
1500	0.983	4.66 <sup>b</sup>	0.092	2.090	10.68	0.0187
2000	0.986	3.56	0.119	2.041	8.286	0.0159
2500	0.987	2.902	0.144	2.000	6.854	0.0152
3000	0.988	2.460	0.169	1.960	5.846	0.0144
3500	0.988	2.147	0.193	1.920	5.119	0.0149
4000	0.988	1.912	0.216	1.880	4.574	0.0153
4500	0.988	1.728	0.239	1.840	4.134	0.0158
5000	0.988	1.581	0.262	1.798	3.770	0.0163
6000	0.988	1.359	0.309	1.710	3.197	0.0174
7000	0.988	1.202	0.356	1.630	2.775	0.0186
8000	0.988	1.084	0.405	1.543	2.440	0.0202
9000	0.988	0.9968	0.456	1.460	2.167	0.0221
10,000	0.988	0.9290	0.511	1.380	1.933	0.0245
220° F.						
39.87 <sup>a</sup>	0	-	0	2.391	-	1.0000
500	0.904	-	0.036	2.321	25.11	0.0996
1000	0.946	-	0.070	2.256	13.51	0.0581
1500	0.960	5.07 <sup>b</sup>	0.102	2.195	9.412	0.0445
2000	0.966	3.87	0.132	2.137	7.318	0.0392
2500	0.969	3.16	0.160	2.082	6.056	0.0369
3000	0.971	2.677	0.187	2.032	5.193	0.0357
3500	0.973	2.334	0.215	1.984	4.526	0.0344
4000	0.974	2.078	0.241	1.931	4.041	0.0343
4500	0.974	1.898	0.267	1.882	3.634	0.0355
5000	0.974	1.718	0.293	1.835	3.324	0.0368
6000	0.974	1.475	0.345	1.740	2.823	0.0397
7000	0.974	1.300	0.396	1.648	2.460	0.0430
8000	0.974	1.170	0.450	1.552	2.164	0.0473
9000	0.974	1.070	0.508	1.448	1.917	0.0528
10,000	0.973	0.9990	0.570	1.347	1.707	0.0628

TABLE II. (Cont.)

Pressure Lb./Sq.Inch	Mole Fraction Hydrogen Dew Point	Volume Cu.Ft./Lb. Mole	Mole Fraction Hydrogen Bubble Point	Volume Cu.Ft./Lb. Mole	Equilibrium Ratio	
					Hydrogen	n-Hexane
280° F.						
84.93 <sup>a</sup>	0	-	0	2.565	-	1.0000
500	0.797	-	0.038	2.489	20.97	0.2110
1000	0.886	-	0.078	2.400	11.36	0.1236
1500	0.914	-	0.115	2.321	7.948	0.0972
2000	0.927	4.17 <sup>b</sup>	0.149	2.250	6.221	0.0858
2500	0.934	3.40	0.181	2.185	5.160	0.0806
3000	0.939	2.887	0.213	2.120	4.408	0.0775
3500	0.942	2.520	0.244	2.060	3.861	0.0767
4000	0.944	2.240	0.274	2.000	3.445	0.0771
4500	0.945	2.025	0.304	1.940	3.109	0.0790
5000	0.946	1.854	0.334	1.882	2.832	0.0811
6000	0.946	1.595	0.393	1.765	2.407	0.0890
7000	0.945	1.411	0.451	1.660	2.095	0.1002
8000	0.944	1.270	0.511	1.545	1.847	0.1145
9000	0.941	1.168	0.576	1.440	1.634	0.1392
10,000	0.931	1.095	0.649	1.332	1.435	0.1966
340° F.						
160.28 <sup>a</sup>	0	-	0	2.806	-	1.0000
500	0.606	-	0.037	2.726	16.22	0.4091
1000	0.772	-	0.086	2.615	8.977	0.2495
1500	0.826	-	0.132	2.510	6.258	0.2005
2000	0.851	4.45 <sup>b</sup>	0.172	2.423	4.948	0.1800
2500	0.865	3.63	0.210	2.340	4.119	0.1709
3000	0.873	3.08	0.249	2.254	3.506	0.1691
3500	0.878	2.690	0.285	2.170	3.081	0.1706
4000	0.882	2.394	0.322	2.096	2.739	0.1740
4500	0.884	2.166	0.359	2.020	2.462	0.1810
5000	0.885	1.986	0.394	1.942	2.246	0.1898
6000	0.884	1.720	0.461	1.800	1.918	0.2152
7000	0.880	1.539	0.528	1.657	1.667	0.2542
8000	0.865	1.410	0.597	1.522	1.449	0.3350
9000	0.815	1.325	0.691	1.382	1.179	0.5987
9200 <sup>c</sup>	0.768	1.333	0.768	1.333	1.000	1.0000

TABLE II. (Cont.)

Pressure Lb./Sq.Inch	Mole Fraction Hydrogen Dew Point	Volume Cu.Ft./Lb. Mole	Mole Fraction Hydrogen Bubble Point	Volume Cu.Ft./Lb. Mole	Equilibrium Ratio	
					Hydrogen	n-Hexane
400° F.						
277.53 <sup>a</sup>	0	-	0	3.23	-	1.0000
500	0.310	-	0.032	3.15	9.688	0.7128
1000	0.568	-	0.103	2.980	5.515	0.4816
1500	0.656	-	0.165	2.840	3.967	0.4120
2000	0.700	4.61 <sup>b</sup>	0.224	2.700	3.125	0.3866
2500	0.722	3.78	0.283	2.581	2.551	0.3877
3000	0.736	3.22	0.341	2.460	2.158	0.4006
3500	0.745	3.82	0.396	2.355	1.881	0.4222
4000	0.749	2.523	0.448	2.250	1.672	0.4547
4500	0.750	2.292	0.500	2.147	1.500	0.5000
5000	0.747	2.105	0.555	2.060	1.346	0.5685
5920 <sup>c</sup>	0.688	1.870	0.688	1.870	1.000	1.0000

TABLE III

ESTIMATED PROPERTIES AT THE UNIQUE STATES IN THE  
HYDROGEN-n-HEXANE SYSTEM<sup>a</sup>

Mole Fraction	Pressure Lb./Sq.Inch	Temperature °F.	Pressure Lb./Sq.Inch	Temperature °F.
	Critical		Maxcondentherm	
0.0	433.9 <sup>b</sup>	454.6 <sup>b</sup>	433.9	454.6
0.1	690	452	620	452
0.2	1000	449	840	449
0.3	1430	445	1150	446
0.4	2000	439	1500	441
0.5	2790	432	2010	435
0.6	4050	419	2750	425
0.7	6300	396	3660	411
0.8	-	277	4590	382
0.9	-	-	5450	327
1.0	188.1 <sup>c</sup>	-399.8 <sup>c</sup>	188.1	-399.8

<sup>a</sup> These data are much more uncertain than the directly measured quantities

<sup>b</sup> Critical of n-Hexane

<sup>c</sup> Critical of Hydrogen

### III. VOLUMETRIC AND PHASE BEHAVIOR OF HYDROCARBON SYSTEMS

#### 2. n-HEPTANE

[illegible]

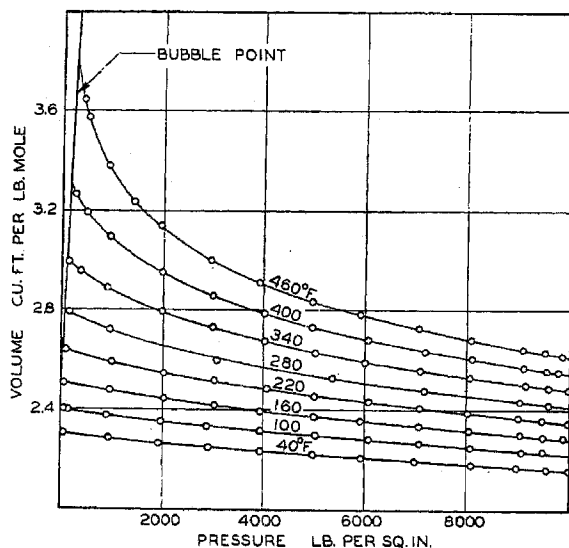
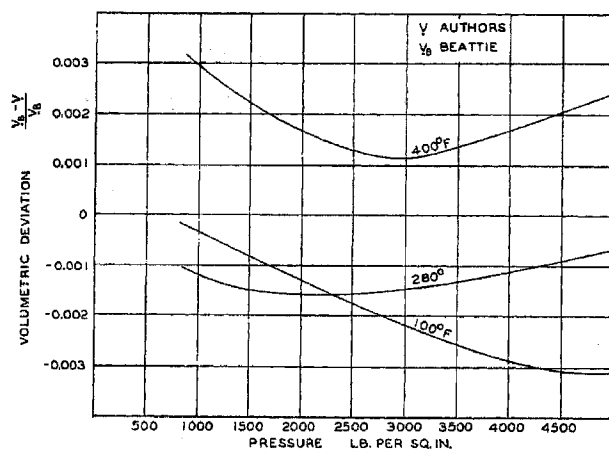
Figure 1. Molal volume of *n*-heptane in liquid phase

Figure 2. Deviation of Beattie's measurements from present investigation

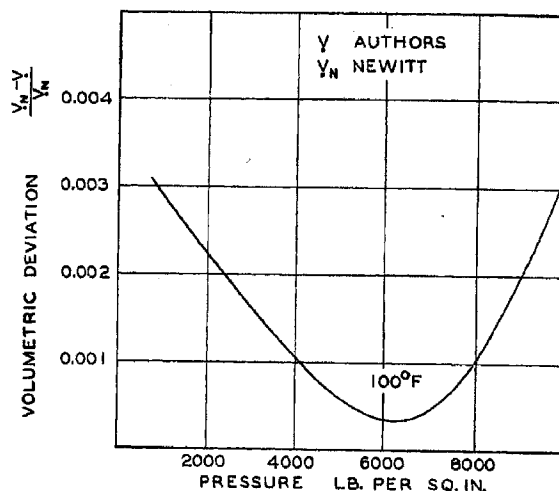


Figure 3. Deviation of Newitt's measurements from present investigation

measurements of Newitt with those of Beattie (10). As it was desired to establish partial volumetric behavior for binary mixtures involving *n*-heptane, the influence of pressure and temperature upon the molal volume of *n*-heptane was studied at pressures up to 10,000 pounds per square inch in the temperature interval between 40° and 460° F.

#### METHODS AND APPARATUS

Methods and equipment employed were the same as those used in the study of *n*-nonane (8) and *n*-hexane (11). The procedure involved confinement of a sample of *n*-heptane of known weight over mercury in a stainless steel chamber and measurement of the volume of the system occupied by the hydrocarbon as a function of state. A detailed description of the equipment is available (8).

Temperature of the sample was determined from the indications of a platinum resistance thermometer of the strain-free type (6) which had been compared with the indications of a reference instrument calibrated by the National Bureau of Standards. Experience indicated that the temperature of the sample was related to the international platinum scale with a

probable error of 0.02° F. Pressures were measured with a balance involving a piston-cylinder combination which was calibrated against the vapor pressure of carbon dioxide at the ice point (2). The pressures were known within 0.1% or 0.2 pound per square inch, whichever was the larger uncertainty. Agitation of the sample was provided in order to hasten physical equilibrium. The volume of the system occupied by *n*-heptane was known with a probable error of 0.25% at pressures below 5000 pounds per square inch and 0.4% at higher pressures. The weight of *n*-heptane was determined by weighing bomb techniques (8) and by comparison of volumetric measurements at atmospheric

Table II. Molal Volumes of *n*-Heptane in Liquid Phase

Pressure, lb./sq. inch Abs.	40° F.	100° F.	160° F.	220° F.	280° F.	340° F.	400° F.	460° F.
B.p.	(0.325) <sup>a</sup> 2.302	(1.58) 2.397	(6.11) 2.508	(17.48) 2.644	(40.96) 2.804	(83.20) 3.01	(151.4) 3.32	(257.8) 3.87
200	2.298 <sup>b</sup>	2.393	2.502	2.631	2.779	2.978	3.28	...
400	2.295	2.388	2.495	2.620	2.762	2.945	3.21	3.63
600	2.291	2.384	2.489	2.608	2.745	2.920	3.16	3.50
800	2.287	2.378	2.484	2.598	2.728	2.896	3.11	3.41
1,000	2.284	2.373	2.477	2.588	2.716	2.876	3.08	3.34
1,250	2.279	2.367	2.468	2.577	2.701	2.852	3.04	3.27
1,500	2.274	2.360	2.461	2.577	2.688	2.830	3.00	3.21
1,750	2.269	2.355	2.454	2.577	2.673	2.807	2.973	3.16
2,000	2.266	2.352	2.446	2.547	2.661	2.787	2.945	3.12
2,250	2.262	2.347	2.440	2.540	2.649	2.772	2.919	3.08
2,500	2.258	2.342	2.434	2.533	2.636	2.756	2.895	3.05
2,750	2.254	2.338	2.427	2.525	2.626	2.740	2.874	3.02
3,000	2.250	2.333	2.421	2.517	2.615	2.726	2.858	2.994
3,500	2.243	2.324	2.410	2.500	2.594	2.699	2.819	2.945
4,000	2.234	2.315	2.398	2.485	2.577	2.676	2.785	2.903
4,500	2.228	2.306	2.386	2.471	2.558	2.653	2.758	2.866
5,000	2.220	2.298	2.378	2.457	2.540	2.630	2.730	2.831
6,000	2.207	2.282	2.356	2.432	2.509	2.591	2.680	2.777
7,000	2.195	2.267	2.337	2.409	2.483	2.560	2.639	2.726
8,000	2.184	2.252	2.320	2.389	2.458	2.530	2.604	2.684
9,000	2.172	2.236	2.302	2.369	2.435	2.503	2.574	2.647
10,000	2.160	2.222	2.286	2.351	2.416	2.482	2.545	2.612

<sup>a</sup> Values in parentheses represent bubble point pressures expressed in pounds per square inch.

<sup>b</sup> Volume expressed in cubic feet per pound mole.



pressure (?) with critically chosen values of specific weight, with a probable error of less than 0.05%.

#### MATERIALS

The *n*-heptane was purchased as research grade from the Phillips Petroleum Co. and was reported to contain 0.0006 mole fraction of impurities. It was fractionated once at reduced pressure in a column containing 16 glass plates at a reflux ratio greater than 20. The first and last 10% of the overhead was discarded. After passage of the liquid through activated alumina and deaeration by prolonged refluxing at reduced pressure, it was dried over metallic sodium.

The specific weight of the sample of *n*-heptane at 77° F. was 42.4232 pounds per cubic foot, which compared with 42.4195 pounds per cubic foot reported by Rossini for an air-saturated sample at the same temperature. The index of refraction for the deaerated sample relative to the *D*-lines of sodium was 1.3853 as compared to a value of 1.3851 reported by Rossini for an air-saturated sample. A comparison of these data indicates that the sample employed for these measurements probably contained less than 0.0005 mole fraction of material other than *n*-heptane. It is believed that the impurities are primarily isomeric hydrocarbons.

#### EXPERIMENTAL RESULTS

The measurements of the volumetric behavior of *n*-heptane are given in Table I. No results were reported for the two-phase region, since the vapor pressure was already well established (1, 7, 10). The experimental results are depicted in Figure 1. The standard deviation of the experimental points from the smoothed curve was 0.0016 cubic foot per pound-mole. Smoothed values of the molal volume of *n*-heptane for each of the temperatures investigated are recorded in Table II. The bubble point pressures included in this table were taken from the critically chosen values of Rossini (?) at the lower temperatures and the measurements of Beattie (1, 10) at the higher temperatures.

The deviation of Beattie's volumetric measurements from the present investigation is shown in Figure 2. The standard deviation of 45 experimental points obtained by Beattie (10) from the smoothed data of Table II was 0.0062 cubic foot per pound-mole.

This corresponded to 0.23% deviation based upon the average molal volume. This variation is within the probable errors of the two sets of measurements. Figure 3 shows the deviation of Newitt's measurements from the present data. In this instance the standard deviation from the information presented in Table II was 0.0043 cubic foot per mole, which corresponds to 0.19% deviation based upon the average molal volume of *n*-heptane.

#### ACKNOWLEDGMENT

This paper is a contribution from American Petroleum Institute Project 37 at the California Institute of Technology. Virginia Berry aided in the reduction of the data and Elizabeth McLaughlin with the preparation of the manuscript, which was reviewed by W. N. Lacey.

#### LITERATURE CITED

- (1) Beattie, J. A., and Kay, W. C., *J. Am. Chem. Soc.*, **59**, 1586 (1937).
- (2) Bridgeman, O. C., *Ibid.*, **49**, 1174 (1927).
- (3) Carmichael, L. T., Sage, B. H., and Lacey, W. N., *IND. ENG. CHEM.*, **45**, 2697 (1953).
- (4) Eduljee, H. E., Newitt, D. M., and Weale, K. E., *J. Chem. Soc.*, **1951**, p. 3036.
- (5) Gilliland, F. R., and Parekh, M. D., *IND. ENG. CHEM.*, **34**, 360 (1942).
- (6) Myers, C. H., *Bur. Standards J. Research*, **9**, 807 (1932).
- (7) Rossini, F. D., Pitzer, K. S., Arnett, R. L., Braun, R. M., and Pimentel, G. C., "Selected Values of Physical and Thermodynamic Properties of Hydrocarbons and Related Compounds," Carnegie Press, Pittsburgh, 1953.
- (8) Sage, B. H., and Lacey, W. N., *Trans. Am. Inst. Mining Met. Engrs.*, **136**, 136 (1940).
- (9) Smith, E. R., and Matheson, J., *J. Research Natl. Bur. Standards*, **20**, 641 (1938).
- (10) Smith, L. B., Beattie, J. A., and Kay, W. C., *J. Am. Chem. Soc.*, **59**, 1587 (1937).
- (11) Stewart, D. E., Sage, B. H., and Lacey, W. N., *IND. ENG. CHEM.*, **46**, 2529 (1954).
- (12) Streiff, A. J., Murphy, E. T., Sedlak, V. A., Willingham, C. B., and Rossini, F. D., *J. Research Natl. Bur. Standards*, **37**, 331 (1946).
- (13) Stuart, E. B., Yu, K. T., and Coull, J., *Chem. Eng. Progr.*, **46**, 311 (1950).

RECEIVED for review January 27, 1955.

ACCEPTED March 9, 1955.

Volumetric data for pure hydrocarbons are of interest in many industrial applications. Because such data for *n*-heptane are not available for the higher temperatures and pressures, the effect of pressure and temperature upon the molal volume of *n*-heptane in the liquid phase was studied.

Measurements were made at pressures up to 10,000 pounds per square inch in the temperature interval between 40° and 460° F. The results are presented in graphical and tabular form.

Data obtained were in good agreement with an earlier investigation by Beattie at states where the two investigations overlapped. Satisfactory agreement with an English investigation was found at 100° F.

## Propositions

1. The following expression was used in correlating the times for the first bubbles to form in supersaturated solutions.

$$\ln[1 - P(0, \theta)] = -\dot{m}_b \theta$$

In evaluating  $P(0, \theta)$ , the probability of a bubble forming up to time  $\theta$ , the use of  $m/n + 1$  is more satisfactory than  $m/n$ , where  $m$  is the number of runs in which a bubble formed up to and including time  $\theta$  and  $n$  is the total number of runs.

2. The "heated thimble" apparatus described in this thesis is believed to be highly satisfactory for the measurement of the rates of bubble formation in supersaturated solutions. The construction of another "heated thimble" of different dimensions is proposed in order to study the effect of volume and surface on the rates of bubble formation. The addition of large (1/8 dia.) spheres of the same material as the thimble is suggested to make large changes in surface and volume.

3. If the rate of bubble formation is being measured in a liquid which is contaminated with foreign nuclei, the first bubble may preferentially form on one of the nuclei. If the nuclei vary in tendency to form bubbles, extreme value theory (1) may be of use in explaining the effect of volume on the mean time for the first bubble to form.

4. The following expression was derived in this thesis for the Fick diffusion coefficient.

$$D_{F,1} = \frac{\dot{m}_1}{\frac{\partial \sigma_1}{\partial x}} \left( \frac{\sigma_1}{\sigma} - 1 \right)$$

If an "integral" coefficient is defined by

$$\bar{D}_{F,1} = \frac{\dot{m}_1 l}{\int_{\sigma_x}^{\sigma_b} \frac{1}{\frac{\sigma_1}{\sigma} - 1} d\sigma_1}$$

this coefficient may easily be calculated for each run. It is proposed to consider this coefficient to represent the "differential" coefficient at the concentration given by

$$\bar{\sigma}_1 = \frac{\int_{\sigma_x}^{\sigma_b} \frac{\sigma_1}{\frac{\sigma_1}{\sigma} - 1} d\sigma_1}{\int_{\sigma_x}^{\sigma_b} \frac{1}{\frac{\sigma_1}{\sigma} - 1} d\sigma_1}$$

5. Pings (2) has suggested that curve fitting by the method

of least squares is formally no more difficult if the method is modified so as to minimize the sum of the squares of the relative deviations. This proposal is numerically feasible if the relative deviation is defined as the difference between the experimental value and the corresponding value on the regression line divided by the experimental value. The method reported by Ergun (3) for fitting families of straight lines may be similarly modified.

6. Abietic acid can be converted to retene by catalytic dehydrogenation. It may be possible to produce phthalic anhydride in good yields from retene by catalytic oxidation. It is proposed that this sequence of reactions be investigated.

7. Air containing a small amount (1-2%) of nitrogen dioxide is frequently the product of a nitration process. Satisfactory methods for removing the nitrogen dioxide are difficult to find. It might be practical to use a process (physical and/or chemical) operating at a temperature below the boiling point of nitrogen dioxide to accomplish this objective.

8. Chang, Schoen, and Grove (4) present some data on the distribution of bubble sizes in foams in order to demonstrate a method of obtaining this data. A further treatment of the data reveals some interesting features not pointed out in the original presentation.

9. An experimental investigation is proposed for the chemical engineering laboratory on the application of the thermodynamics of irreversible processes to corrosion. Van Rysselberghe (5) has presented the basic theory, and Johnson and Babb (6) made a simple calculation of an interaction coefficient using some preliminary data of Schwerdtfeger and McDorman (7). The experimental equipment is not extensive and the program might be carried out by students at the first year graduate level. The data may be treated simply in an approximate manner or much more elaborately.

10. a. Both games of a baseball doubleheader are more likely to be won by the same team than to be divided between the two teams.

b. The winning team in a major league baseball game will score at least twice as many runs as the losing team more often than not.

c. The most probable number of games played in a World Series is six.

## Nomenclature

$D_{F,1}$	Fick diffusion of component 1
$Q$	diffusion path length
$m$	number of runs in which a bubble formed
$\dot{m}_1$	transport rate of component 1
$n$	total number of runs
$\dot{n}_b$	rate of bubble formation
$P(0,\theta)$	probability of a bubble forming up to time $\theta$
$x$	distance along diffusion path
$\theta$	time
$\sigma$	specific weight
$\sigma_1$	concentration of component 1
$\sigma_{1x}$	concentration of component 1 at top of diffusion path
$\sigma_{1b}$	concentration of component 1 at bottom of diffusion path

## References

1. Gumbel, E. J. "Statistical Theory of Extreme Values and Some Practical Applications" U. S. Department of Commerce, National Bureau of Standards, AMS-33 Washington 1954
2. Pings, C. J. Ph. D. Thesis California Institute of Technology 1955
3. Ergun, S. Ind. Eng. Chem., 48, 2063 (1956)
4. Chang, R. C., Schoen, H. M., and Grove, C. S. Ind. Eng. Chem., 48, 2035 (1956)
5. Van Rysselberghe, P. J. Phys. Chem., 57, 275 (1953)
6. Johnson, P. A., and Babb, A. L. Ind. Eng. Chem., 46 518 (1954)
7. Schwerdtfeger, W. J., and McDorman, O. N. J. Electrochem. Soc., 99, 407 (1952)